CHAPTER 4

Test Results and Discussions

CHAPTER 4
TEST RESULTS AND DISCUSSION

The results obtained from the experimental work are summarized in this chapter. Theseresults were conducted in four main parts:

1- Test results of experiments that were carried out on conventional concrete.
2- Test results of experiments that were carried out on modified concrete.
3- Test results of experiments that were carried out on mortars (as an external protection for the concrete).
4- A case study.

The results were tabulated and analyzed as follows:

4.1 Phase 1: Results of experiments carried out on conventional concrete.

4.1.1. Compressive strength test results.

Compressive strength test results of conventional concrete (control mix) cubes 100x100x100mm for28days were tabulated in **Table 4.1** at normal ambient temperature and after being exposed to different degrees of temperature at 200, 400 and 600ºC for 2 hrs.

Table 4.1: Compressive strength test results of control concrete at different elevated temperatures for 2 hrs.

Mix designation	Compressive Strength (MPa)			
	Temperature (ºC)			
	20	200	400	600
Control mix	36.2	30.1	27.9	20.2

One of the main adverse effects of high temperatures onconcrete structures is the reduction in compressive strength of concrete. From **Fig. 4.1** it is evident that the compressive strength decreases with the increase of elevated temperature. The residual compressive strength of the concrete is reduced by about 17, 23 and 45% at 200, 400 and 600ºC respectively.

The compressive strength is lost inheated concretes mainly from the changes that occur in the concrete microstructure during the heating process. Some complicated processes of shrinkage,

decomposition, expansion and crystal destruction occur during exposure to fire.The reduction in the concrete compressive strength, whenexposed to elevated temperatures, can be attributed also to thedehydration of concrete by the driving out of free water, interlayerwater and chemically combined water. The loss of physicallybound water significantly affects the mechanical properties ofthe concrete which is exposed to elevated temperatures.Build-up pore pressure is induced due to the evaporation of pore water as well as by the shrinking of the binder due to water loss. Furthermore, the coefficient of thermal expansion of the binder is different from that of the aggregate. Therefore mere increase in temperature increase induces microcracking and changes the pore structure of concrete, thus reduces its strength and stiffness **[Diederichs et al. 1989].**

Also the explosive thermal spalling of concrete during exposure to fire occursmostly without prior notice. Different researchers foundsimilar results regarding the effects of high temperatureson the properties of concrete. Similar to the results of thecurrent study, **[Chan et al. 1999]** found that the range between 400 and 800°C was critical to the loss in strength. The compressivestrength of the specimens was lowered drastically when thetemperature reached above 400 °C.

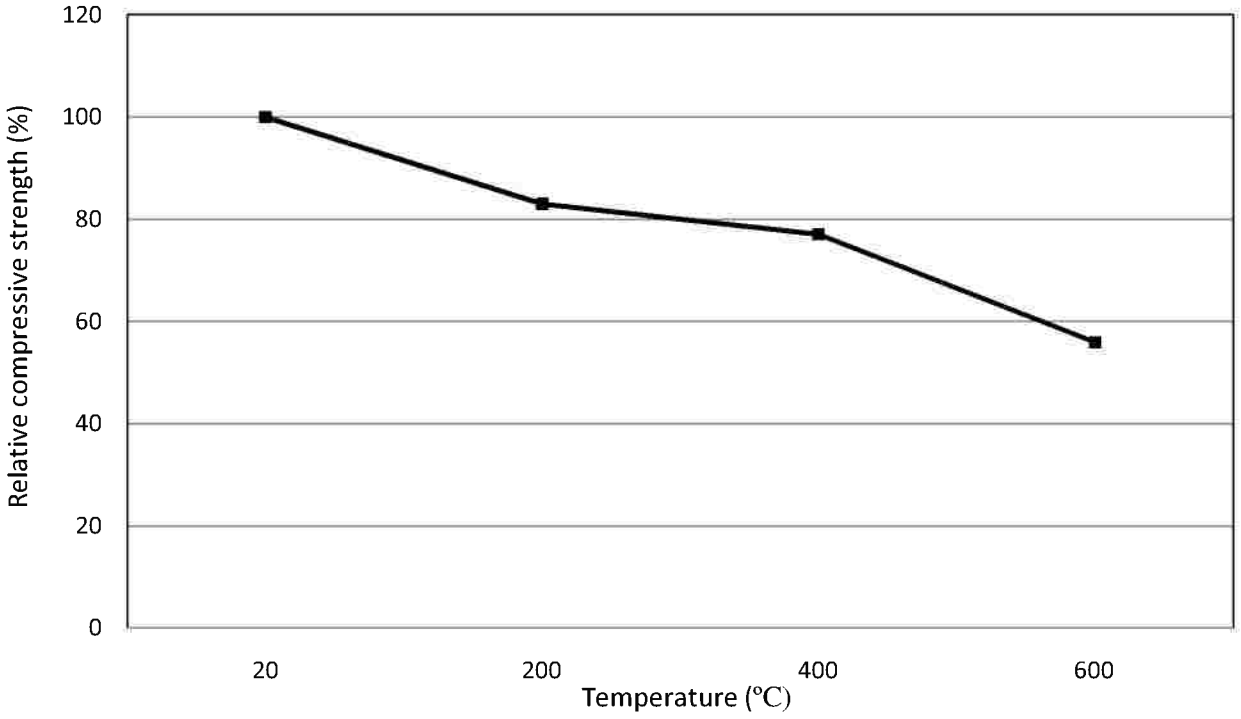

Fig. 4.1- Relative compressive strength of the control mixture at room temperature andresidual compressive strength after exposure to 200, 400 and 600°C for 2 hrs.

4.1.2. Tensile strength test results.

Twelve cylinders 100x200 mm wereinvestigated at 20, 200, 400 and 600ºC for tensile strength and the results are presented in **Table 4.2**. The relative tensile strength was plotted in **Fig. 4.2**. Analysis of the tensile strength results shows that theywere reduced considerably at elevated temperature. Clearly, from **Fig. 4.2** it can be noted that with the increase in the elevated temperature from 20 to 200, 400 and 600ºC the tensile strength is decreased to 22, 47and 65% respectively.The loss in tensile strength is considerably sharp, which is clearly different from the loss of compressive strength. This is due to the fact thatthe tensile strength is more sensitive to macro- or non-micro-scale cracks, which are caused by high temperature in concrete**[Chan et al, 1999]**.

The tensile strength of concrete is much lower than the compressive strength, due to the ease with which cracks can propagate under tensile loads **[Mindess, et al. 2003]**. Concrete is weak in tension, and for NSC, tensile strength accounts for only 10% of its compressive strength. Thus, tensile strength of concrete is often neglected in strength calculations at both room and elevated temperatures. Yet it still remains an important, because cracking in concrete is generally due to tensile stresses and the structural damage of the member in tension that is often generated by progression in micro cracking. Under fire conditions tensile strength of concrete can be even more crucial in cases where fire induced spalling occurs in a concrete structural member **[Khaliq, and V. Kodur, 2012]**. Tensile strength of concrete depends on almost the same factors as compressive strength of concrete **[Neville, 2004 and Shah, 1991]**.

Hence, the tensile strength is similar to the compressive strength – or even more severely - reduced, due to themicrostructure damages that result frommicro cracks.

Table 4.2: Tensile strength results of conventional (control) concrete after exposure to20, 200, 400 and 600ºC for 2 hrs.

Mix designation	Tensile Strength (MPa)			
	Temperature (°C)			
	20	200	400	600
Control mix	3.6	2.8	1.9	1.3

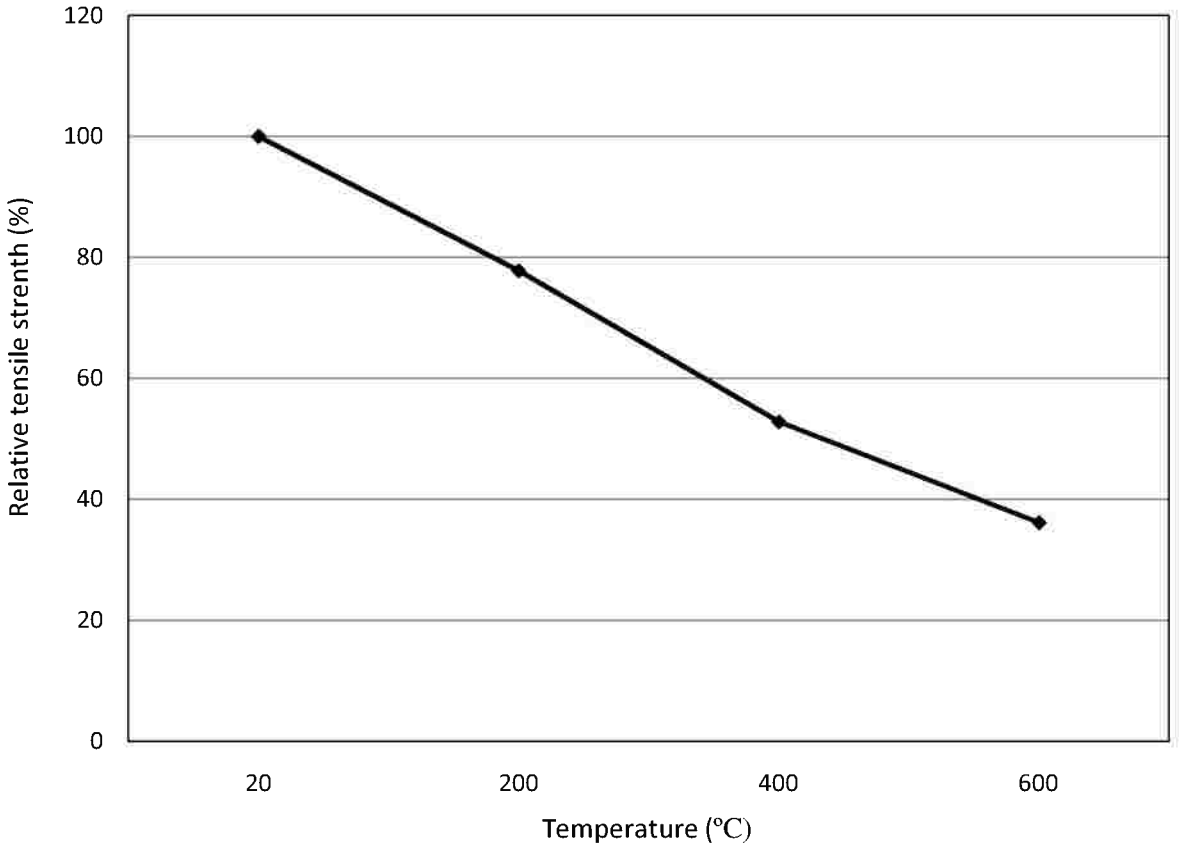

Fig. 4.2- Relative tensile strength of the control mixture at room temperature and after exposure to 200, 400 and 600°C for 2 hrs.

4.1.3. Flexural strength test results.

Flexural strength test results areplotted in**Fig. 4.3.**The figureshows the decrease in flexural strength with elevated temperature. The residual flexural strength decreases gradually when temperature rises from 20ºC up to 600ºC. It can be observed the stabilization decrease for ordinary concrete mix between 20ºC and 200ºC, the flexural strength decreases by about 20%. After this moderate decrease in residual flexural strength, another important decrease of (about 82%) is observed at 600ºC. This dramatic reduction in flexural strength is due to many micro and macro cracks that were produced in the specimens due to the thermal incompatibility between aggregates and cement paste**[Hanaa et al. 2009]**.

Table 4.3: Flexural strength test results of conventional (control) concrete after exposure to 20, 200, 400 and 600ºC for 2 hrs.

Mix designation	Flexural Strength (MPa)			
	Temperature (ºC)			
	20	200	400	600
Control mix	5.6	4.5	2.36	1

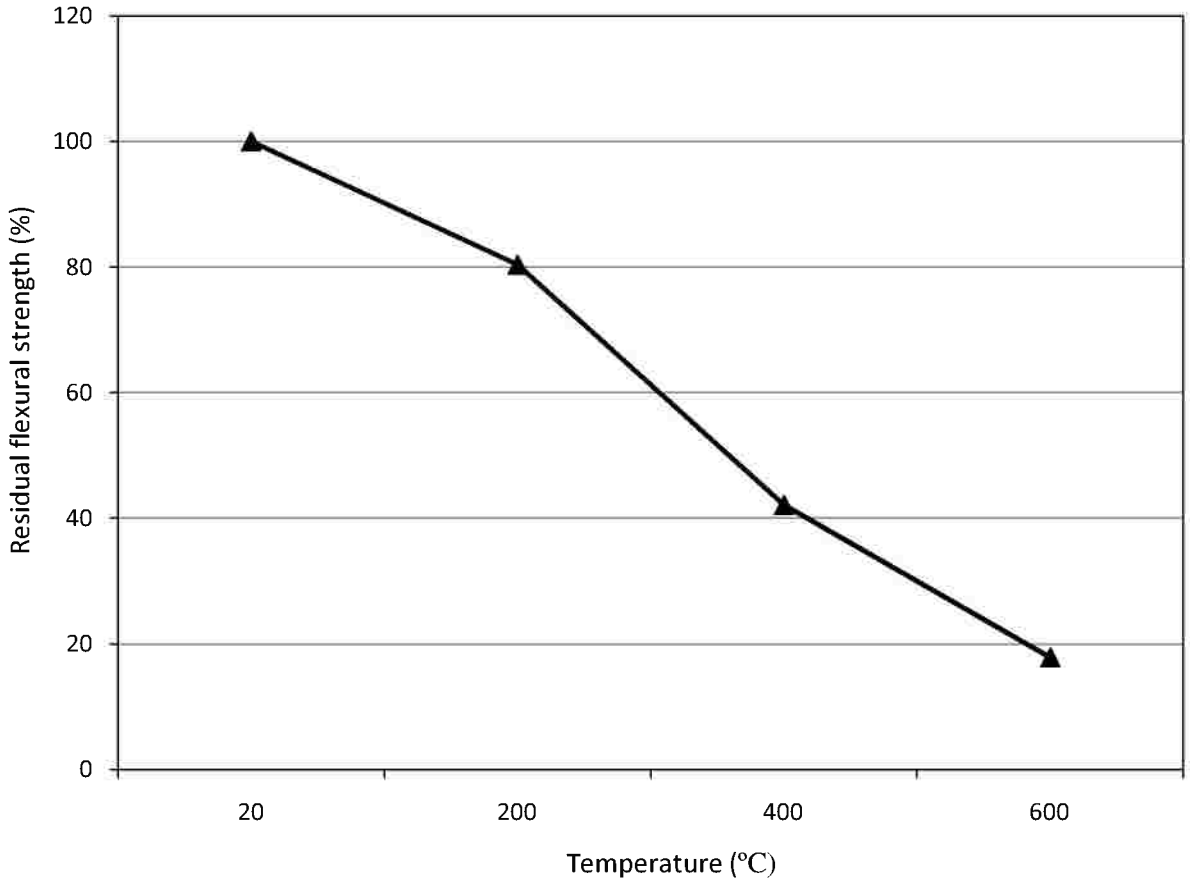

Fig. 4.3-Relative flexural strength of the control mixture at room temperature and after exposure to 200, 400 and 600°C for 2 hr.

4.1.4 Weight loss test results.

The weights of the conventional concretecube specimens before and after exposure to high temperature were determined and plotted for the weight loss evaluation. **Fig. 4.4** presents the effect of elevated temperatures on the weight loss of the concrete specimens. It can be seen

from this figure that the evolution of weight loss versus temperature. The variation of weight loss versus exposure to different temperatures can be divided into three phases ending up 600°C. Between the ambient temperature and 200°C, the variation of mass is rather big. The loss in weight in this domain corresponds to the departure of free water contained in the capillary pores beside the chemical decomposition of some components such as ettringite. When the temperature rises from 200 to 400°C, an important increase in weight loss corresponds to about 2.6% of the initial weight loss can be observed. The mass loss of this domain is owing to the release of both capillary water and gel water **[Hoff, et al. 2000]**. At the range of 400 to 600°C, the rate of weight loss comparatively slows down due to the decomposition of $Ca(OH)_2$ (portlandite)in this phase.

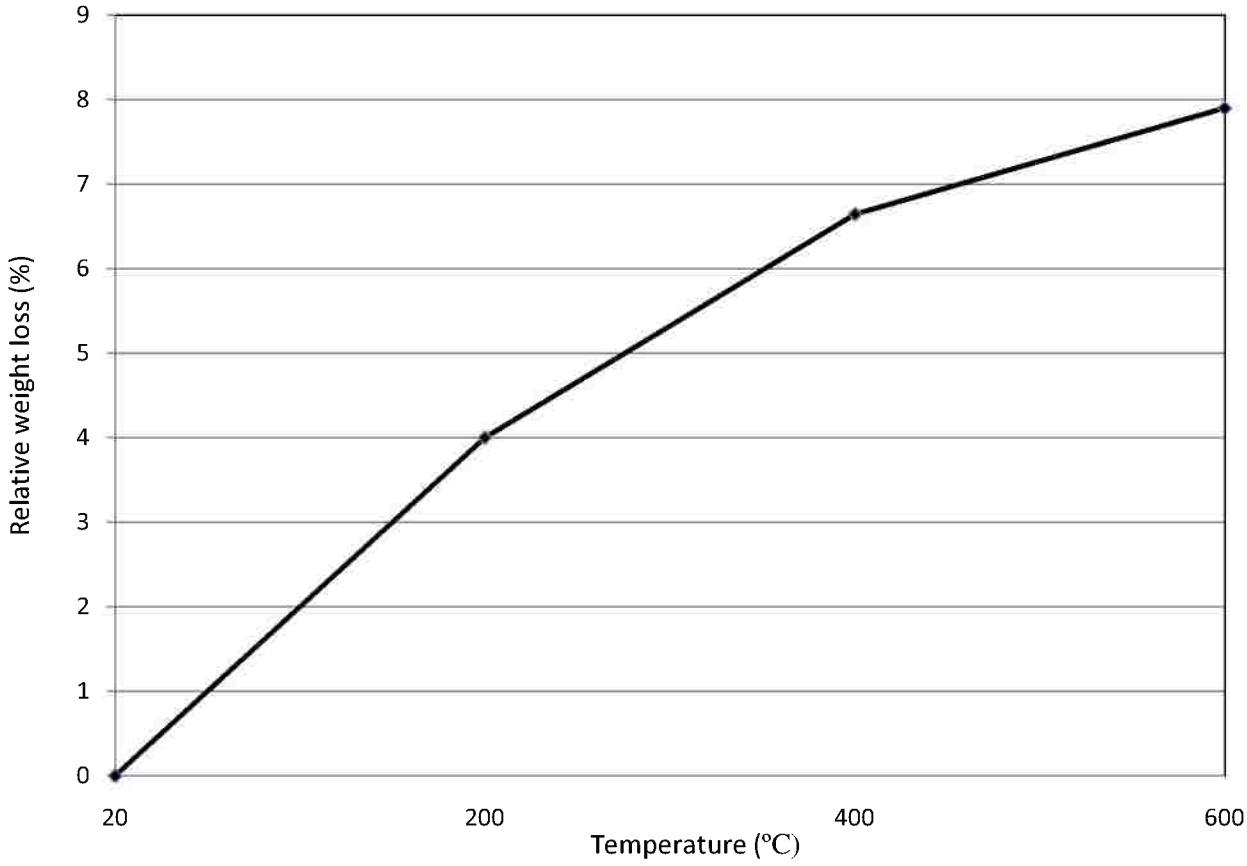

Fig. 4.4- Relative weight loss of control concrete specimens while being subjected to elevated temperature up to 600°C.

4.1.5 Visual inspection test results.

A visual investigation on the surface of the concrete cubes was done in order to evaluate the impact of elevated temperatures on the growth of the surface cracks. It is evident from **Fig 4.5** that the surface cracks were increased with the increasein the exposure to high

temperature degrees.Especially at 600°C, experiments showa network of surface cracks. This investigation was supported the results that were obtained from the compressive strength test results and was given more vision about the role at the surface cracks,effec on the reduction of the concrete strength.

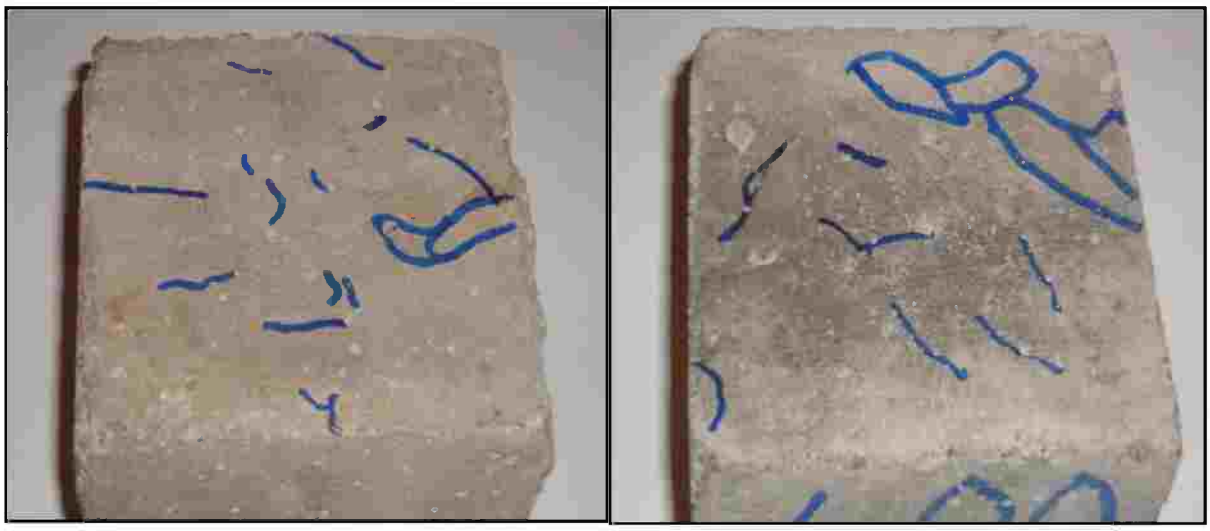

(a) 200ºC (b) 400ºC

(c) 600ºC

Fig. 4.5- Maps of the cracking of control concrete specimens after being exposed to 200, 400 and 600°C for 2 hrs.

4.1.6 Effect of water cooling regime on the residual compressive strength.

The effect of water cooling regime on the properties of concrete was studied in terms of compressive strength.The results of relative residual compressive strength of the air and water cooling regime'sspecimens are given in **Table. 4.4**. The strength decreases gradually with the increase in temperature for the entiretemperature range without any recovery.

From **Fig. 4.6** it is observed that air-cooling exhibits superior qualities over water-cooling through maintaining higher residual properties. At 200, 400ºC and 600ºC the retained residual performance by air-cooling regime over water-cooling regime was up to 3, 9 and 6% respectively. It must be noted that the reduction in the residual compressive strength between air and water cooling regime may be rather small with respect to the small specimen's dimension.

This reduction in residual compressive strength of the concrete specimens with water cooling regimeis due to the fact that water cooling causes significant thermal shocks to the hot concrete and as a result, severe in deterioration has taken place. Sudden water cooling regime causes a negative thermal shock for the concrete specimens and thereby increases the near-surface cracks **[Kristensenl and Torebn, 1994]**.

On another hand, As soon as concrete is heated to a temperature of 500ºC to 550ºC, portlandite decomposes according to the following reaction:

$Ca(OH)_2 \rightarrow CaO + H_2O$ and its content drops rapidly, but when sudden cooling was done, the dehydration process of $Ca(OH)_2$ with more volume and less strength was performed causing more cracks and weak microstructures.

Table 4.4: Relative compressive strength under air and water cooling regime.

Cooling regime	Exposed temperature (°C)			
	20	**200**	**400**	**600**
Under air	100	83	77	56
Under water	100	80	68	50

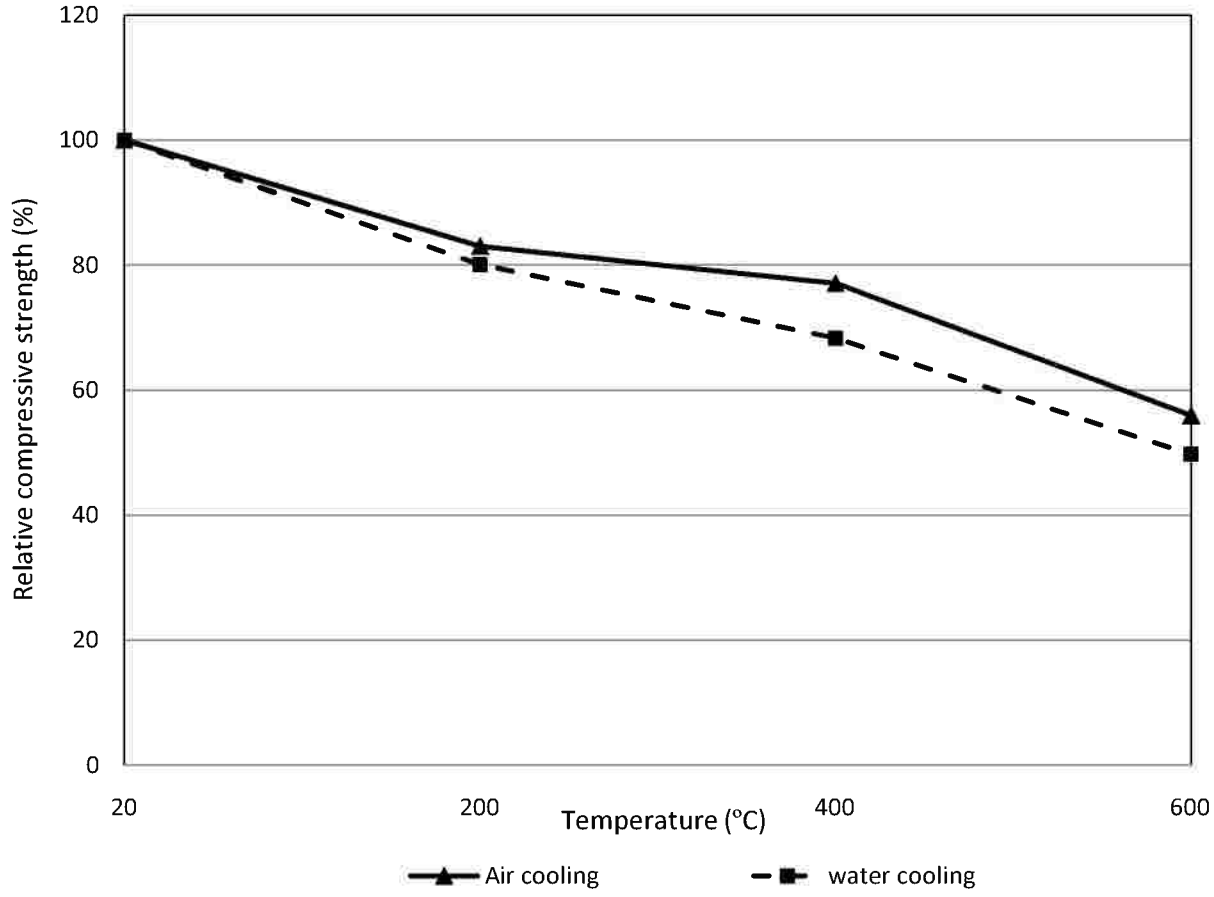

Fig. 4.6-Relative compressive strength of conventional concrete specimens after air and water cooling regime.

4.1.7Thermogravimetric analysis (TGA/DTG).

Thermogravimetric analysis(TGA) consists of finding changes in the weight of a material with increasing in temperatures. This plot is called a Thermogram. The loss of weight indicates decomposition or evaporation of the material. This technique allows finding out the temperature range at which a material will remain stable and the temperature at which it would undergo decomposition.The (TGA/DTG) curves are presented in **Fig. 4.7 (a-b)** whichshows three significant weight loss stepsthat correspond to endothermic processes. The first,at about 100ºC, is attributed to surface water desorption as well as water loss from C-S-H gel layers and the dehydration of ettringite. Further mass loss at 400°C indicates continuous thermal decomposition of the complex mixture of hydrated silicate- and aluminate-type compounds. The second step was conducted at about 480ºC and is due to the dehydration of $Ca(OH)_2$ (portlandite)according to the following reaction:

$Ca(OH)_2 \rightarrow CaO + H_2O\uparrow$ and its content drops rapidly.

The third weight loss step,was at about 780ºC, and it can be attributed to the decarbonation of $CaCO_3$which is correlated with the portlandite content which has tendency to increase in the concrete. At the third step, may be the peak has a slight difference between the unheated (825ºC) and the preheated specimens (780-800ºC). The first step of weight loss is almost completely hidden by the drying and dehydration processes of the ettringite and C-S-H gel for all the preheated samples at 200,400 and 600ºC.Total mass losses of unheated and preheated control samples at 20, 200, 400 and 600ºC after TGA test were about25, 22, 14 and 8.5% respectively.Although TGA curves are similar in shape, significant differences can be observed in DTG profiles of portlandite and carbonated phases' decompositions. It can be obvious from **Fig. 4.7(a)** that theweight loss at the second step of the control mixtureis reduced with the increase of the elevated temperatures of the preheated concrete.It means that, as example, the weight loss of the preheated sample to 400ºC is less than the weight loss of unheated sample. This is a result of the difference in the amount of decomposed $Ca(OH)_2$ before the test.

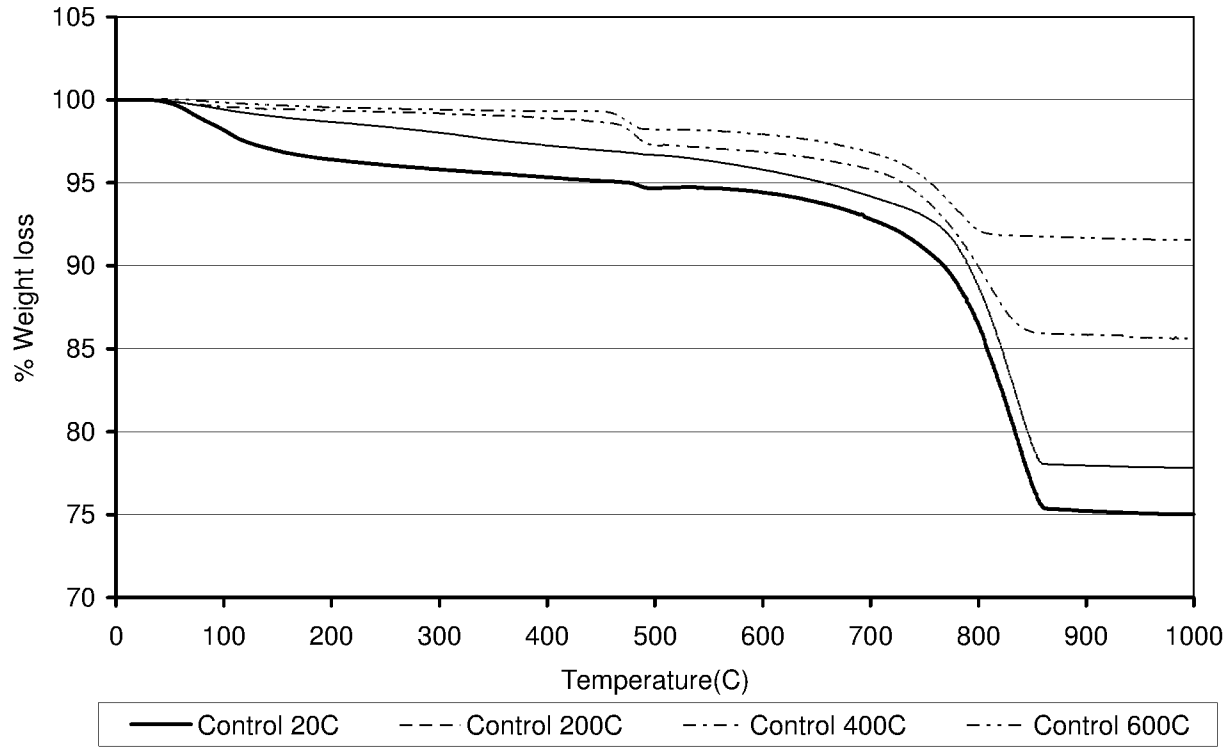

(a)

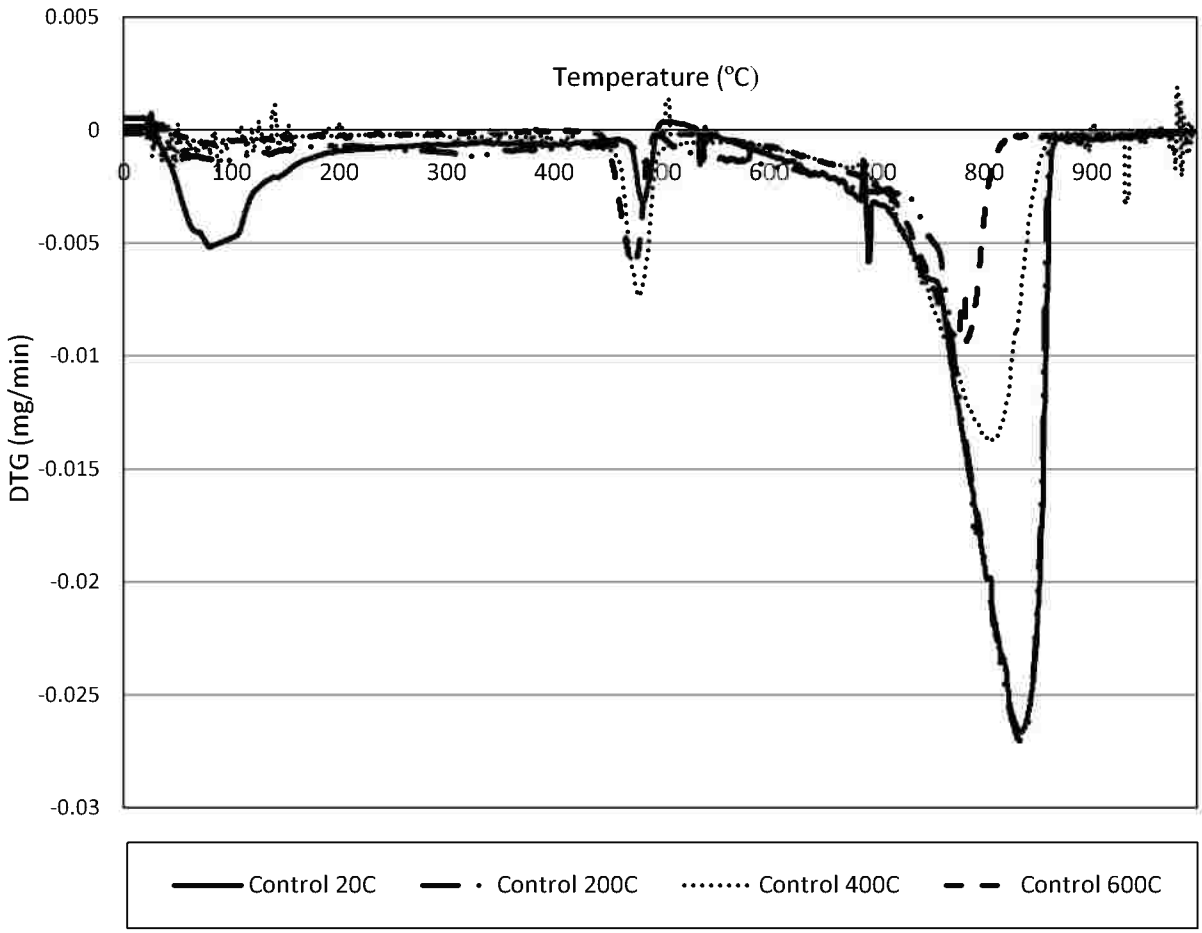

(b)

Fig. 4.7-(TGA/DTG) curves of control mix a) TGA b)DTG

4.1.8Scanning electron microscope (SEM).

Scanning electron microscopy (SEM) allows the examination of microstructural details.In this study fragments of specimens were broken off, and SEM was carried out on M-Cat 20, 200, 400 and 600ºC.Evidently, as shown in **Fig. 4.8-a.1**, the microstructure of the mixture concrete at 20ºC displays the existence of microcrystalline and nearly amorphous, there is calcium silicate hydrate (marked ''CSH'')which is the main product together with the calcium hydroxide(marked ''CH'') which occurs as relatively crystalline plates and mono-sulpho-aluminate hydrate (ettringite) (marked ''AFt'').Also it can be observed that there is a very goodadhesion between the matrix and the fine aggregate as shown in **Fig. 4.8-a.2**

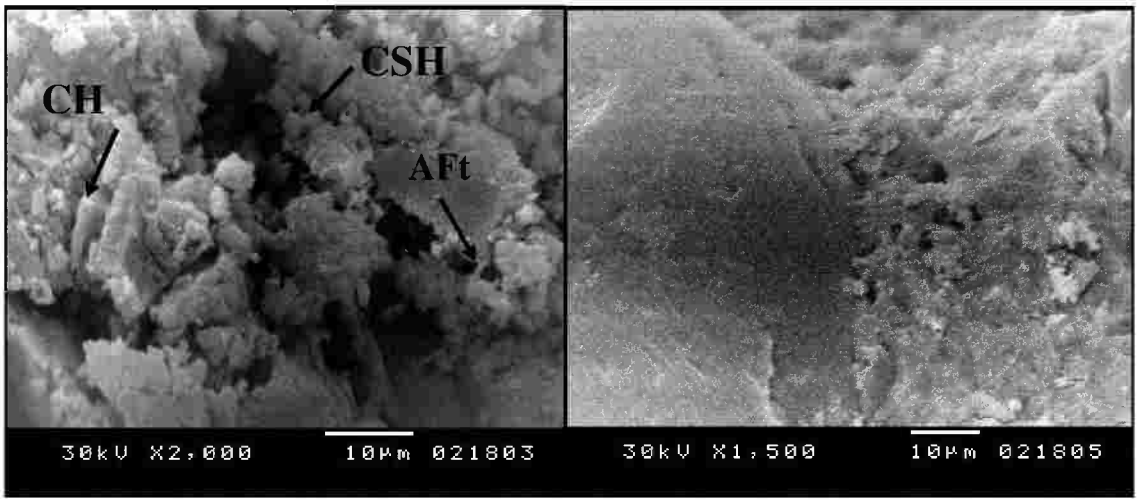

(1) (2)

(a) 20ºC

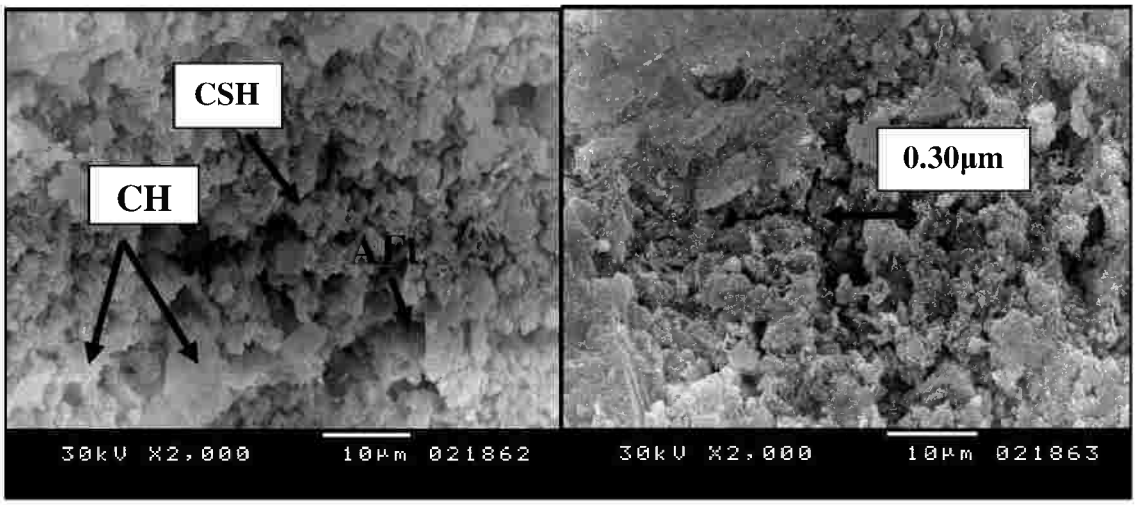

(b) 200ºC (c) 400ºC

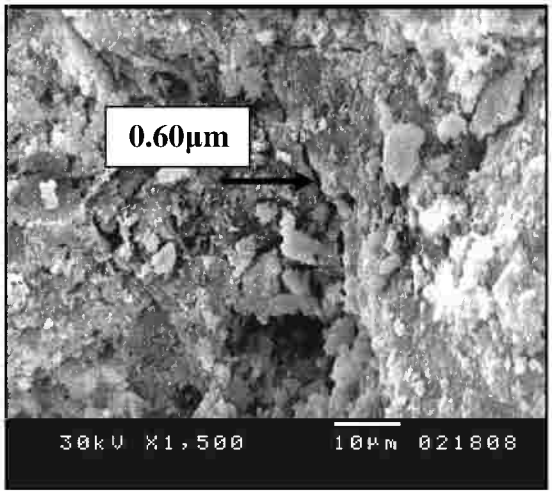

(d) 600ºC

Fig. 4.8- SEM images of conventional concrete specimens after being exposed to elevated temperature at 20, 200, 400 and 600°C for 2 hrs.

SEM image shows plenty in all hydrated productsat 200ºC. At 400ºC and from **Fig. 4.8-c**, the control specimen shows the beginning of cracks with about 0.30 µmwidthand the concrete start to be poor in hydration products.On the other hand at 600ºC, the SEM micrograph displays the formation of microcracks with average width of 0.6 µm and also the decomposition of the hydration products as shown in**Fig. 4.8-d**.

4.1.9Effect of elevated temperature on small scale reinforced concrete slabs.

The slabs were exposed to three different degrees of temperature at 600, 800 and 1200ºC. The results of reinforcement temperatures inside the slabs with 25 mm concrete cover, with both unexposed and exposed surface temperatures of concrete are tabulated in **Tables4.5, 4.6** and **4.7**.The results are plotted in **Figs. 4.9, 10** and **11**, where the vertical axis shows the temperature and the horizontal axis resembles the duration. From **Figs. 4.9, 10** and **11** it is evident that the temperature of the reinforcement, unexposed and exposed surface increases with the increasein the term of exposed temperatures. After 2 hr. exposure, the reinforcement temperatureswere 220, 275 and 391ºC when the slabs were exposed to 600, 800 and 1200ºC respectively, it can be noted that the reinforcement temperature is less than 550ºC, at which the steel loses 50% of its strength.It can be noted that after 2 hrs. of air cooling, the difference in reinforcement temperature inside the exposed slabs at 600, 800 and 1200ºC is rather small, and the reinforcement temperatures were 50, 52 and 60ºC respectively. Also it appears that the unexposed surface temperature is slightly more than the exposed surface after 2 hrs of air cooling, this may be attributed to the heat transportationfrom exposed (with higher temperature) to unexposed surface (lower temperature) after being heated.

Table 4.5: Temperature of reinforcement, unexposed and exposed surface of conventional concrete slabs when exposed to 600ºC for 2 hrswith air cooling for 2 hrs.

Time (min)	Reinforcement temperature (°C)	Unexposed surface temperature (°C)	Exposed surface temperature (°C)
0	20	20	20
10	83	51	600
20	135	118	600
30	145	127	600
40	153	139	600
50	166	145	600
60	171	147	600
70	176	154	600
80	182	163	600
90	190	172	600
100	196	176	600
110	205	183	600
120	220	186	600
130	187	171	370
140	154	156	139
150	131	132	118
160	109	108	97
170	97	94	86
180	85	81	76
190	77	72	69
200	69	64	63
210	63	59	58
220	58	54	53
230	54	50	50
240	50	47	46

Table 4.6: Temperature of reinforcement, unexposed and exposed surface of conventional concrete slabs when exposed to 800ºC for 2 hrswith air cooling for 2 hrs.

.

Time (min)	Reinforcement temperature (°C)	Unexposed surface temperature (°C)	Exposed surface temperature (°C)
0	20	20	20
10	115	86	800
20	148	117	800
30	178	137	800
40	205	154	800
50	224	175	800
60	244	199	800
70	256	208	800
80	264	222	800
90	270	228	800
100	269	233	800
110	272	236	800
120	275	239	800
130	230	214	464
140	185	190	178
150	155	152	145
160	126	115	113
170	111	105	101
180	97	95	89
190	85	83	77
200	74	70	64
210	66	64	60
220	59	58	55
230	54	53	51
240	52	48	47

Table 4.7: Temperature of reinforcement, unexposed and exposed surface of conventional concrete slabs when exposed to 1200ºC for 2 hrswith air cooling for 2 hrs.

Time (min)	Reinforcement temperature (°C)	Unexposed surface temperature (°C)	Exposed surface temperature (°C)
0	20	20	20
10	124	83	1200
20	177	123	1200
30	221	142	1200
40	263	187	1200
50	296	216	1200
60	321	237	1200
70	337	251	1200
80	352	263	1200
90	363	268	1200
100	373	276	1200
110	384	280	1200
120	391	286	1200
130	345	255	719
140	299	224	238
150	243	193	193
160	187	161	149
170	160	134	129
180	133	107	110
190	113	93	91
200	94	80	73
210	85	69	69
220	76	58	65
230	68	55	58
240	60	53	51

.

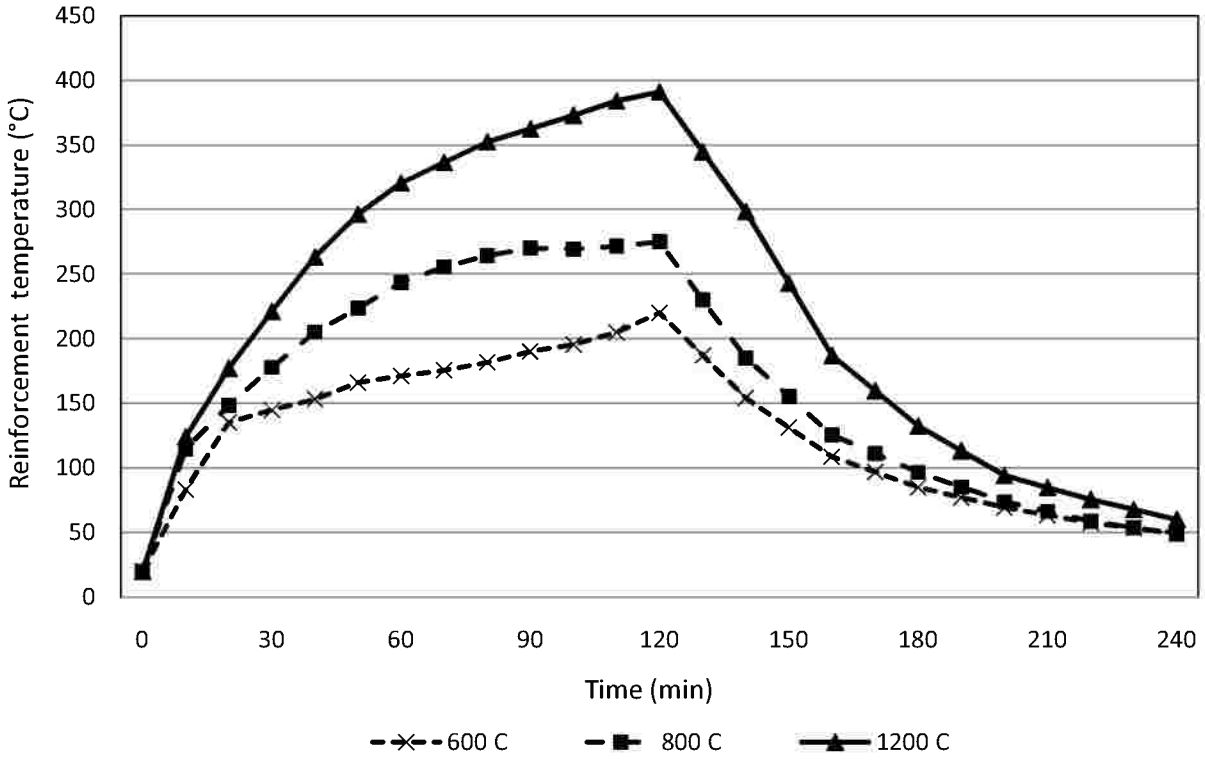

Fig. 4.9-Time – temperature curves of reinforcement inside reinforced conventional concrete slabs when exposed to 600, 800 and 1200ºC for 2 hrs and cooled by air for 2 hrs.

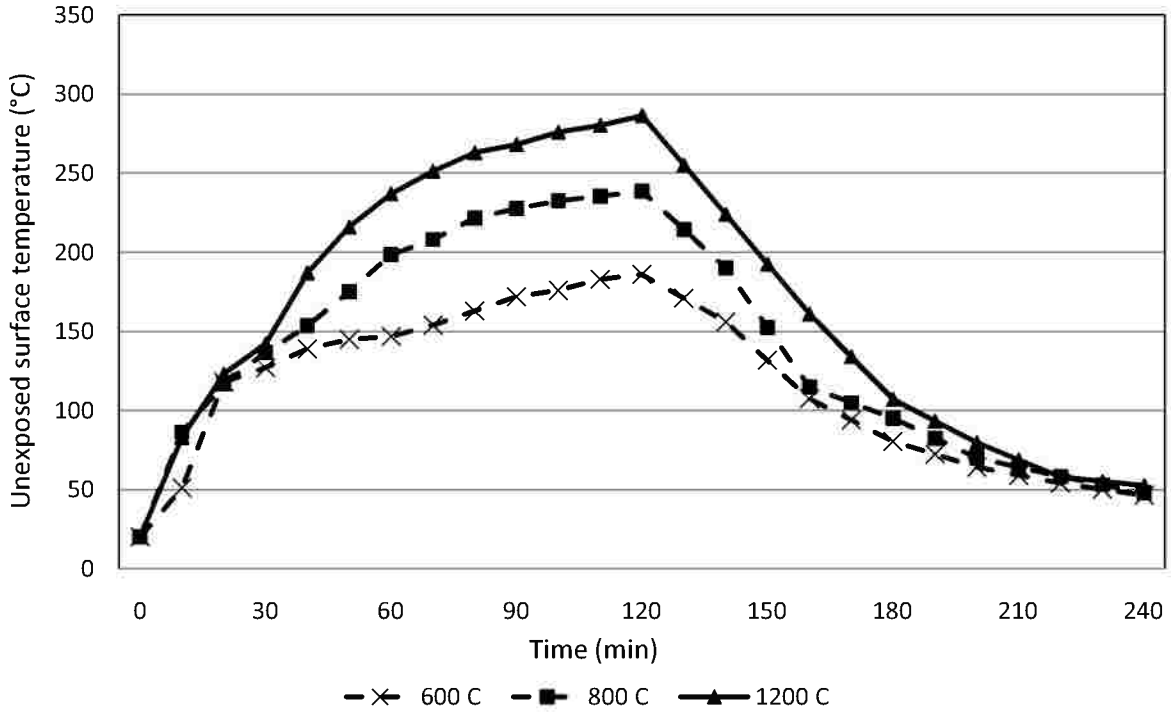

Fig. 4.10-Time-temperature curves of unexposed surface of reinforced conventional concrete slabs when exposed to 600, 800 and 1200ºC for 2 hrsand cooled by air for 2 hrs.

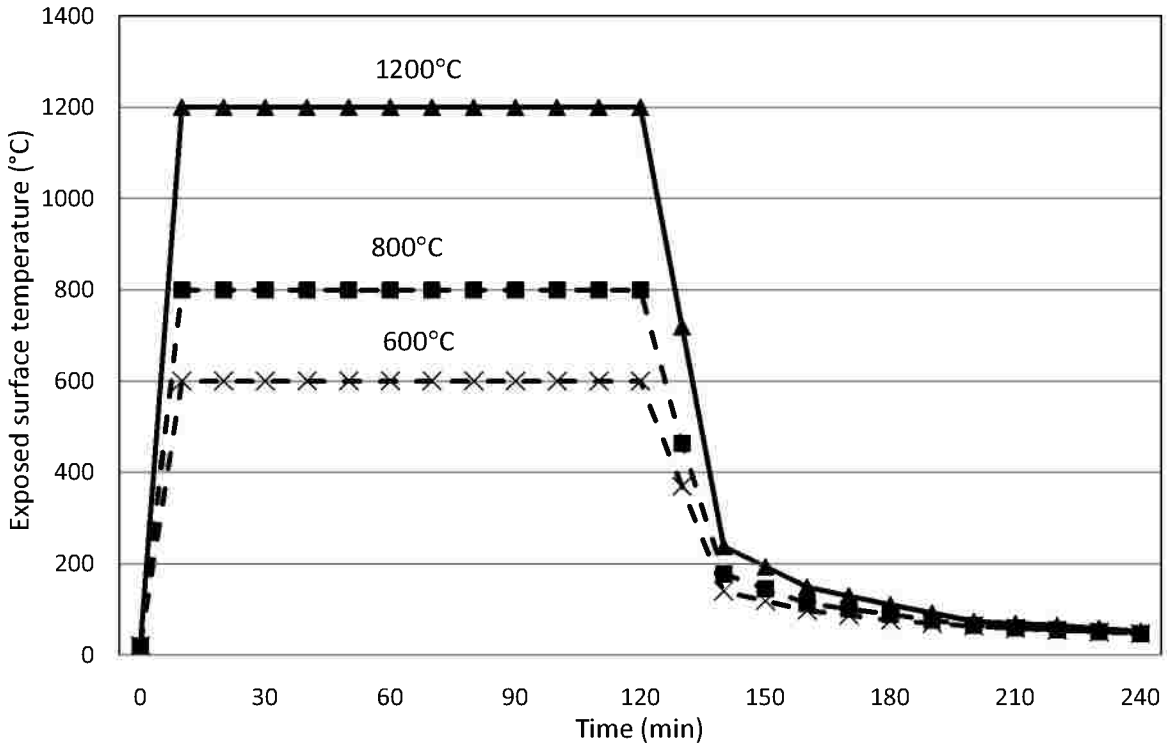

Fig. 4.11-Time-temperature curves of exposed surface of reinforced conventional concrete slabs when exposed to 600, 800 and 1200ºC for 2 hrs.and cooled by air for 2 hrs.

4.1.10Effect of the concrete cover thickness on the protection of the reinforcement.

One of the major safety requirements in the design of buildings is the provision of appropriate fire endurance of structural members. The fire endurance in this part is defined in terms of the temperature of the reinforcement. In this context one of the main factors that influence the fire resistance of conventional reinforced concrete slabs is: the concrete cover thickness.

Small scale slabs with the dimensions 300x250x100 mm having a 25, 50 and 75 mm concrete cover,were exposed to 800°C from beneath and the temperature of the steel bars inside the slabs were recorded with the time as presented in **Table 4.8** and plotted in **Fig. 4.12**.It is evident that the thickness of the concrete cover to the reinforcement has a pronounced effect on the fire resistance of the slabs. This can be attributed to the fact that failure of the slabs is assumed to be governed by the critical temperature of the reinforcement. Larger concrete cover thickness delays the transmission of heat to the reinforcement, therefore enhancing fire resistance.It is evident that the average Rft temperatures were less for slabs with a greater overall cover thickness,as should be expected. From **Fig. 4.12,** it can be seen that increasing the concrete cover thickness from 25 mm

to 50 and 75 mm is reduced the temperature of reinforcement, after 2 hrsof exposure, by about 16 and 58%, thus it is that clear the passive effect of increasing concrete cover on protecting the Rft from elevated temperature.

Table 4.8: Temperature of the Rft inside conventional concrete slabs with 25, 50 and 75 mm cover thickness during exposure to 800°C for 2 hrs and air cooled for 2 hrs.

Time (min)	Concrete cover thickness (mm)		
	Rft. Temperature (°C)		
	25	50	75
0	20	20	20
10	115	89	27
20	148	99	45
30	178	104	59
40	205	121	71
50	224	135	87
60	244	150	98
70	256	166	99
80	264	182	101
90	270	201	103
100	269	210	107
110	272	222	110
120	275	232	114
130	260	214	117
140	230	196	119
150	220	180	119
160	205	163	119
170	195	147	113
180	180	130	107
190	160	119	94
200	140	108	82
210	127	97	79
220	115	86	75
230	95	79	73
240	88	72	68

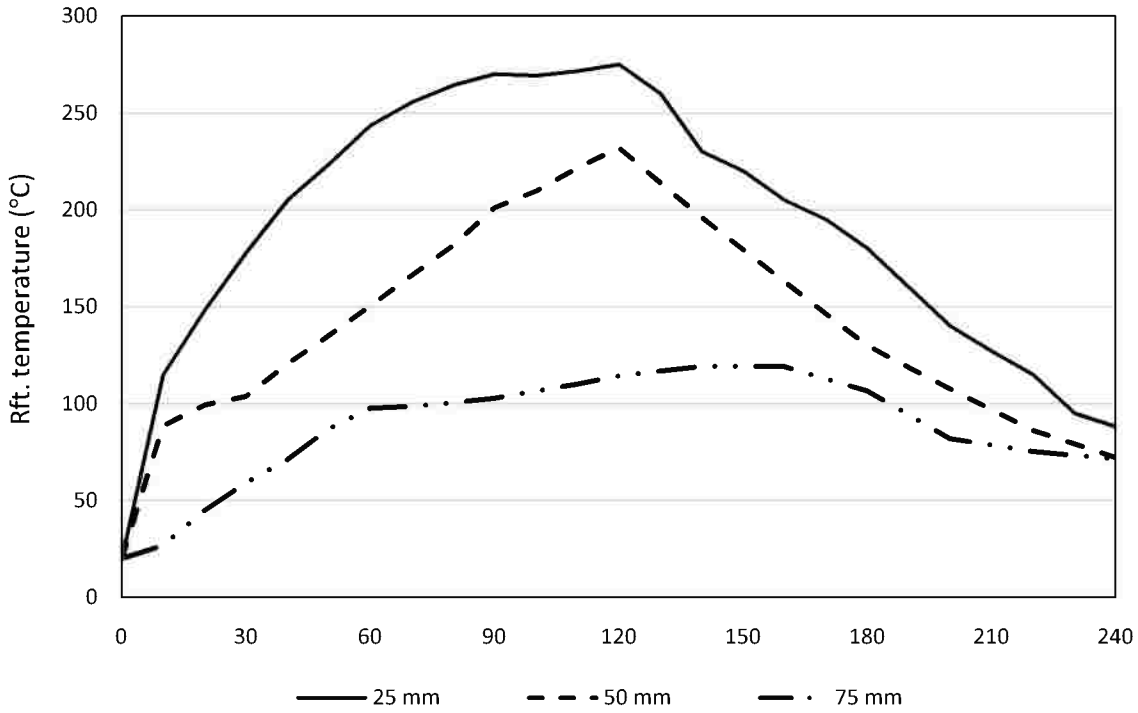

Fig. 4.12- Time-temperature curves of reinforcement insideconventional concrete slabs with 25, 50 and 75 mm cover thickness during exposure to 800°Cand cooled by air for 2 hrs.

As an important result, **Fig. 4.12-a** clarifies the temperatures distribution inside small scale slabs with 10 cm thickness after exposed to 800°C for 2 hrs, where shows that the temperature inside the concrete slabs were reduced by about 67, 72, 86 and 87% when the depth of the concrete was increased to 25, 50, 75 and 100 mm from the exposed surface.

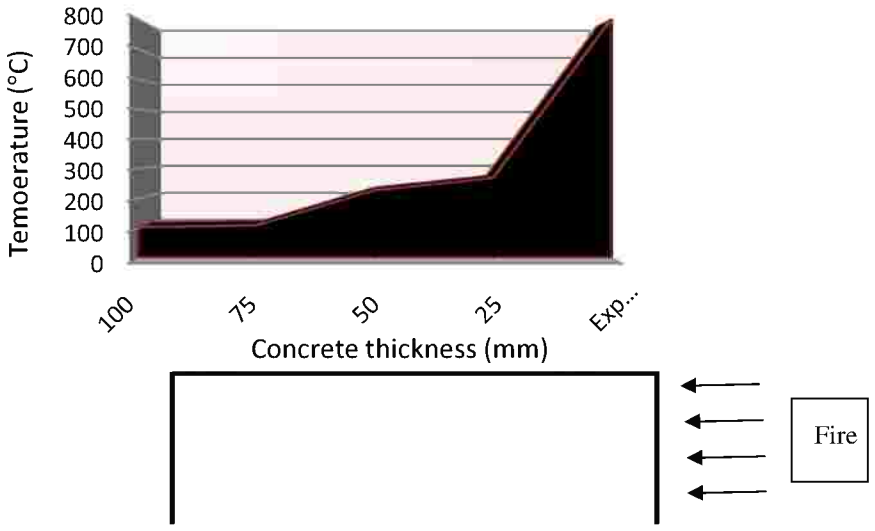

Fig. 4.12-a – Temperatureswithin slabs during fire tests carbonate aggregate (limestone) concrete.

4.1.11Deceitful pull out test results.

Pull out test results are graphically presented in **Fig. 4.13**and showthe major reduction in pull out test with the temperature increase. It seems that the experiment is very sensitive to the elevated temperatures. The pull out strength was reduced by about 60, 84 and 92% at 200, 400 and 600°C respectively.

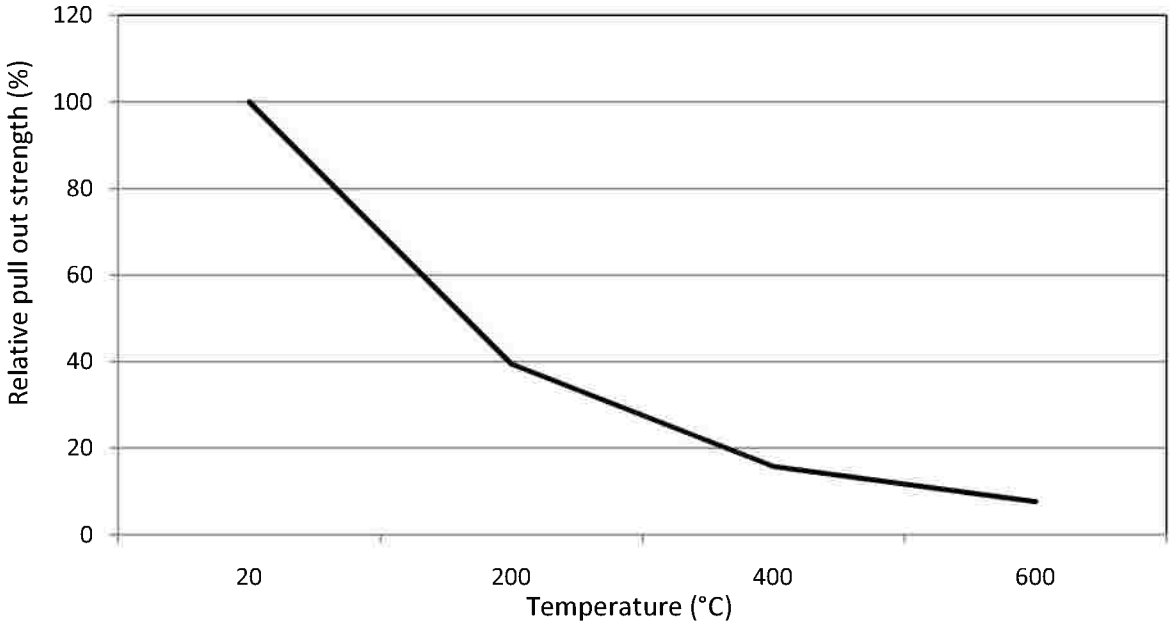

Fig. 4.13- Relative pull out strength between the Rft and the concrete cylinder at room temperature and after exposure to different elevated temperatures at 200, 400 and 600°C.

4.2 Phase 2: Results of experiments carried out on modified concrete.

4.2.1 Compressive strength test results.

The compressive strength of heated concrete specimens after air cooling regime was determined. The results which are listed in **Table 4.9**indicate the compressive strength of each mixture at 20, 200, 400and 600° C. The results show a loss in the concrete strength with increased maximum heating temperature.

Table 4.9: Compressive strength of concrete specimens at different elevated temperatures for2 hr.

Mix designation	Compressive Strength (MPa)			
	Temperature (°C)			
	20	200	400	600
M-Control	36.2	30.1	27.9	20.2
M-Silica	38.9	34.6	28.8	16.0
M-PPF	38.6	34.3	23.4	18.4
M-(Silica+ PPF)	46.5	38.9	31.7	24.5
M-(Steel.F)	49.5	41.4	41.1	24.6
M-(L.P.10R)	35.5	28.5	24.7	16.7
M-(L.P.15R)	32.0	23	19.0	13.0
M-(L.P.10A)	45.3	38.4	34.8	23.6
M-(L.P.15A)	47.0	36.0	34.0	26.0
M-(Ben.10R)	32.6	27.9	26.4	19.2

4.2.1.1 Effect of silicafume on residual compressive strength.

The effect of silicafume (10% replacement by weight of cement content) on the compressive strength of the 100 mm cubes were observed in this study. **Fig. 4.14** shows that silicafume increases the compressive and residual compressive strength at 20, 200, 400ºC by about 7, 15, 3% respectively, but reduces it by about 21% at 600ºC if it is compared to the residual compressive strength of the control mix. The silicafume increases the compressive strength until 400ºC ranges more than the control concrete. This increase may be due to the hydrothermal interaction of the silicafume particles as a result of temperature rise with the

liberated free lime during hydration reaction.After 400ºC, internal stress and thus micro and micro cracks are generated due to the heterogeneous volume dilatations of the ingredients and the buildup of vapor in the pores. Therefore, at higher temperature, especially above 400ºC, the observed specimens decrease in their compressive strength of silicafume concrete may be due to internal thermal stress generated around pores which generate micro cracks or in another way the compact microstructure is highly impermeable and under high temperature becomes detrimental as it does not allow moisture to escape, resulting in the building-up of pore pressure and rapid development of micro cracks in the silicafume concrete, hence leading to a faster deterioration of strength and occurrence of spalling**[Poon et al.2001 and Chen et al. 2004]**.Thus, it can be said that the silicafume concrete is more sensitive to high temperatures than ordinary cementconcrete. The previous results are compatiblewith **[Morsy, 2010]**.

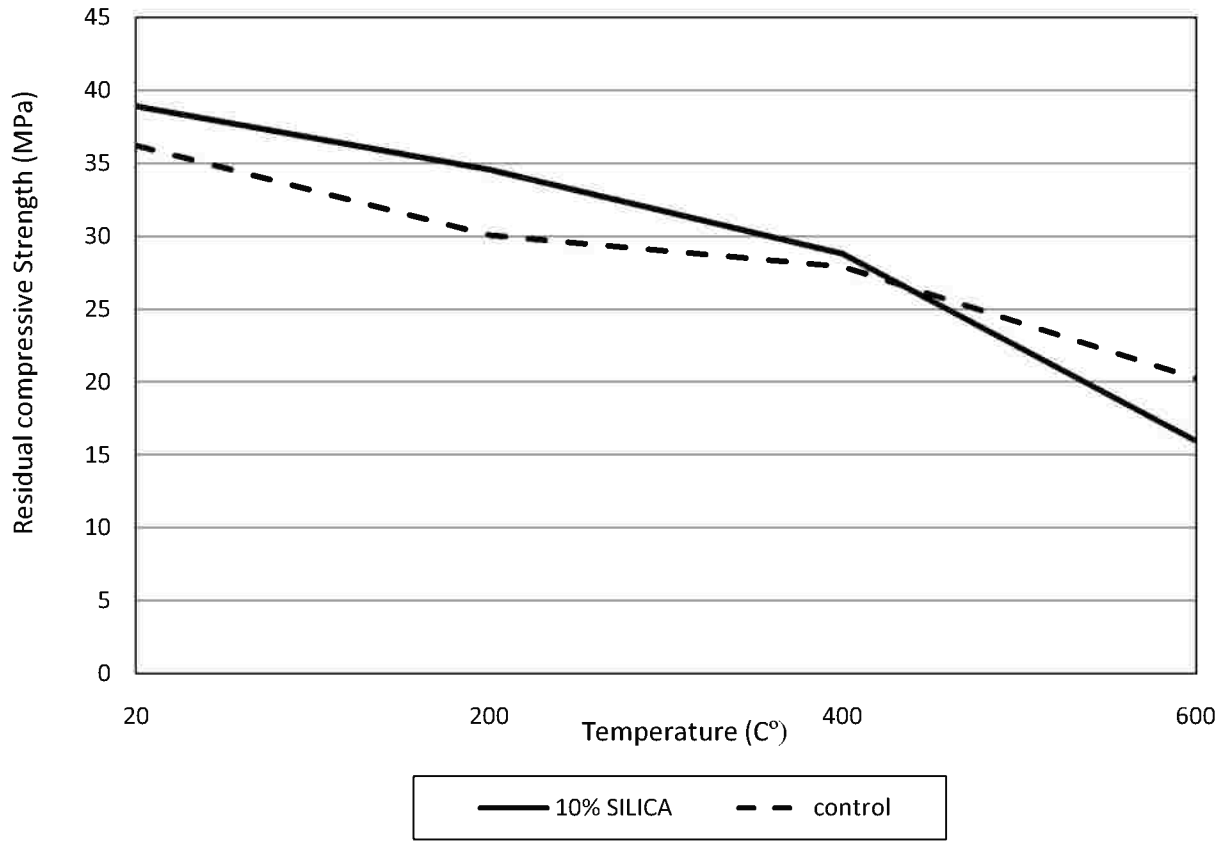

Fig. 4.14 – Residual compressive strength of control and 10% silicafume concrete at room temperature and after being exposed to elevated temperature at 200, 400 and 600°C.

4.2.1.2 Effect of polypropylene fibers on residual compressive strength.

From the common researches such as **[Ramamurthy et al, 2009] and [Cheon, 2005]**,It was decided to take 0.90 kg/m³ polypropylene fibers as additive to conventional concrete in this study.From **Fig. 4.15** it can be seen that the addition of 0.90kg/m³ polypropylene fibers increases the compressive strength at 20, 200ºC by about 6, 14% and reduces it by about 16, 9% at 400, 600ºC compared to the compressive strength of the control mix at the same temperature The improvement at 200ºC is attributed to the amount of water vapor that escapes freely through the pathways formed by the melting of the PP fibers between 165 and 170ºC and getting out the of surface of the concrete through the pores so reducing the water vapor pressure. Furthermore, the decomposition of the PP fibers may reduce the results of thermal incompatibility between aggregates and cement paste due to the provision of more free space which acts as a thermal shock absorber. Also **[Kalifa et al. 2001]** suggested that the cement matrix is able to absorb the melted PP, despite the large size of the molecules compared to diameter of paste pores. The reduction in residual compressive strength of PP fibers at 400 and 600ºC may be ascribed to the formation of a multifilamentstructure due to the insufficient diffusion of this amountof PP fibers in the mixture**[Lankard, et al. 1971].** It should be noted that the polypropylene fibers do not influence the physico-chemical changes.

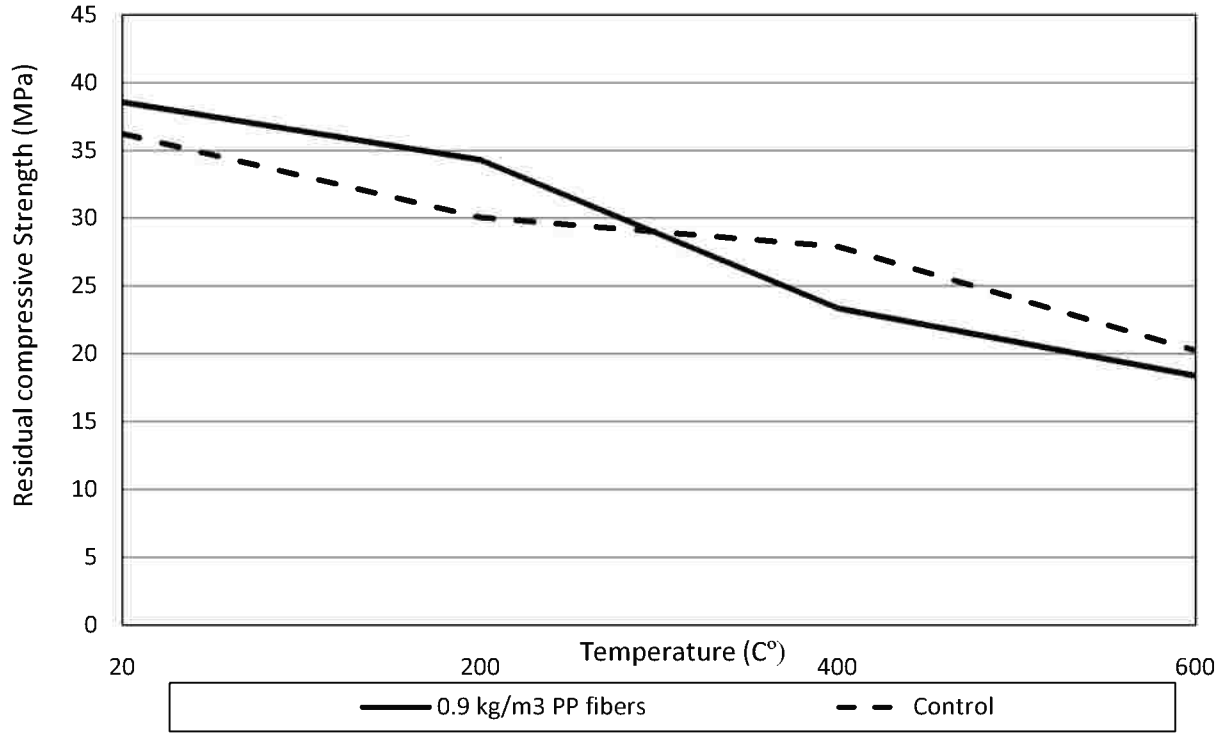

Fig. 4.15 – Residual compressive strength of control and polypropylene fiber concrete at room temperature and after being exposed to elevated temperature at 200, 400 and 600°C.

4.2.1.3 Effect of silicafume with polypropylene fibers on residual compressive strength.

The effects of the addition of polypropylene fibers to silicafume concrete on the enhancement of its properties were studied in many researches in the last decade. **Fig. 4.16**illustrates that the addition of polypropylene fibers to blended concrete increase the compressive strength by about 28,29,13 and 21% respectively comparing with the control mix at 20, 200, 400 and 600ºC. In the same time the silicafume with polypropylene fibers mix shows enhancement in the compressive strength when compared to silicafume concrete mix at all studied elevated temperatures. This confirms that the polypropylene fibers can remarkably improve the resistance of the blended concrete subject to temperature by reducing its explosive spalling, its surface cracking and deterioration as reported by**[Min et al. 2004].**

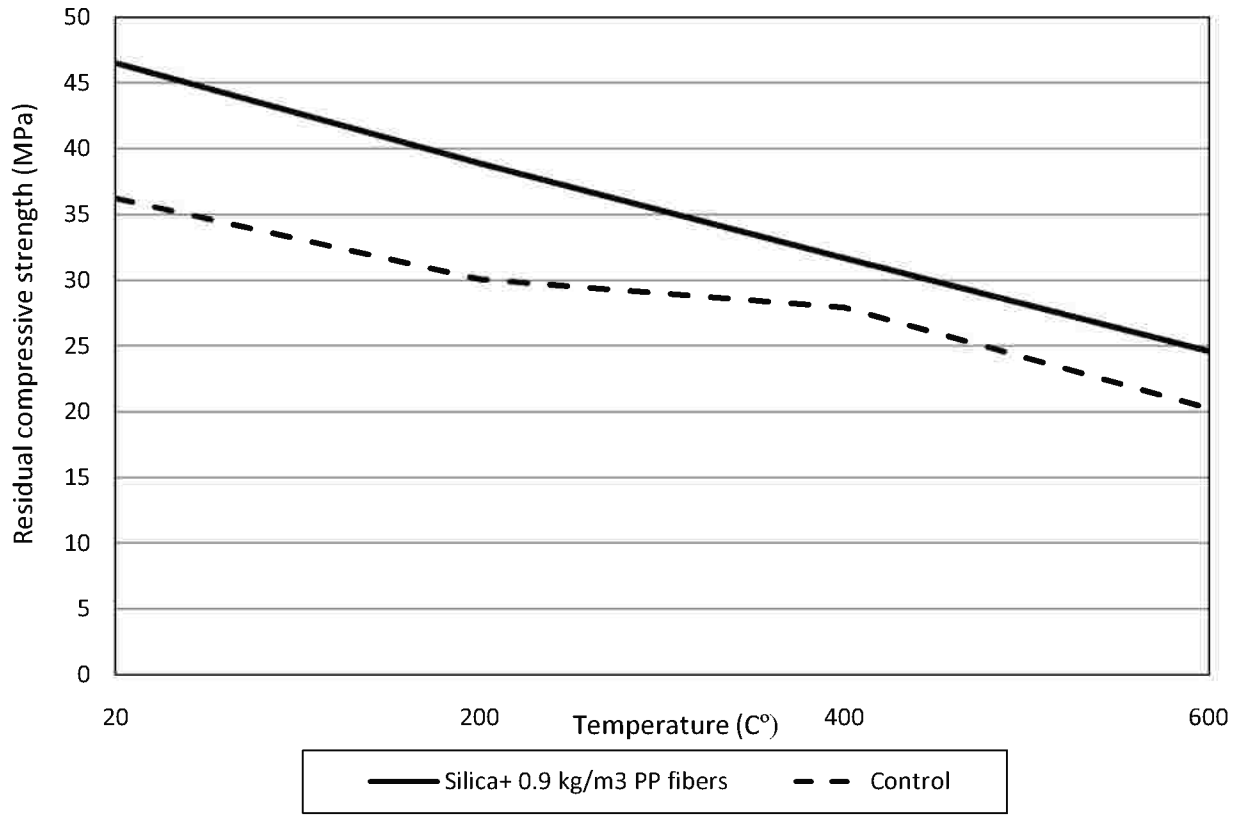

Fig. 4.16– Residual compressive strength of control and (silicafume + polypropylene fiber) concrete at room temperature and after being exposed to elevated temperature at 200, 400 and 600°C.

4.2.1.4Effect of steel fibers on residual compressive strength.

Steel fibers are used instead of ordinary steel reinforcement or in addition to reinforcing bars. The effect of steel fiber on the compressive strength of concrete under elevated temperatures

isinvestigated in this study. **Fig. 4.17**shows that the presence of the steel fibers increases the residual compressive strength when compared to the control mix by 37, 38, 47 and 22% at 20, 200, 400 and 600ºC.This result is compatible with **[A. Lau and el, 2006],** which illustrates that the presence of steel fibers in concrete helps to slow down the strength loss at elevated temperatures.

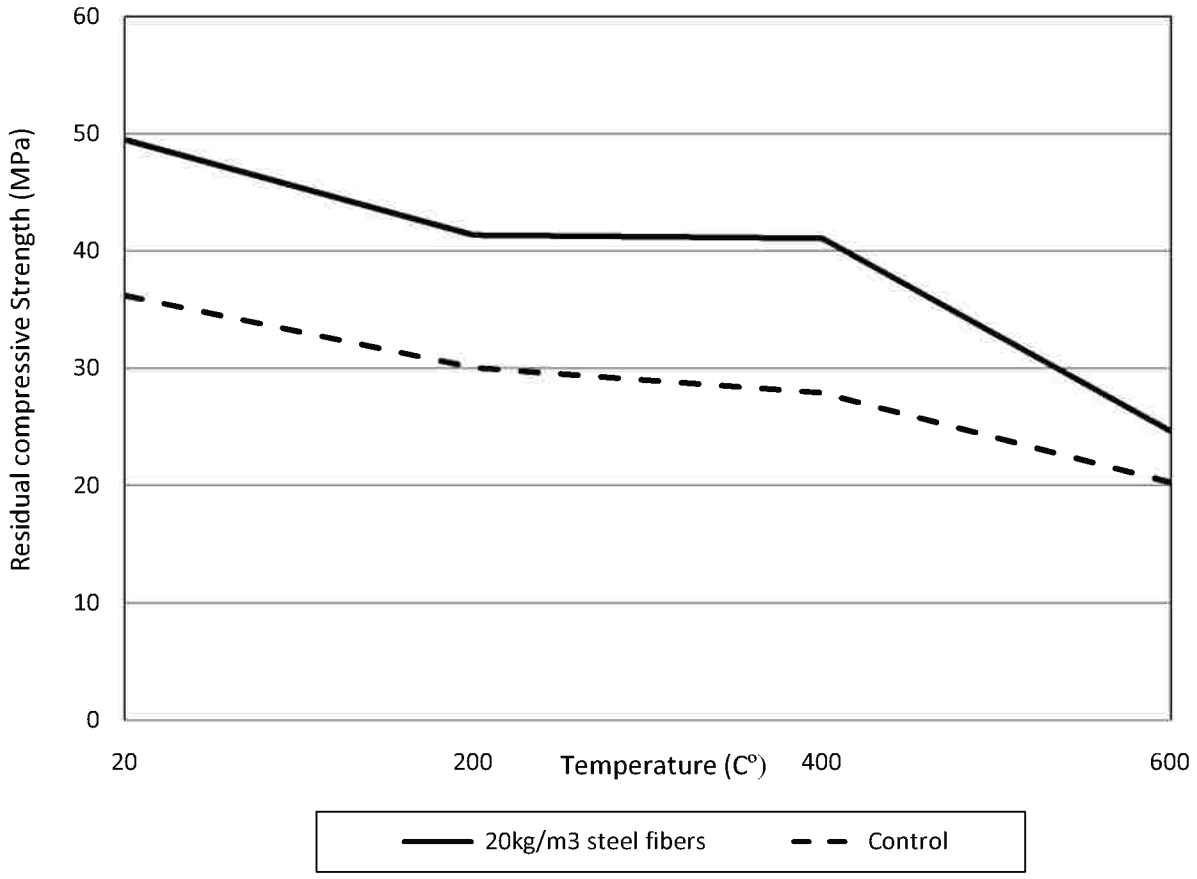

Fig. 4.17– Residual compressive strength of control and steel fiber concrete at room temperature and after being exposed to elevated temperature at 200, 400 and 600°C.

4.2.1.5 Effect of limestone powder on residual compressive strength.

Evidently from **Fig. 4.18,** it is clear that the use of L.P as a cement replacement reduces the residual compressive strength of the specimens when compared to the control mix. The obtained percentages of reduction were about 2, 5, 11 and 18% for M-(L.P10R) and 12, 23, 34 and 35 % for M-(L.P 15R) comparing to M-C at different studied temperature. The replacement of portland cement by limestone powder caused a reduction in the compressive strength that can

be explained as a result of the cement dilution effect. It is indicated that the filler effect of limestone cannot compensate for the dilution effect of cement at all stages.

On the other hand, the addition of limestone powderto the cement content increases the compressive strength by about 25,21, 20 and 24% for M-(L.P 10A) and 30,21,24 and 31% for M-(L.P 15A) at 20,200,400 and 600ºC respectively comparing to M-C at the same temperature. During hydration of portland cement some calcium carbonate reacts with the alumina phases of cement to form carboaluminates and delays or impedes the ettringite-monosulphate transformation **[Menendez et al. 2003]**. This leads to the stabilization of the ettringite and will result in an increase in the total volume of the hydration products, which might result in a decrease in porosity and thus an increase in strength. Also this increase in compressive strength may be attributed to the fact that the limestone fulfills the pores between cement particles.

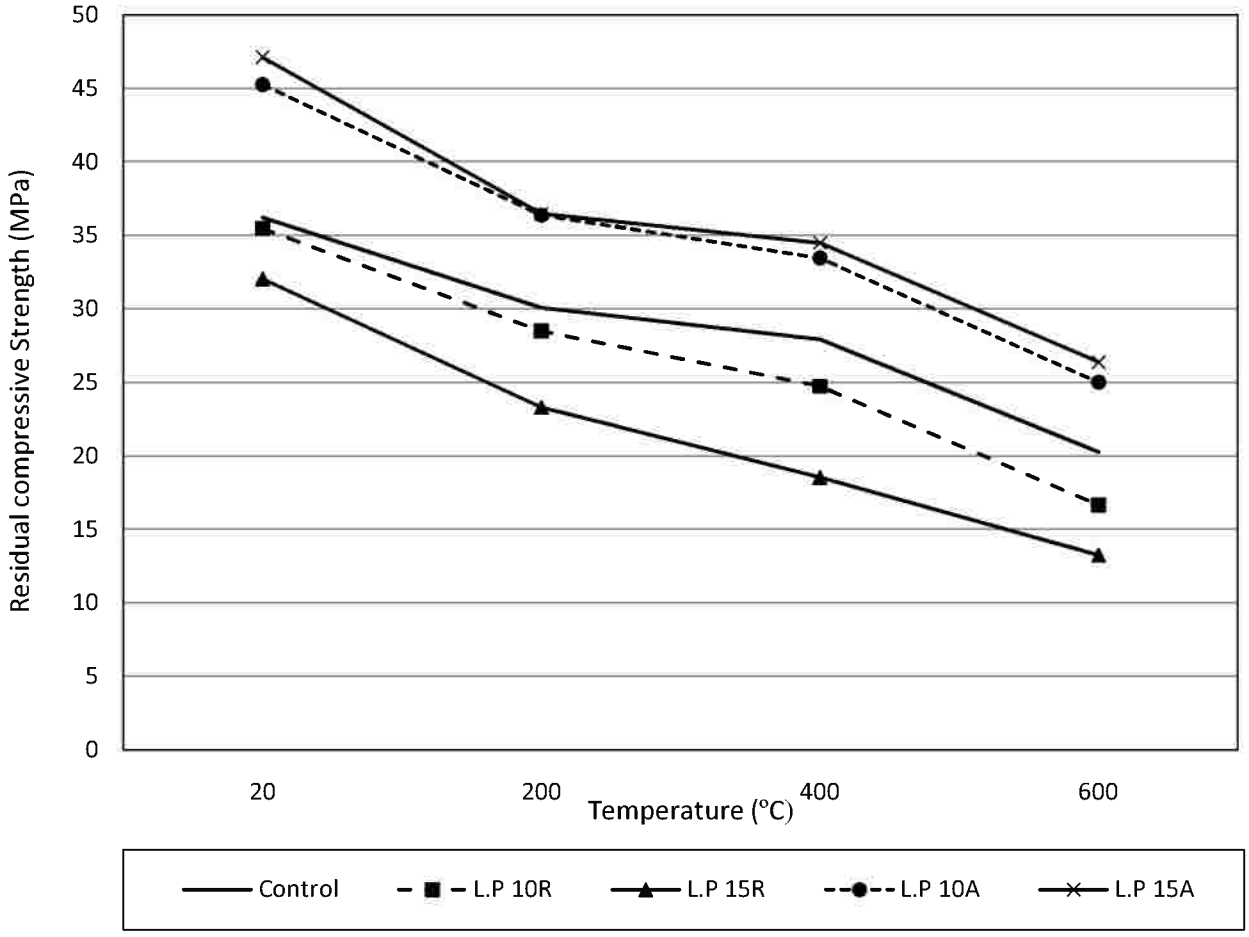

Fig. 4.18– Residual compressive strength of control and limestone powder concrete at room temperature and after being exposed to elevated temperature at 200, 400 and 600°C.

4.2.1.6 Effect of bentonite on residual compressive strength.

The effect of bentoniteas 10% of cement content as a replacement by massis illustrated in **Fig. 4.19**. (M-Ben.10R) has a residual compressive strength less than M-C at all studied elevated temperatures. The compressive strength is reduced by 10, 7, 5 and 5% at 20,200,400 and 600° C respectively. Also the M-(Ben.10R) cubes are clearly loose at elevated temperature. This result could be attributed to the increase in the alkali metal concentrations in the prepared mixture at the expense of alumino-silicates, which could affect the whole integrity of the pastes **[El-Kamash, 2006].**

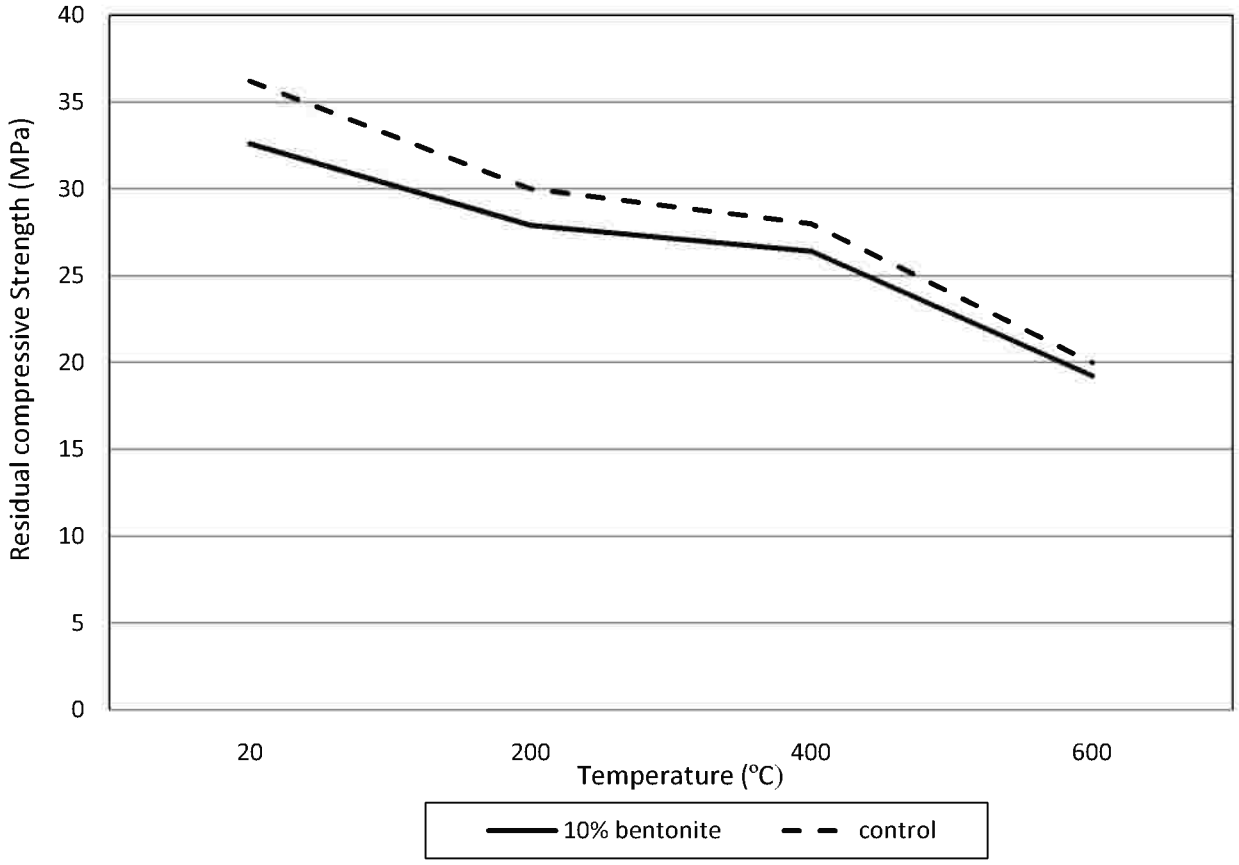

Fig. 4.19– Residual compressive strength of control and bentonite concrete at room temperature and after being exposed to elevated temperature at 200, 400 and 600°C.

4.2.2. Flexural strength test results.

Analysis of the fourpoints bending elevated temperature flexural strength of all mixtures is presented in **Figs.4.20 (a, b, c, and d)**. Theresults indicate a reduction in flexural strength for all mixtures with increasingtemperature.

Flexural strength of silicafume concrete at room temperature is more than the conventional concrete and this may be due to the fact that when water is added to cement, hydrationoccurs forming two products, as shown below:

OPC + H_2O CSH (Calcium silicate hydrate) + $Ca(OH)_2$.

In thepresence of Silicafume, the silicon dioxide will react with the calcium hydroxide to produce moreaggregate binding CSH as follows:

$Ca(OH)_2 + SiO_2 H_2O \rightarrow$ CSH.

The reaction reduces the amount of calcium hydroxide in theconcrete. The weak calcium hydroxide does not contribute tostrength. When combined with carbon dioxide, it forms asoluble salt, which will leach through the concrete causingefflorescence, a familiar architectural problem.

Experimental results of the effect of limestone powder, as a replacement and an additive to cement content, on the flexural strength development are investigated in this study.**Fig. 4.20**shows the reduction in the flexure strength of beams when exposed to elevated degree of temperature up to 600°C. As shown in the **Fig.4.20,**the flexural strength decreases as limestone fines ratio is increasedas a cement replacement by mass up to 15% at all the studied elevated temperature values. The performance of limestone fines as a cement additive is better than thatof the conventional concrete at all elevated degree of temperature up to 600°C as illustrated in **Fig.4.20**.It can be observed that the addition of limestone fines to the conventional concrete increases the flexural strength by about 24, 9, 20 and 40% for M-(L.F10A) and by about 29, 31, 35 and 60% for M-(L.F15A) at the same temperature, thus, as the limestone fines increase the flexural strength increase up to 15% as additive to cement content. This may be attributing to that the limestone particles fulfill the pores between the cement particles without any dilution on the cement content, so enhances the microstructure of the specimens. Polypropylene fibers and steel at flexural, the presence of ductile fibers in the matrix significantlyaltered brittle behavior by limiting rapid crack propagation and unstable failure. The presence of fibers notonly slows down the cracks propagation with increasing loads, but also allows a stress transferacross (the lips) the cracks openings. This effect allows the composite to have a postcrackingresistance and thus withstand deformations much larger than the matrixalone.Analysis of the 4 point bending flexural test results indicates that throughout theentire temperature range, the strength of steel fiberconcrete is significantly greaterthan that of the standard concrete and polypropylene fiberconcrete. The thermal damage of steel fiberconcrete is less than the standard mortar.In effect, the steel fibers do not limit physico-chemical changes but control the thermalcracking and

limit the spread of cracking during mechanical testing.As previously noted, at 200°C, the polypropylene fiberconcrete degrades nearly at the same rate ofthe ordinary concrete; but in excess of 400°C, this positive effect disappears.

The polypropylene fibers can reduce cracking by controlling the vaporpressures, but do not influence the physico-chemical changes. This suggests that thetensile strength is more sensitive to cracking than physico-chemical changes whilethe compressive strength is sensitive to these two phenomena.

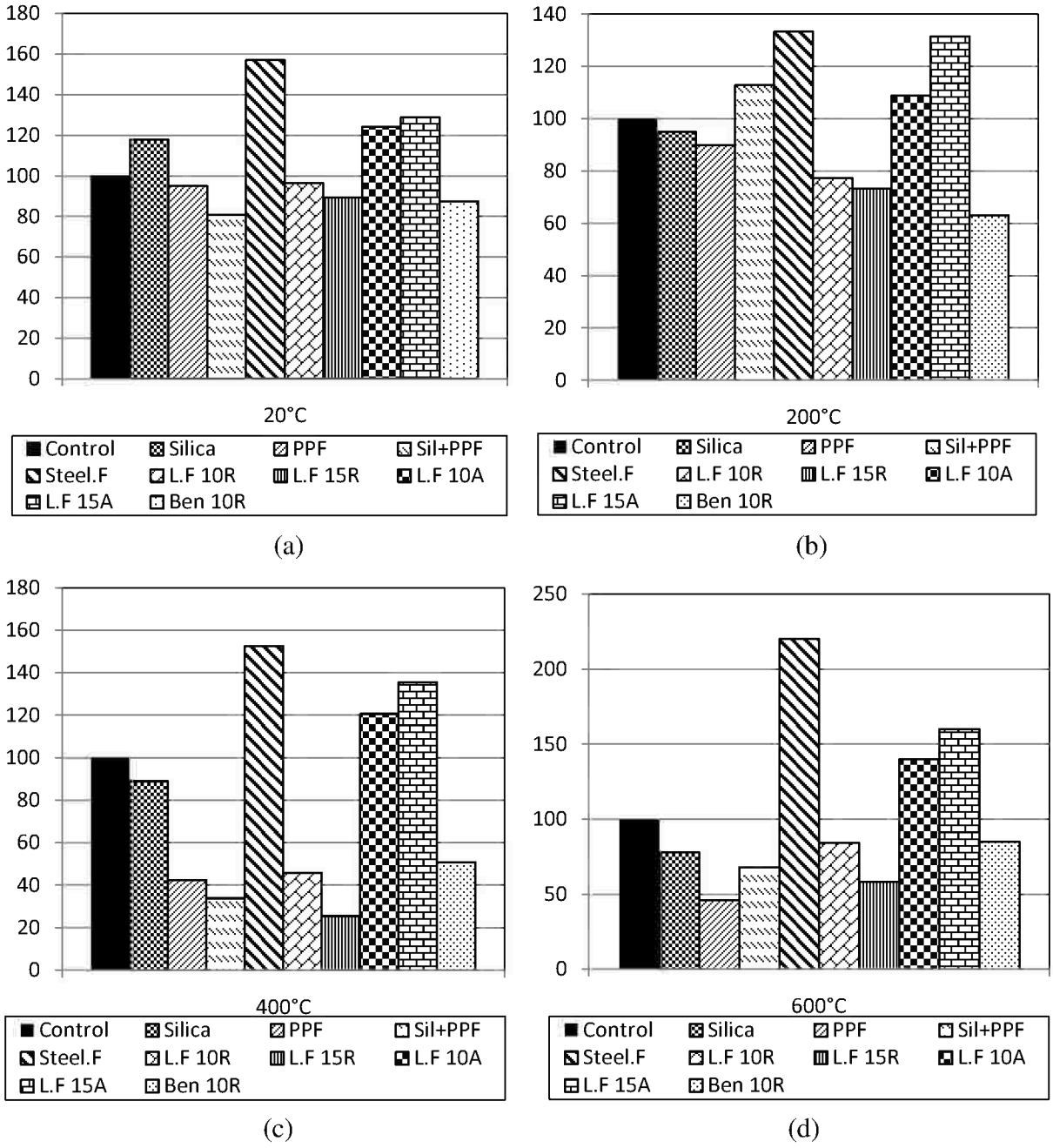

Fig. 4.20–Flexural strength of all concrete mixtures beams at 20, 200, 400 and 600°C.

4.2.3. Concrete weight loss.

The average relative weight loss of three cubes at 20, 200, 400 and 600ºC of all mixtures are recorded in **Table 4.10**and compared to that of the control mix.At the beginning and in general for all mixtures, as seenin **Figs. 4.21, 4.22** theunitweightsdecreasewithincreasing temperature. Weightreductiontakesplaceinthespecimensdue tothereleaseofwater.Becauseofthereleaseofboundwater from thecementpaste,airvoidsareformedintheconcrete.The structural integrityofthespecimensdeterioratesasconfirmedby the increaseinweightreductionwithincreasedtemperatures.The reduction inweightconfirmsthelossofmassbytheconcrete material andtheincreaseintheproportionofairvoids. It can be seen from the **Fig. 4.21** thatthe unit weight of all mixtures except M-(Steel.F) is less than M-C at 20º C. This reduction is attributed to that silicafume, polypropylene fibers, limestone powder and bentonitewhich has a lower bulk density than ordinary portland cement.It can be seen from **Figs. 4.22 (a,b,c)** that the 10% silicafume concrete as cement replacement by mass exhibits a weight loss more than the control mix.**[Balakrishnaiah.D1, et al 2013]**illustrates that as the temperature increase as all the hydrated phases including C-S-H and $Ca(OH)_2$ appeared to have amorphous structures at this temperature instead of their characteristic crystaline structures especially at 600ºC which was considered the critical temperature.

The weight loss of polypropylene fibers concrete and steel fibers concrete is less than that of the control mix. The reduction in weight loss of steel fibers concrete may impute to the fact that the steel fibers inside the specimens were still firm without any loss.The concrete mixtures containing limestone powder exhibit less mass loss than the normal concrete this is so clear at 400°C and 600°C as shown in **Figs. 4.22 (b,c),** this is attributed to the lower porosity of concrete mixtures containing limestone powder than normal concrete **[Lothenbach, et al 2008]**. Also limestone powder mainly constitutes of $CaCO_3$ which decomposes at 600ºC. From **Figs. 4.22 (b,c)** it can be noticed that the rate of weight loss of specimens containing10% bentonite as cement replacement has been reduced at 400 and 600ºC. The weight loss is 6.51 and 6.65% respectively, which means that it has a weight loss less than the control mix. This may attribute to the fact that the bentonite clay has a high resistance to elevated temperatures**[Inglethorpe,et al 1993].**

Table 4.10: Weight Loss (%) of allconcrete mixtures at 20, 200, 400 and 600º C.

Mix designation	Weight loss (%)			
	Temperature (ºC)			
	20	200	400	600
M-C	0	4.0	6.6	7.9
M-Silica	0	6.1	7.7	8.5
M-PPF	0	5.2	6.1	7.0
M-(Silica+ PPF)	0	5.3	8.4	9.2
M-(Steel.F)	0	4.0	5.8	7.6
M-(L.P.10R)	0	5.5	6.2	7.1
M-(L.P.15R)	0	5.4	6.0	7.4
M-(L.P.10A)	0	3.5	6.3	7.7
M-(L.P.15A)	0	3.0	4.6	5.8
M-(Ben.10R)	0	5.0	6.5	6.7

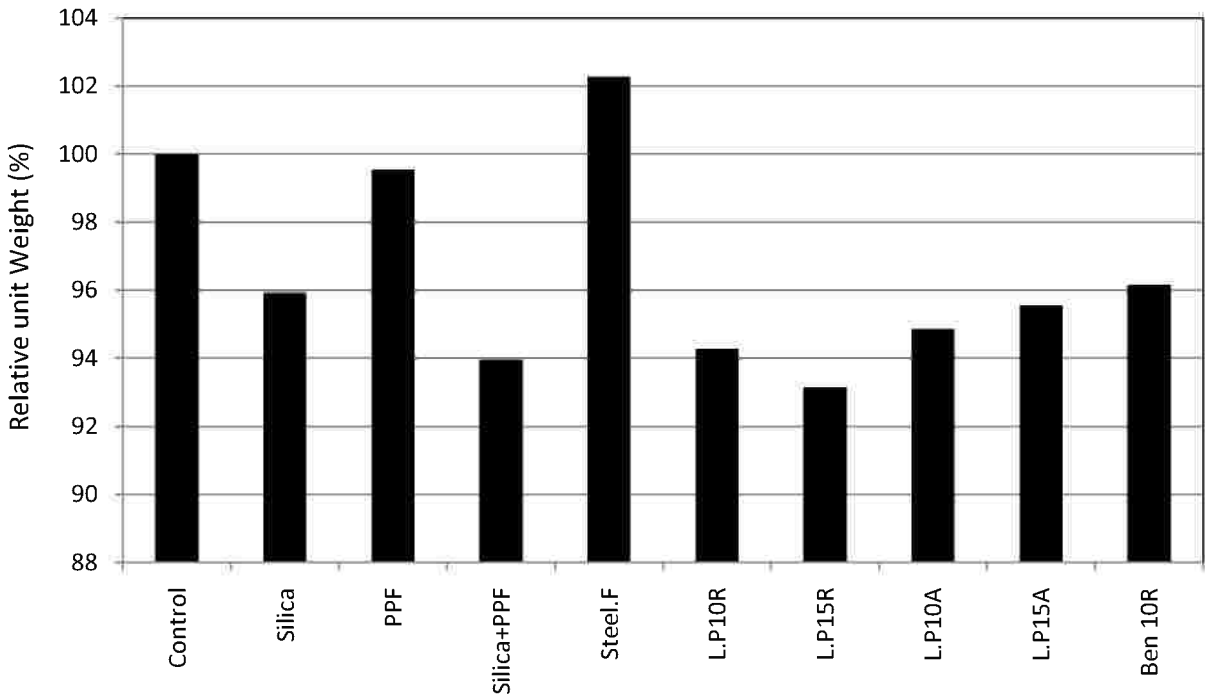

Fig. 4.21 - Relative unit weight of all mixtures at 20ºC.

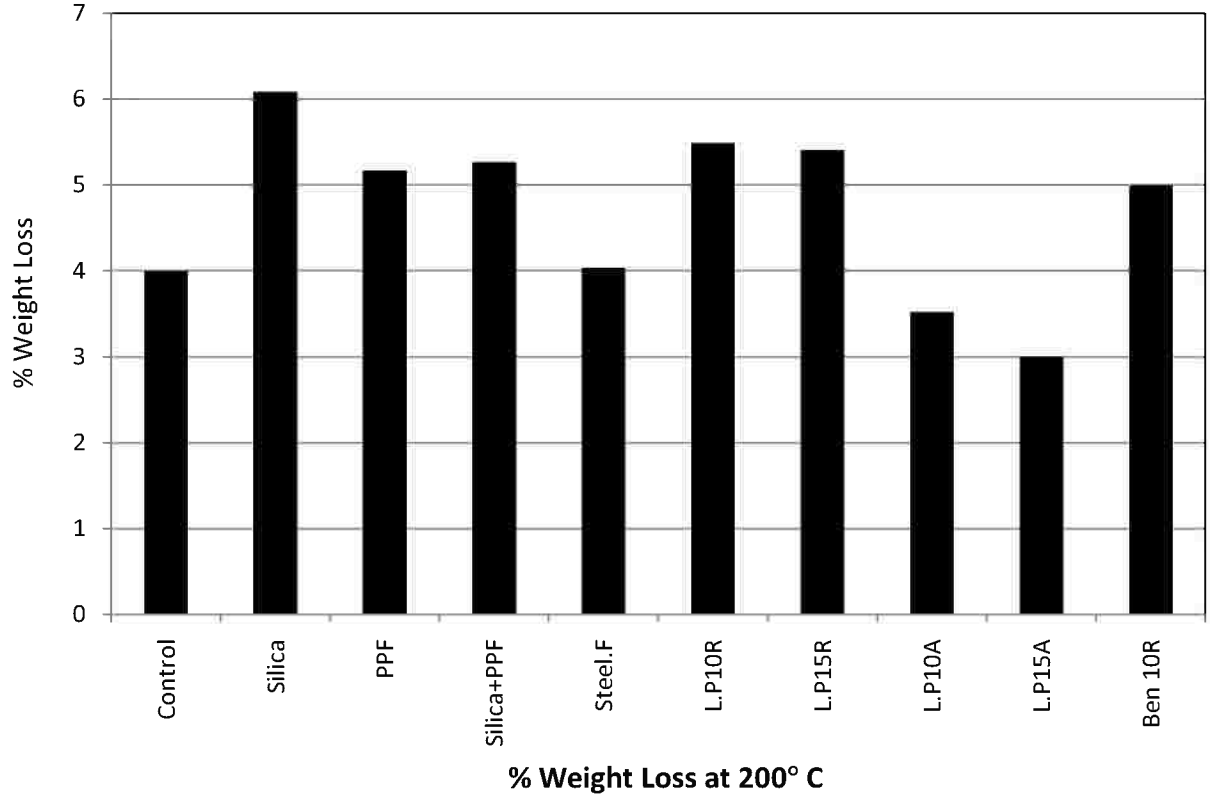

(a)

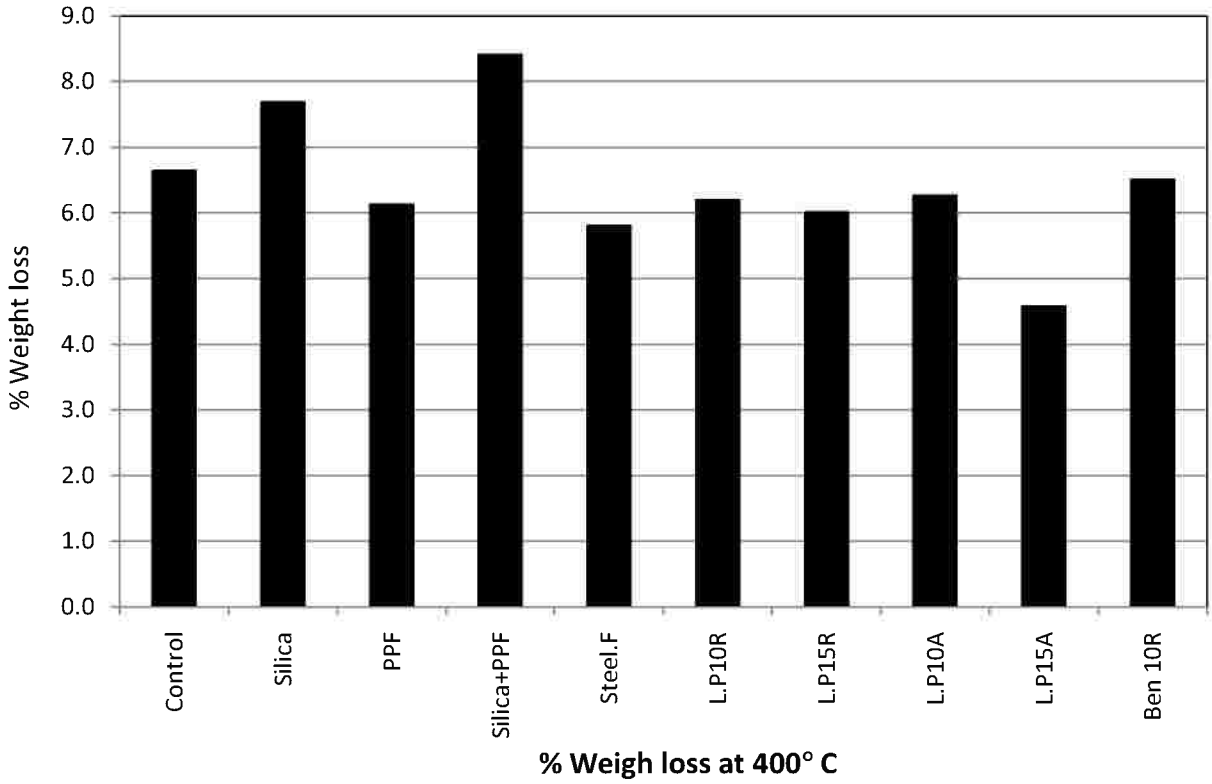

(b)

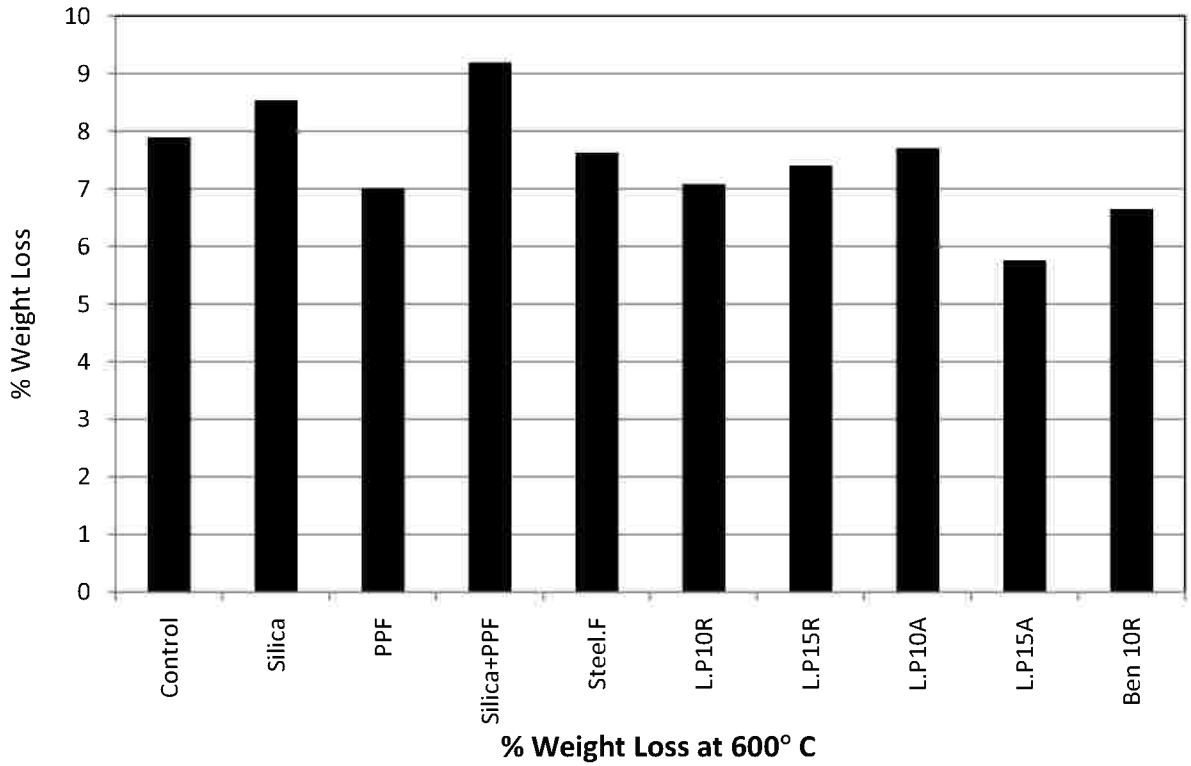

(c)

Fig. 4.22 -% Weight loss of the mixtures at a) 200ºC b) 400ºC c) 600ºC.

4.2.4. Scanning electron microscope (SEM).

The scanning electron microscope(SEM) of the mixtures was carried out on specimens at 20, 200, 400 and 600ºC. In this study fragments of specimens broke off and SEM was carried out.

4.2.4.1SEM on silicafume concrete mix.

The concrete specimenswith 10% silicafume as cement replacement by mass were observed by SEM. Samples were taken fromthe surface of the destroyed specimens to observethe concrete's microstructure. Dense concretematrix-aggregates are visible in**Fig. 4.23-a**whichreveals dense structure of calcium silicate hydrates (C-S-H) due to the reaction between silica ions and calcium hydroxide forming additional C-S-H as described in the following equation:

$$Ca(OH)_2 + SiO_2 + H_2O \Rightarrow C\text{-}S\text{-}H$$

So the SEM micrographs which are obtained for the pozzolanic concrete products obtained after 28 days of hydration were mainly calcium silicate hydrates and calcium hydroxide as

shown in **Fig. 23-a**, this can be clearly understood from the microstructure of the hardened blended concrete. The blended concrete is richer with C-S-H andettringiteat 200ºC as described in **Fig. 4.23.b.** Also an observation should be deserve from **Fig. 4.23-d** that the cracks' width of silicafume concrete at 600ºC (about 0.9 µm) are more than the cracks' width in the control mix.Thus, this result confirms the role of that the densesilicafume microstructure increases the spalling and micro cracks in concrete specimens when exposed to elevated temperatures.

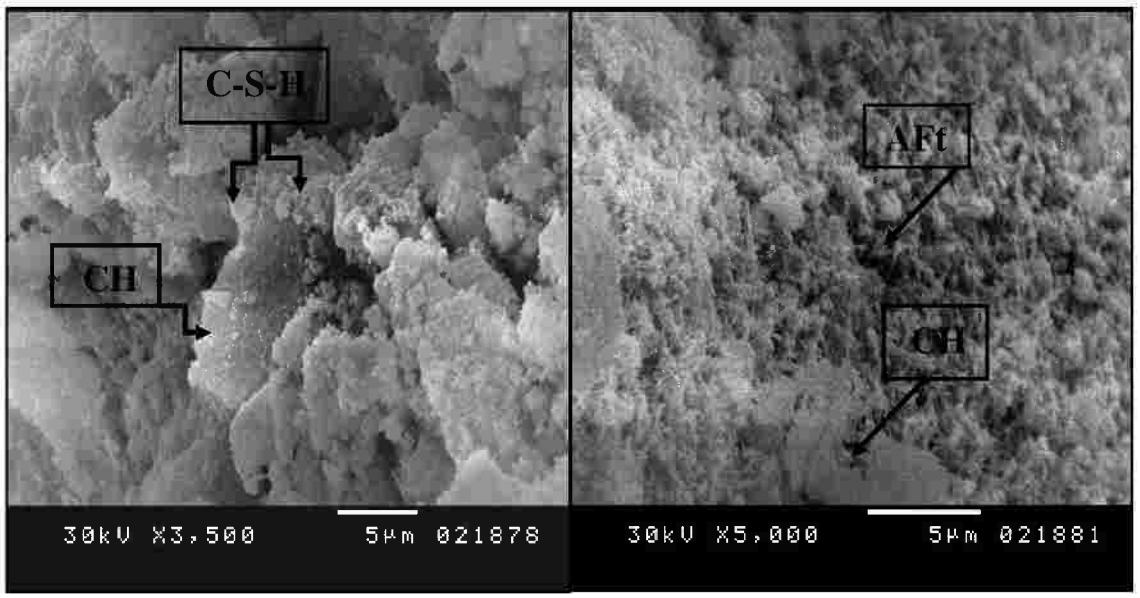

a) 20°C b) 200°C

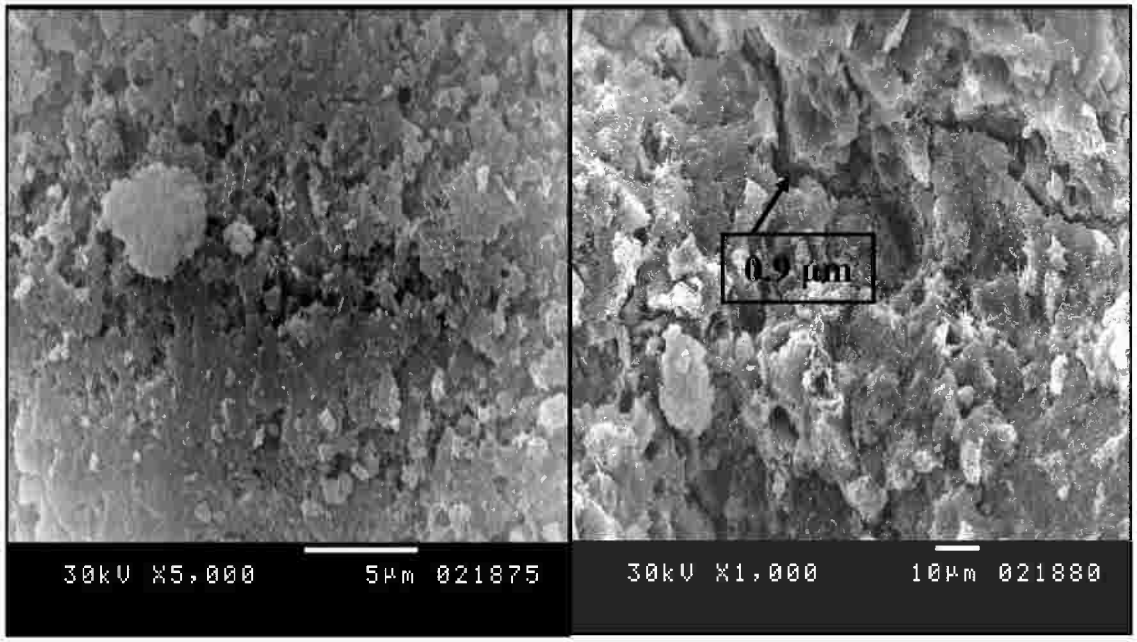

c) 400°C d) 600°C

Fig.4.23 - SEM images of concrete with 10% silicafume as cement replacement at a) 20ºC b) 200 c) 400 and d) 600ºC.

4.2.4.2 SEM on polypropylene fiber concrete mix.

Images are taken to polypropylene fibers concrete at 20, 200, 400 and 600ºC. The cohesion between polypropylene fibers and the matrix is clearly observed in **Fig. 4.24.a**. The melting polypropylene fiber appears in **Fig. 4.24.b** at 200ºC which in agreement with that the PPF is melted at about 170ºC, whilst **Fig. 4.24.c** shows no mark of polypropylene fibers after being exposed to elevated temperaturedegree at 400ºC where the PPF is evaporated at about 340ºC. The results of recent researches have shown the great influence of the presence of polypropylene fibers on the spalling behavior of the concrete under fire loading. The impact of polypropylene fibers in reducing the micro-cracksclearly came out as shown in **Fig. 4.24.d** after being exposed to 600ºC for 2 hrs. The micro-cracks were reduced due to bridging-effect that limits the propagation of cracks. Whilst, as a result of polypropylene fibers evaporation, **Fig. 4.24.d** shows that the specimen has small aimless channels that reduces the residual compressive strength of the polypropylene fibers concrete.

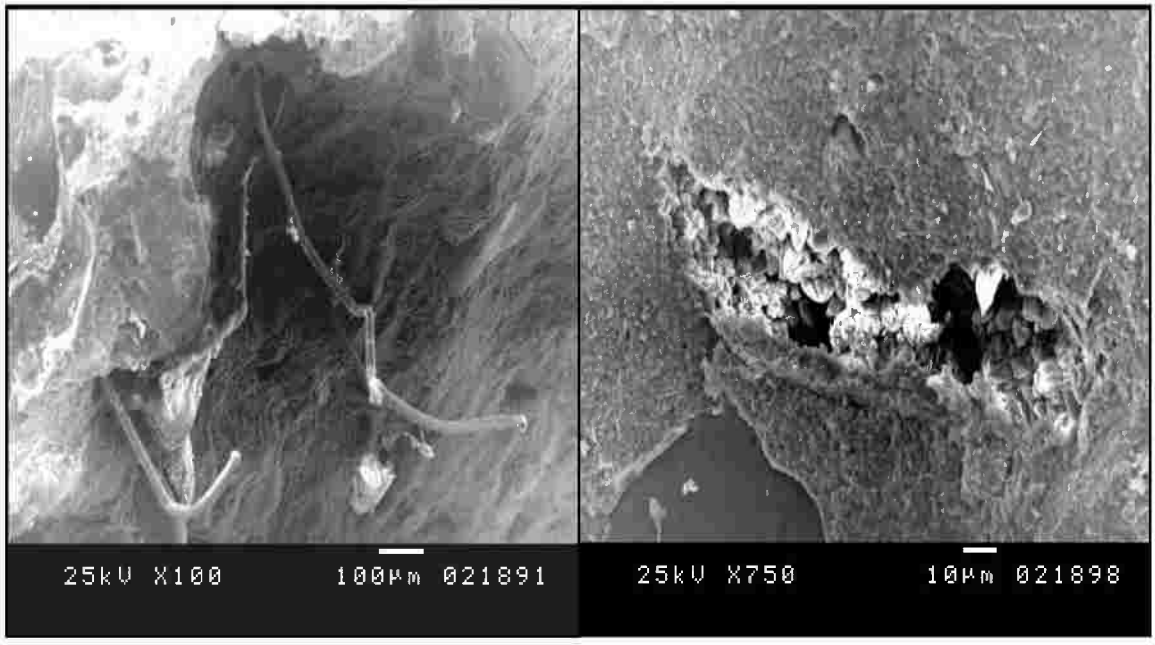

a) 20 b) 200

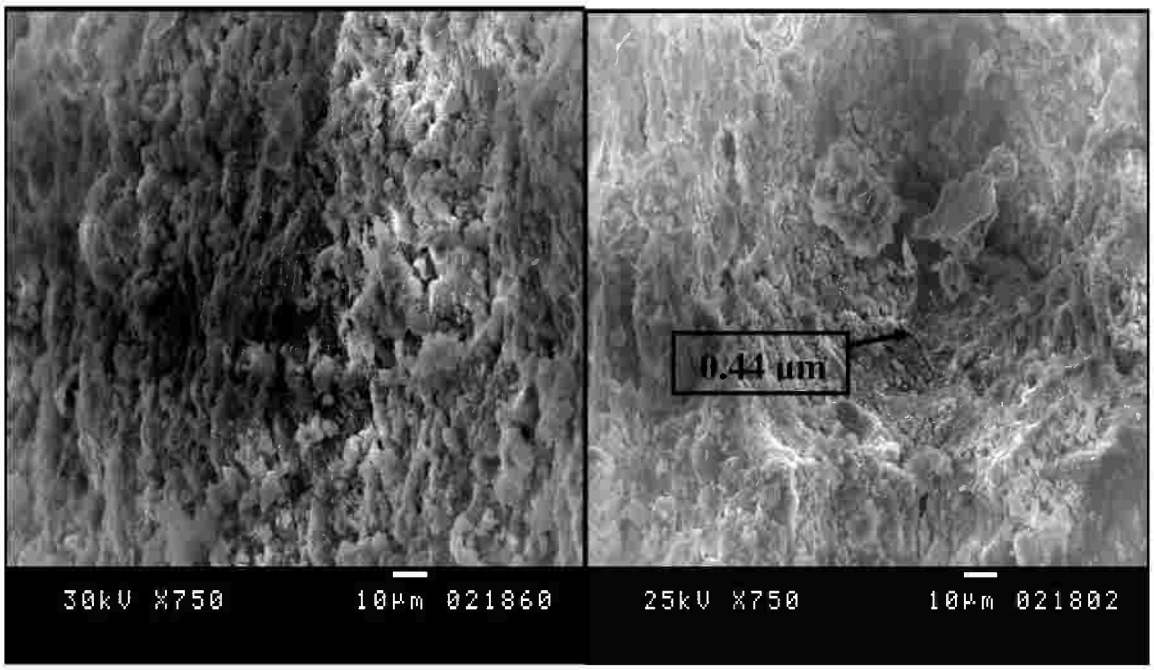

c) 400 d) 600

Fig. 4.24 - SEM images of concrete with 0.90 kg/m³ polypropylene fibers at a) 20ºC b) 200 c) 400 and d) 600ºC.

4.2.4.3 SEM on limestone concrete mixes.

At the beginning, SEM is carried out on raw materials of limestone powder as shown in **Fig.4.25**. In this study fragments of specimens are broken off and SEM was carried out on M-(L.F 15R) and M-(L.F 15A) at 20, 200, 400 and 600ºC.

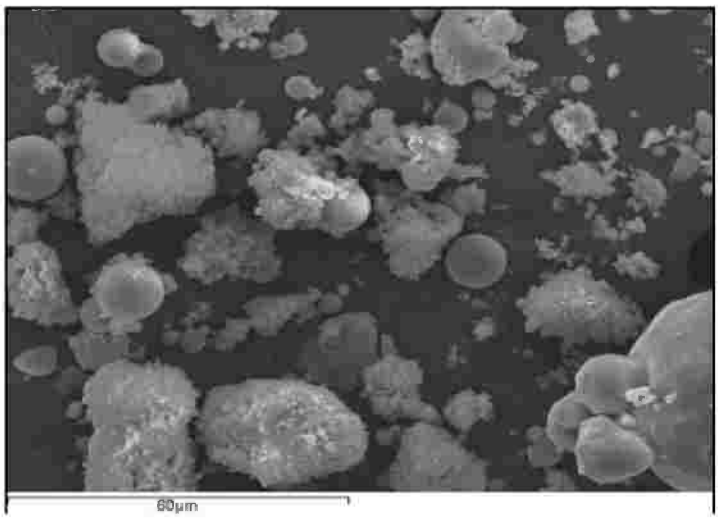

Fig.4.25 -Raw material of limestone powder under SEM.

SEM of the concrete with 15% limestone as additive shows dense concrete when compared to the control mixture and 15% limestone concrete as cement replacement. This is as a result of the limestone particles filling the pores between cement and aggregate and the formation of monocarboaluminates. Also it can be observed that a very goodadhesion between the matrix and the fine aggregate as shown in **Fig. 4.26-a.**M-(L.P 15R) and (M-L.P 15A) at 200ºC exhibitplenty in all hydrated products and unreacted $CaCO_3$ (marked ''C'')large crystals are observed in limestone concrete as presented in **Fig.4.26-b**. At 400ºC and from **Fig. 4.26-c,** the limestone concrete mixturesare still without obvious cracks and the image of 15% limestone as additive renders wealth of $Ca(OH)_2$.On the other hand the limestone particles became more manifested in limestone concrete at 600ºC, whether M-(L.P.15R) or M-(L.P15A) as clearly obvious in **Fig. 4.26-d**.

M-(L.P15R) M-(L.P15A)

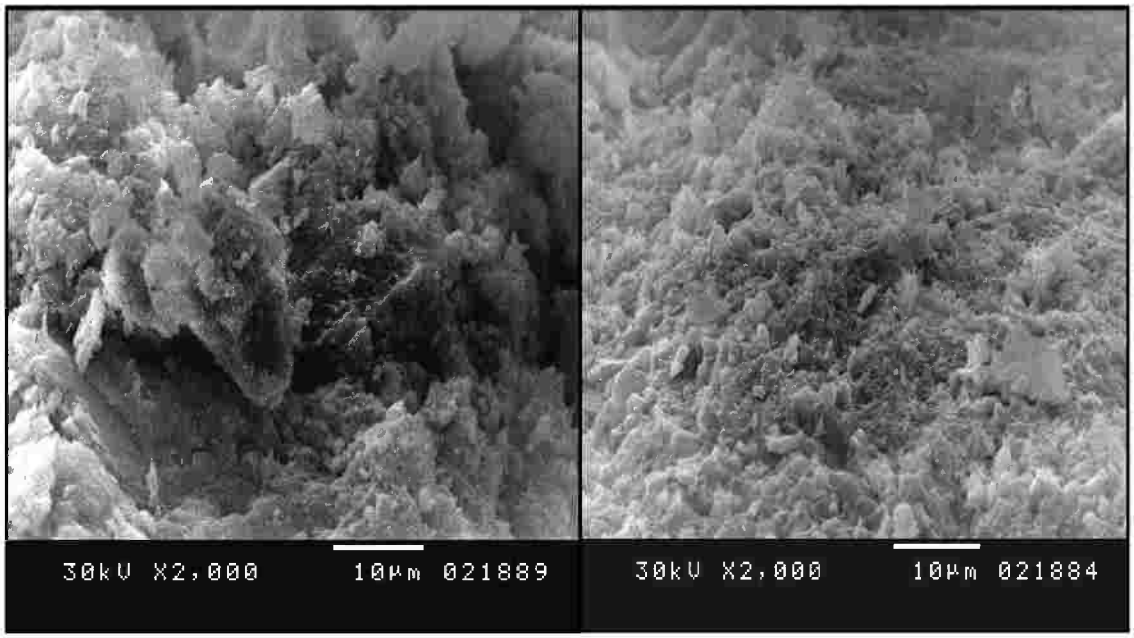

a) 20

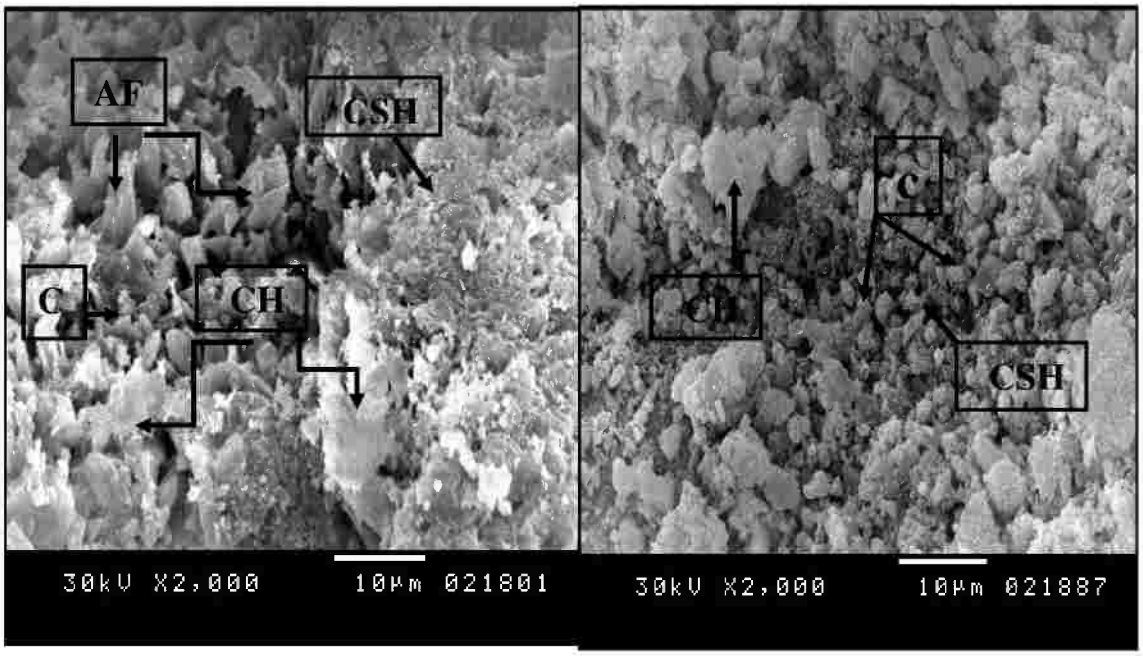

b) 200° C

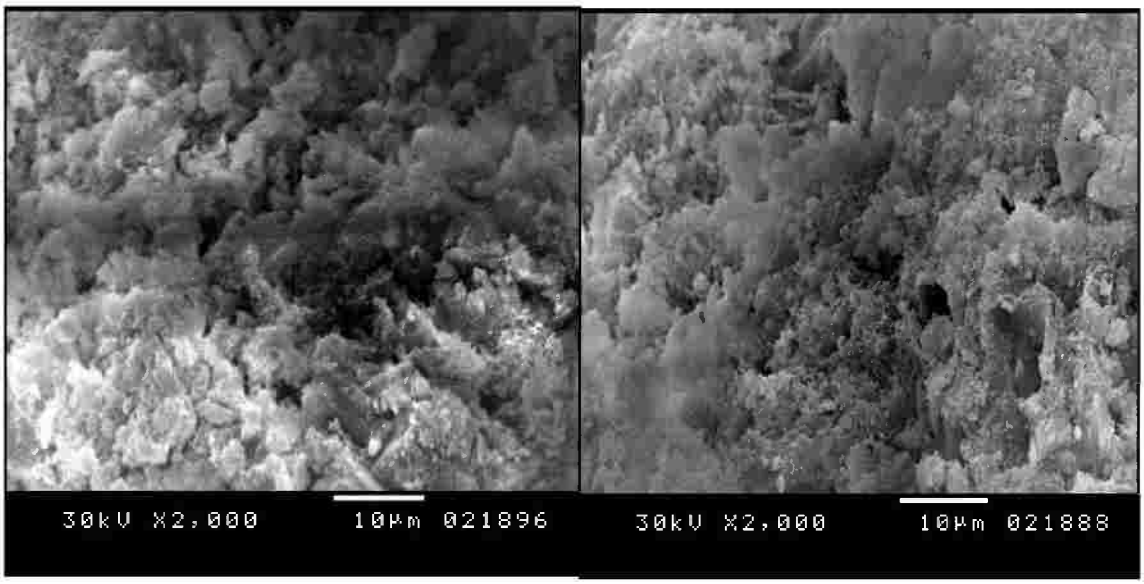

c) 400º C

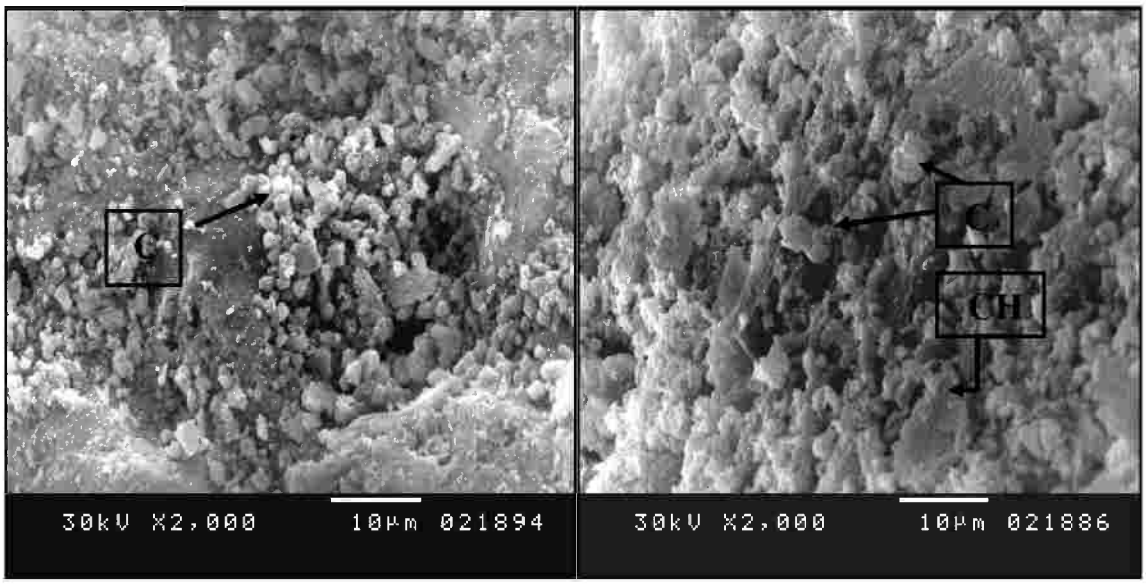

d) 600º C

Fig.4.26 -SEM images of 1-M-(L.P15R) 2-M-(L.P15A)at a) 20 b) 200 c)400 and d) 600ºC.

4.2.4.4. SEM on bentonite concrete mix.

Scanning electron microscopy is best suitable for observation of bentonite structure. First, the sample of initial raw bentoniteis examinedby SEMwhich shows clay platelets of varying size that are clearlyvisible in **Fig. 4.27**. They are arranged in face-to-face patterns. Some well crystalline pseudo-hexagonal edges arealso observed.The sample of bentoniteis examinedby SEM and results are presentedin **Fig. 4.28**.At 20ºC, clay platelets of varying sizes are clearly

visible in **Fig. 28-a,**and the surface of the sample is smooth and flat. It is clear from **Fig.28-e** that the bentonite concrete after being exposed to 600ºC has cracks less than in the control mix.Thus this result is consistent with the results observed from visual inspection. Also the clay flat or platelets particles are still found in numerous numbers.

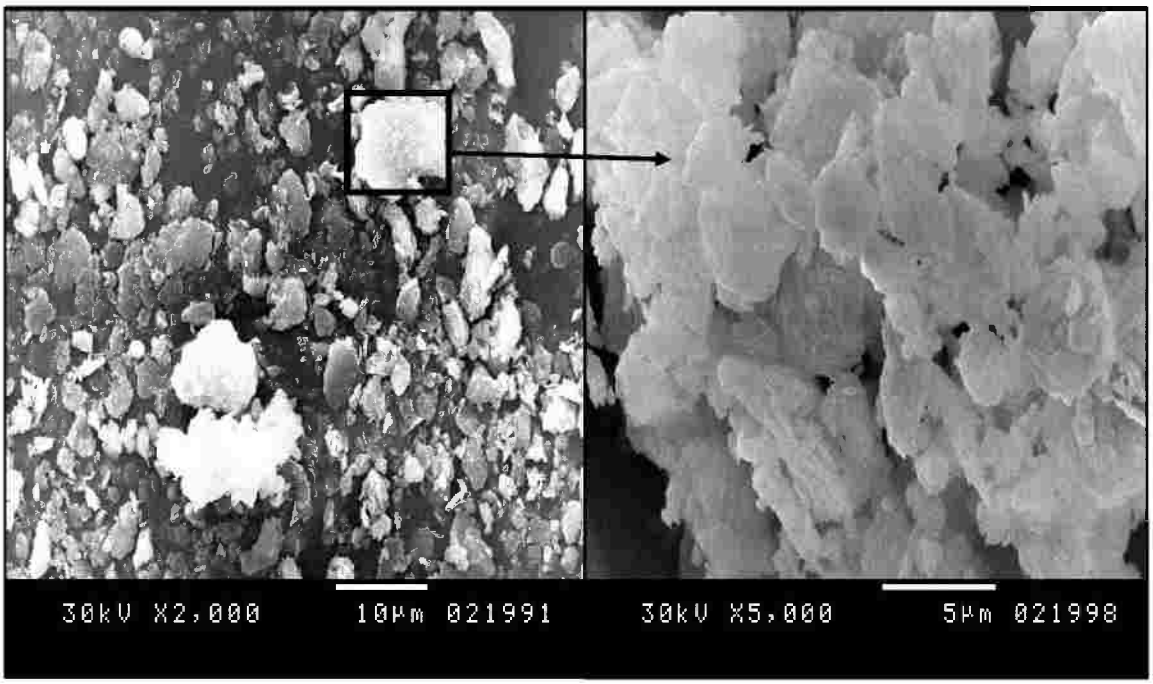

Fig. 4.27- SEM micrographs of raw bentonite at different magnifications: a) 2000× and b) 5000×

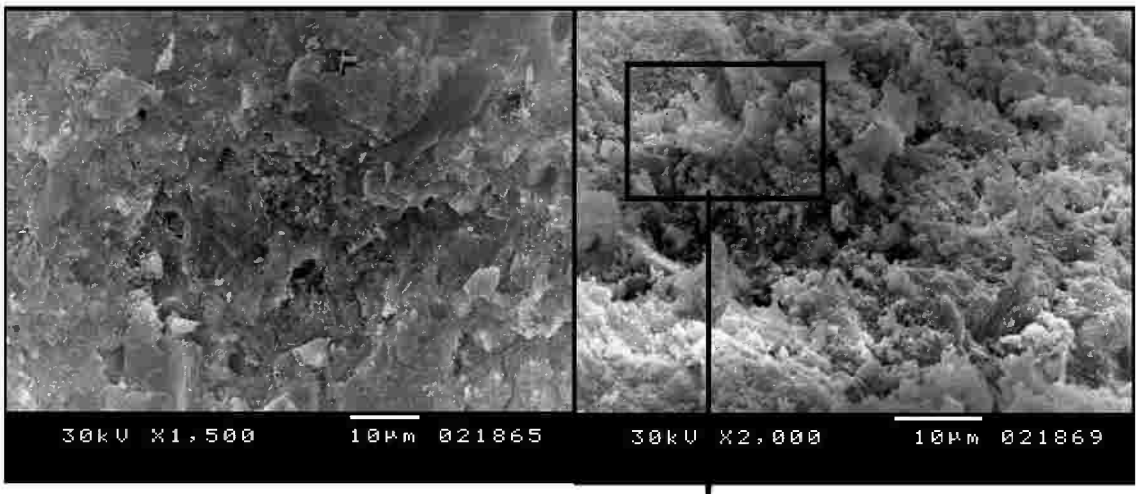

a) 20ºC b) 200ºC

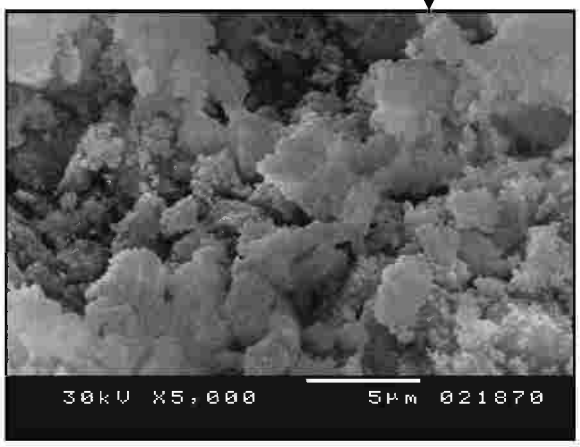

c)Bentonite particles

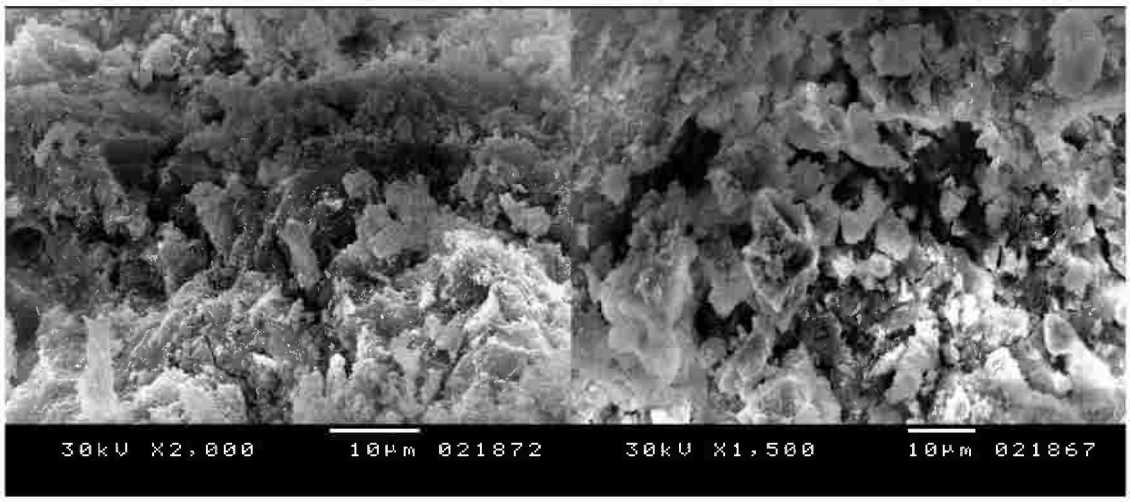

d) 400 ºC e) 600ºC

Fig. 4.28 - SEM images of concrete with 10% bentonite as cement replacement at a) 20ºC b) 200 c) bentonite plates d) 400 e) 600ºC.

4.2.5 Thermogravimetric analysis (TGA/DTG).

The (TGA/DTG) is done to all mixtures except M-(PPF), M-(Sil+PPF) and M-(Steel-F) because of the thermogravimetrywhich is often used to investigate chemical reactions in which weight changes occur. In theory, it is not expected to observe a gravimetric effect when a substance melts, for that PPF and steel fibers are melted at different elevated temperature degrees then the thermogravimetry should not be done.

(TGA/DTG) ofunheated and preheated silicafume concrete shows as presented in **Fig. 4.29-b** a peak (A) at about 70°C dute to free water desorption and the decomposition of C-S-H gel. The second peak (B) obviously appeares for unheated specimen at about 100°C which is related to ettringite and C-S-H decomposition. Peaks (A) and (B) are observed considerably resulting from an increased content of C-S-H gel structural OH- groups.Further mass loss up to approx. 400 °C indicates continuous thermal decomposition of a complex mixture of hydrated silicate- and aluminate-type compounds.Peaks (C) and (D) take placedue to portlandite and carbonated phases decomposition. It should be noticed that the peaks (A, B, C, D) are shifted with the different preheated degrees of temperature where as a sample, peak (D)has been shifted to a lower temperature from 825 to 790, 780 and 770°Cat 20, 200, 400 and 600°C respectivelydue declining order of the C-S-H gel structure that increases with the increaseof the preheated degree of temperature.Peak (A) completely disappears for preheated Silica fume concrete at 600°C as a result of that the free water,ettringite and C-S-H gel are completely decomposed.

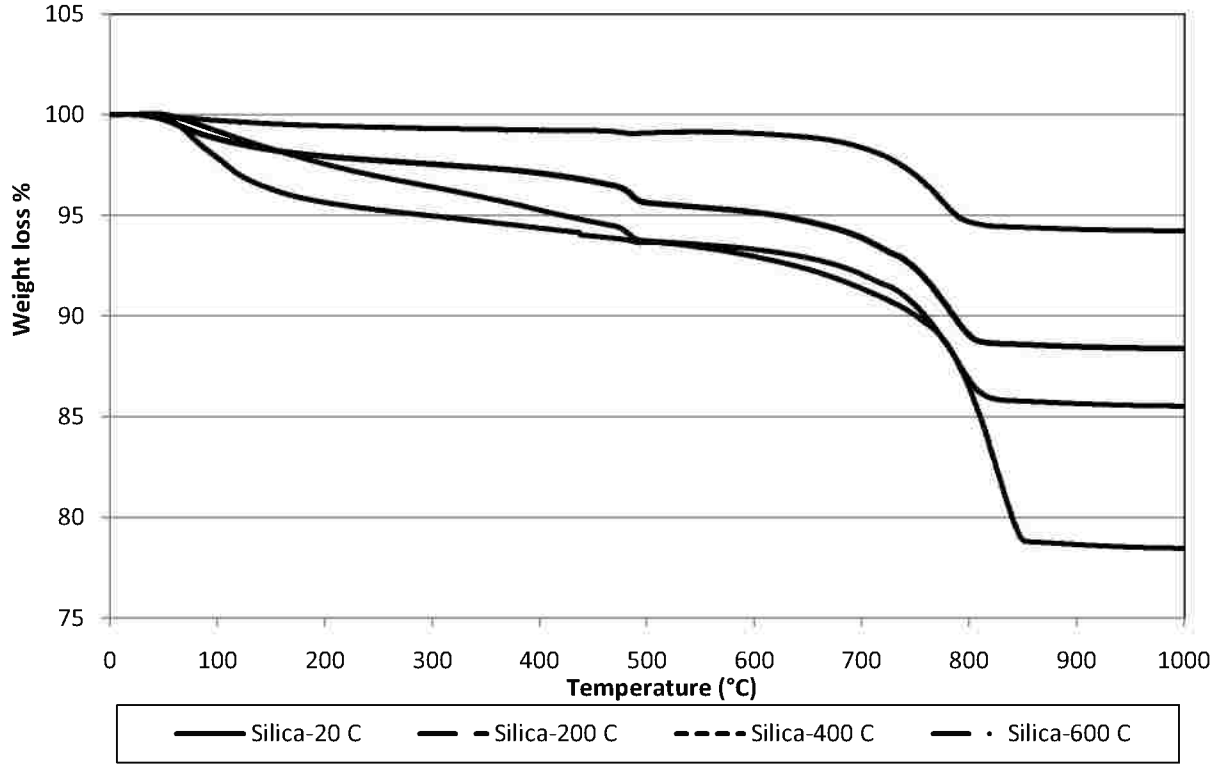

(a)

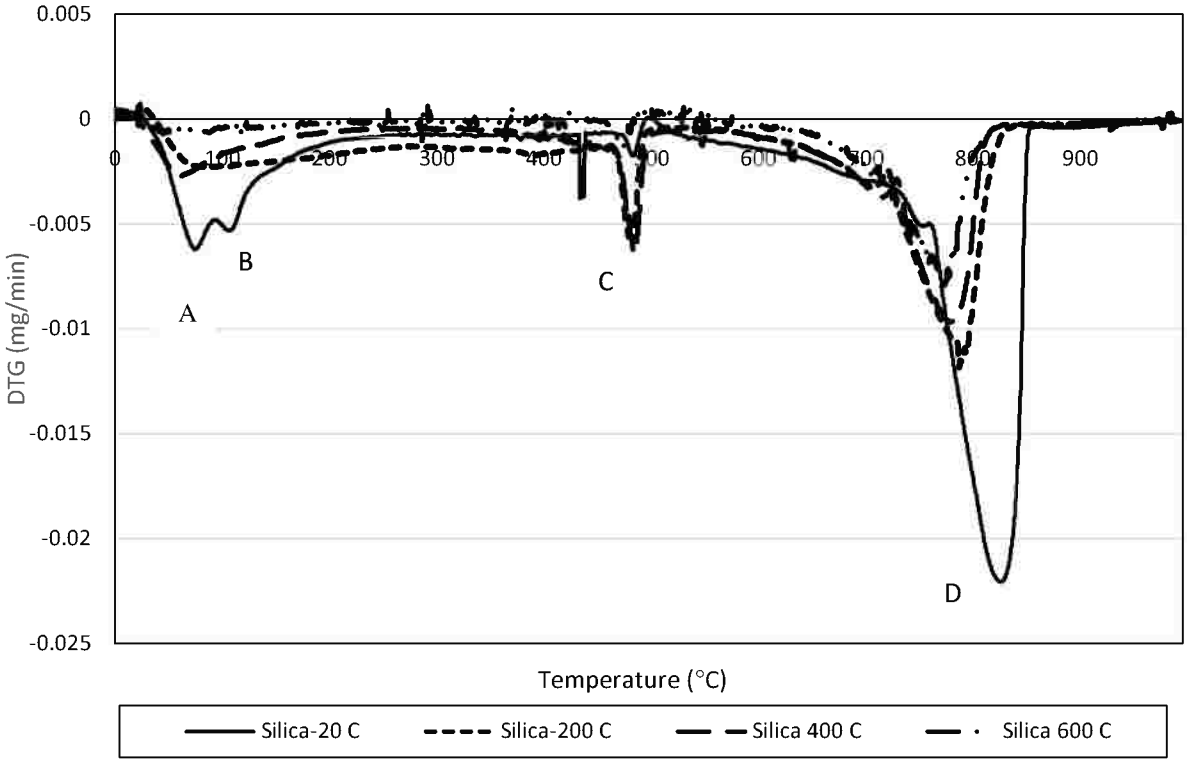

(b)

Fig.4.29 -(TGA/DTG) curves of concrete with 10% silicafume as cement replacement by mass

a) TGA b)DTG

Fig. 4.29-a shows weight losses obtained from thermogravimetric analysis of small samples from silicafume concrete and control mix. From **Fig. 4.29-a** it can be noted that the weight loss of unheated and preheated silicafume concrete are more than the weight loss of control mix up to TGA-800°C, from TGA-800°C up to TGA-1000°C the weight loss can be reversed, so the weight loss of the control mix became more less.

The rate of reduction in weight lossof unheated and preheated silicafume concrete was mild up to TGA-500°C followed by a sharp decreasein a broad temperature interval from 500 to 800 °Ccaused by carbonated phases decomposition. Preheated silicafume concrete at 200, 400 and 600°C show a reduction in weight loss over TGA-800°Cwhencompared with control mix.Also, as control mix and from **Fig 4.29-a** it can be seen that the total weight loss of the spcimens at TGA-1000°C decreases with the increase of the preheated degree of temperature. The weight loss results from TGA are in agreement with the weight loss from the heated cubes in sec 4-2-4.

The limestone concrete also was investigated by (TGA/DTG) test. TGA/DTG curves for unheated and preheated limestone concrete are presented in from **Fig. 4.30to Fig. 4.33.** Total mass losses for unheated concretes with 10 and 15% limestone as replacement and additive to cement content were 13.2, 13, 16.4 and 17.4 % respectively and less than the total weight loss of control mix which is 25%.From TGA/DTG curves it can be noticed that the weight losses for unheated concrete at about 500ºC, were about 5.5, 7, 5, 9 and 8 % for M-C, M-(L.P 10R), M-(L.P 15R), M-(L.P 10A) and M-(L.P15A). This result attributes to the carbonationofCaCo$_3$ which produces more Ca(OH)$_2$.

The thermograms show that hydrated C$_3$A exhibits a small endothermal effect with a peak at about 320º C and additions of CaCO$_3$ suppress this peak especially as shown in **Fig. 4.32-b** and for unheated and preheated concrete at 200ºC. In unheated samples of limestone concrete a little endothermic peaks appears at about 140ºC due to the presence of monocarboaluminateas observed clearly in **Fig. 4.31-b** for unheated concrete**[Handoo, et al. 2002]**. By some implantation, **Fig. 4.32-b and Fig. 4.33-b**show, in unheated and in some cases of preheated specimens, a small endothermal peak at about 815ºC is noticeddue to the CO$_2$release.

This could suggest that with limestone additions the composition of the C-S-H,the formation of ettringite and the carboaluminatephases change.

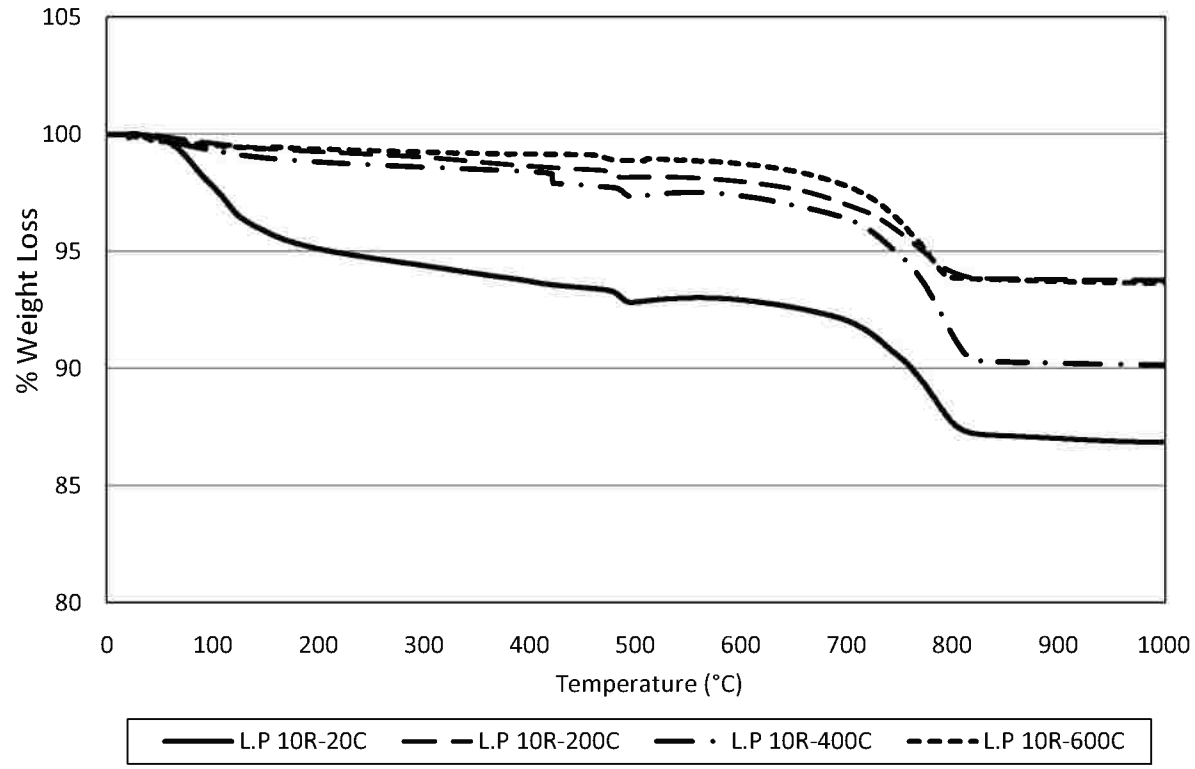

(a)

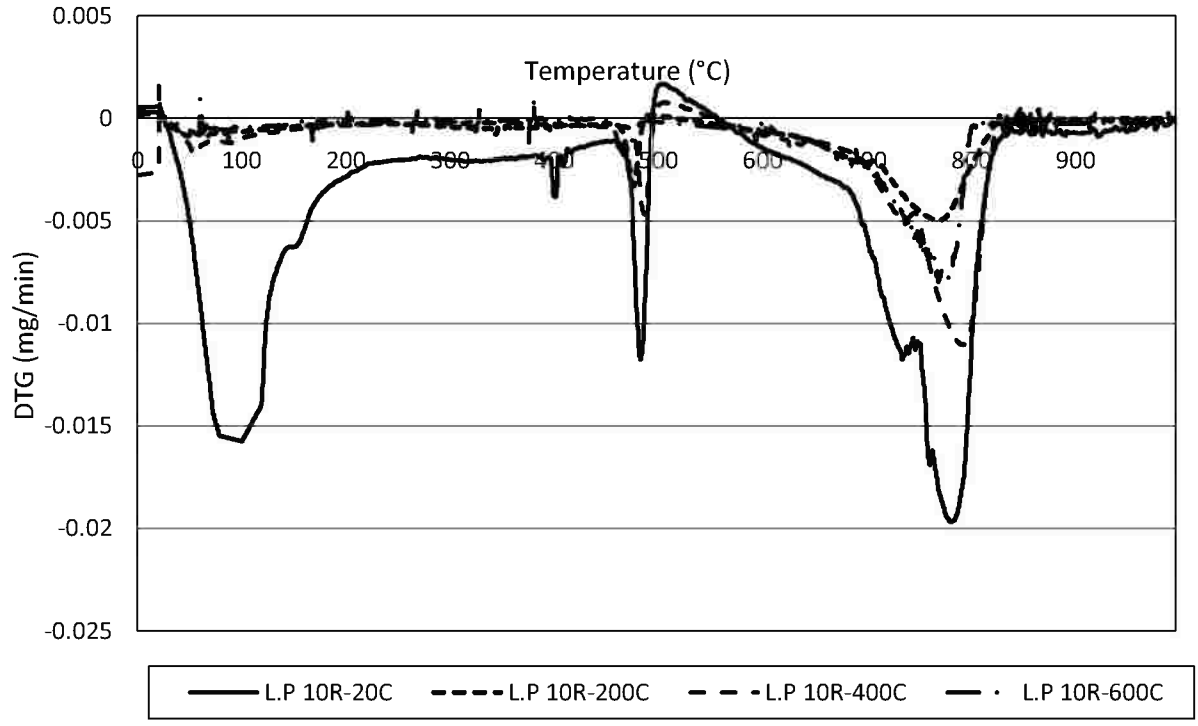

(b)

Fig.4.30 - (TGA/DTG) curves of concrete with 10% limestone powder as cement replacement by mass a) TGA b)DTG

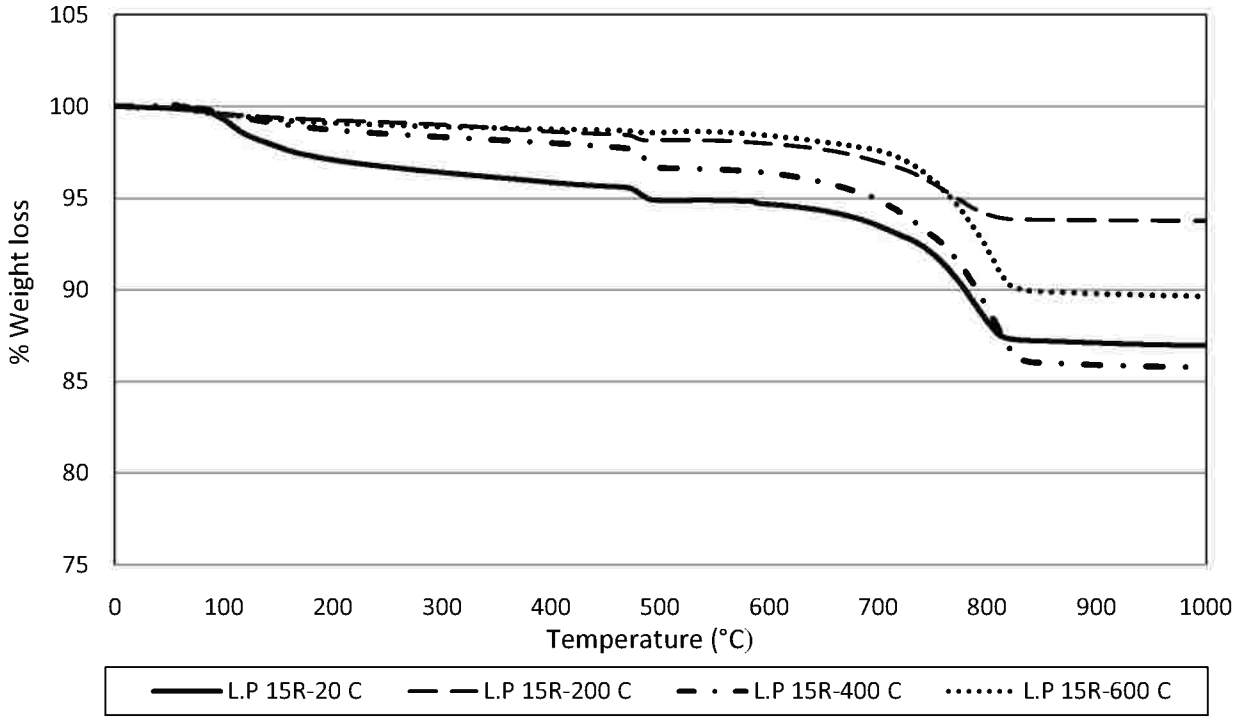

(a)

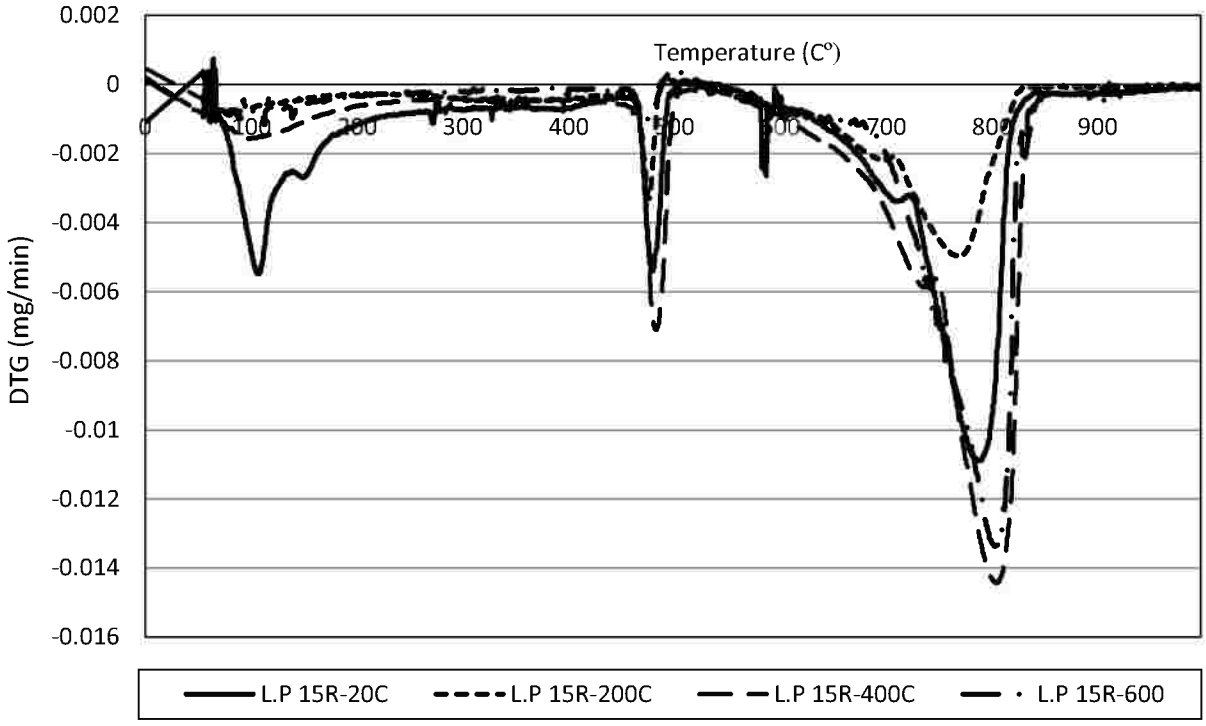

(b)

Fig. 4.31 - (TGA/DTG) curves of concrete with 1٥% limestone powder as cement replacement by mass a) TGA b)DTG

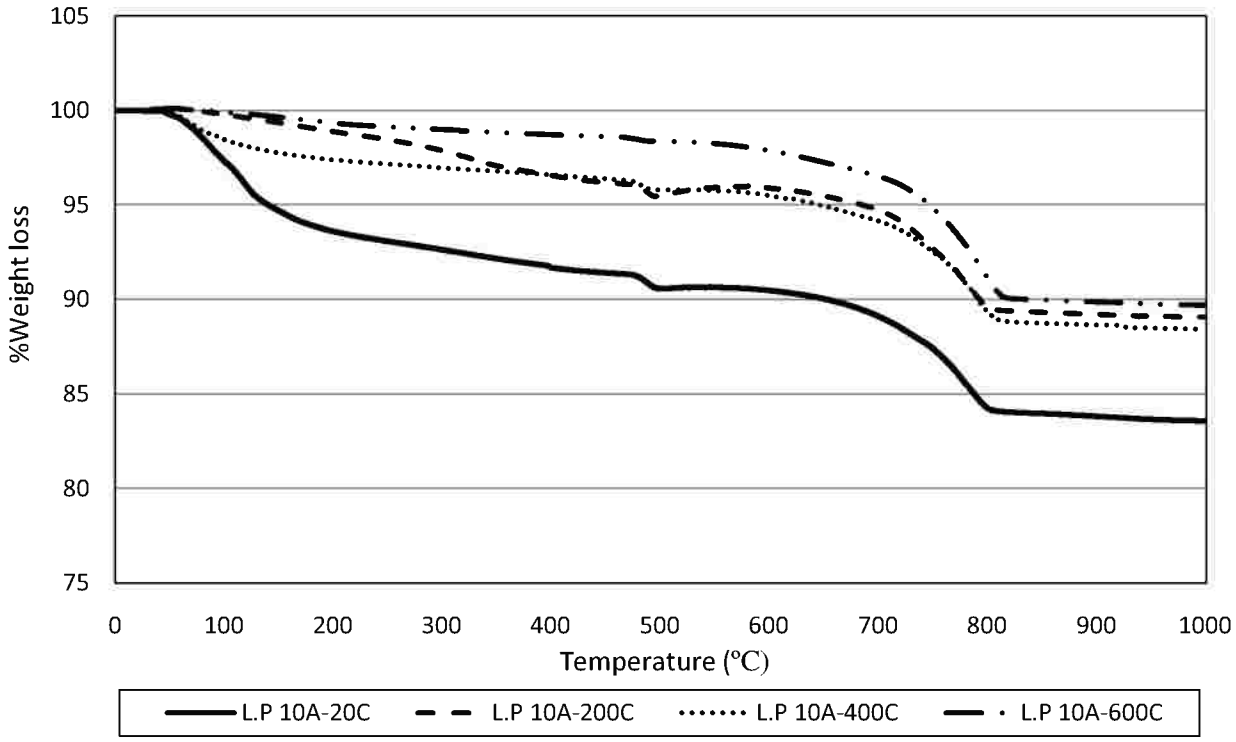

(a)

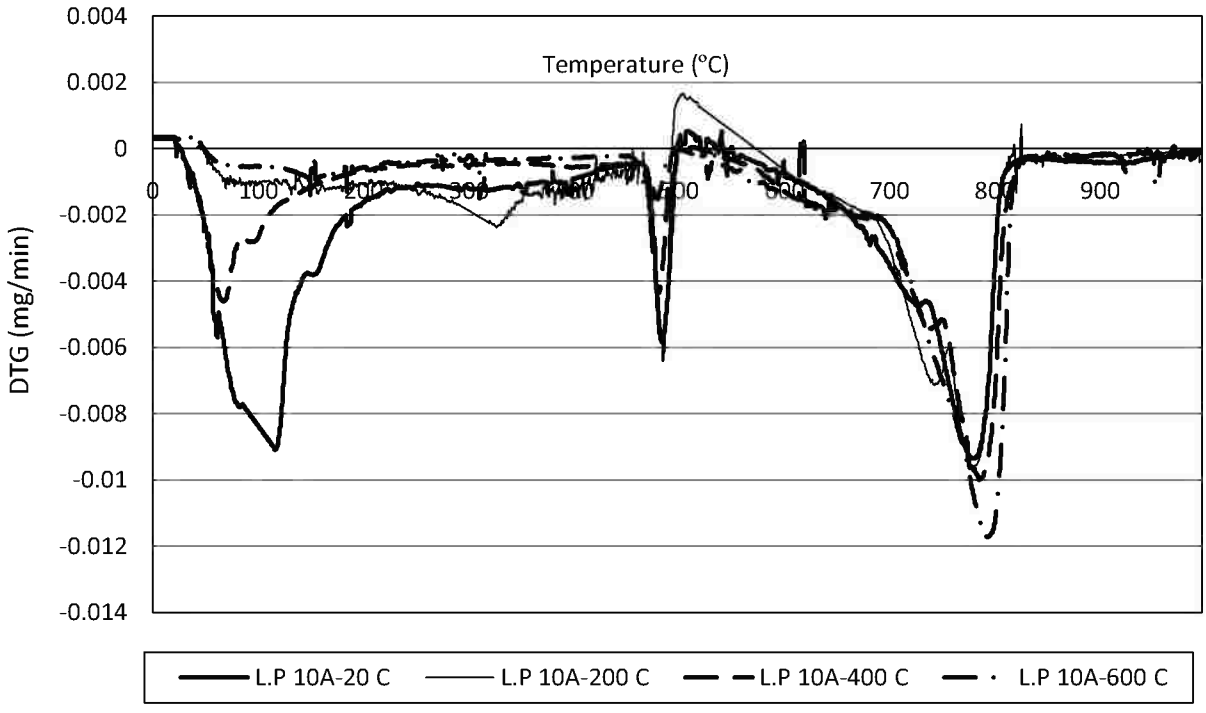

(b)

Fig. 4.32 - (TGA/DTG) curves of concrete with 10% limestone powder as cement additive by mass a) TGA b) DTG

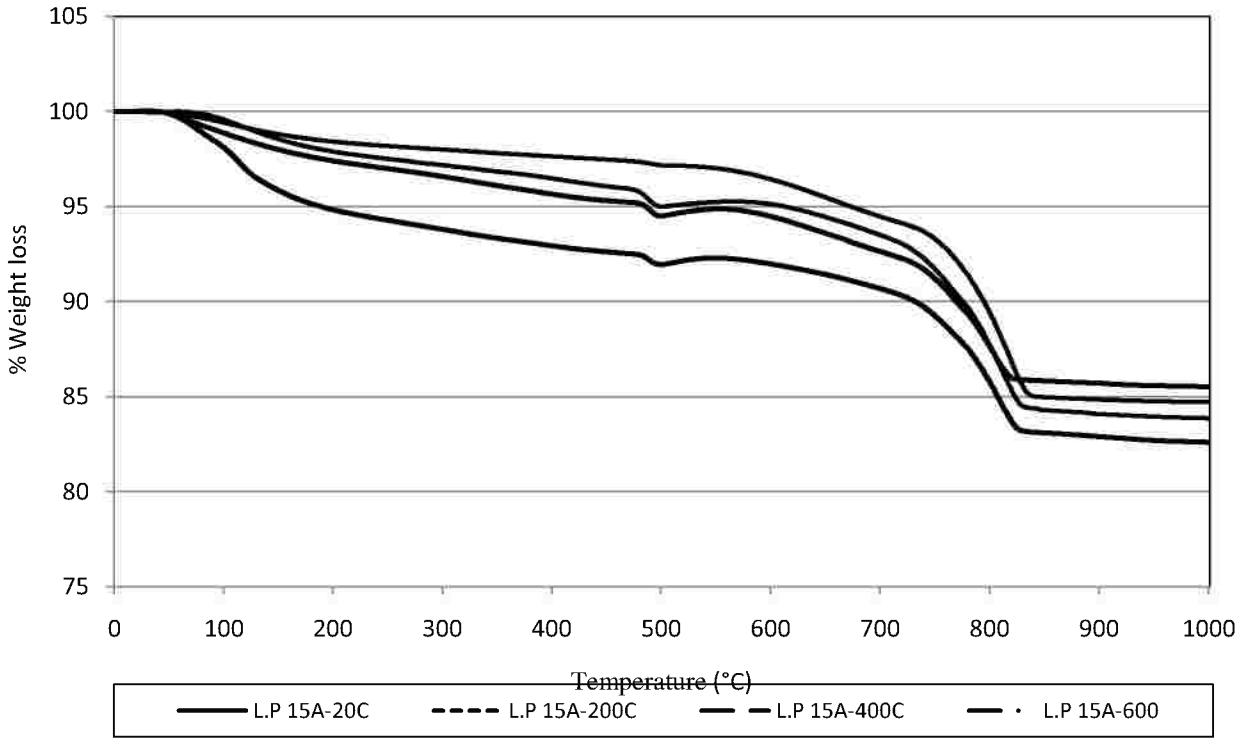

(a)

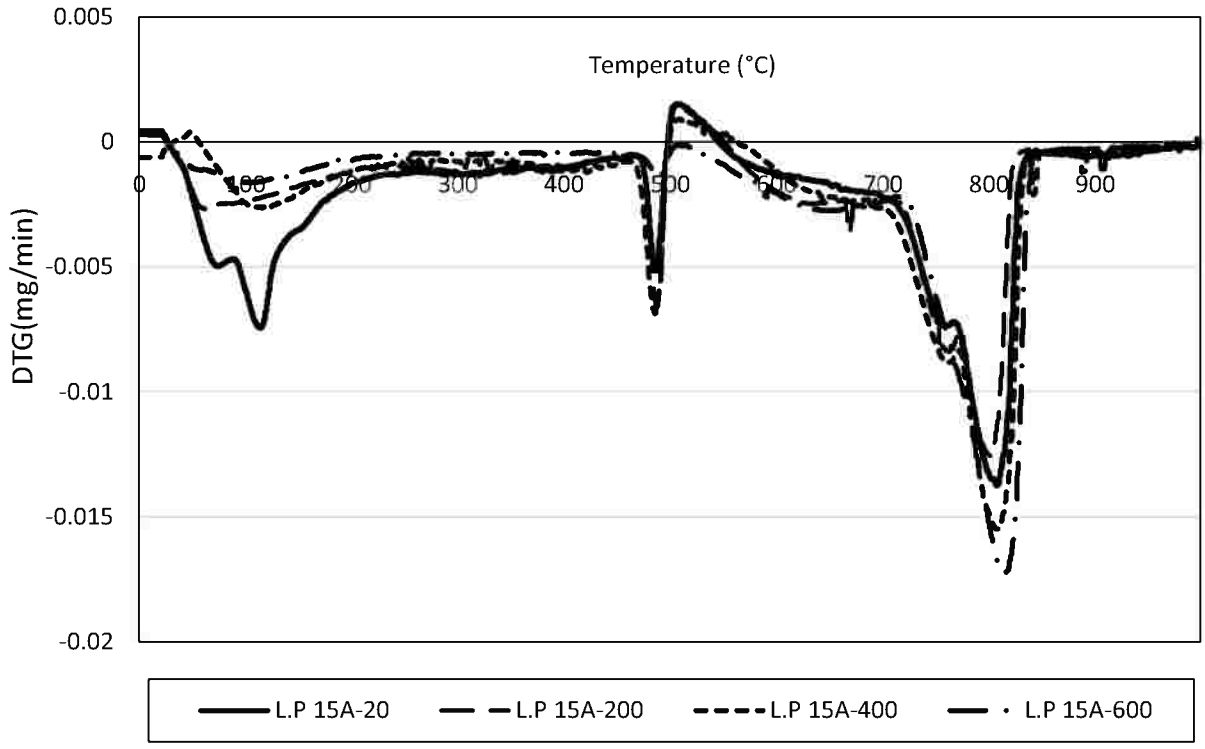

(b)

Fig. 4.33 - (TGA/DTG) curves of concrete with 15% limestone powder as cement additive by mass a) TGA b)DTG

The EDAX analysis of bentoniteshows high silica content and the presence of Al^3 and Fe^3 and alkaline earth metal.As shown in **Fig. 4.34**. A significant endothermic peak at 93°C can be attributed to the removal of adsorbed andinterlayer water of the clay. Also, at 198°C the smallpeak-limb can be observed, which represents simultaneousreaction, such as boiling reaction of water **[Bish, et al. 1990]**. Inaddition, a large exothermic reaction between 250 and450°C is related to the decomposition of organic matter.A broad endothermic band centred at 500°C was due tothe dehydroxylation. An exothermic peak was obtainedat 1033°C due to recrystallization of montmorillonite but was not observed in this study.The DTG curve shows a slight endothermic peak around998°C, immediately before the exothermic peak, due tothe breakdown of the montmorillonite structure.

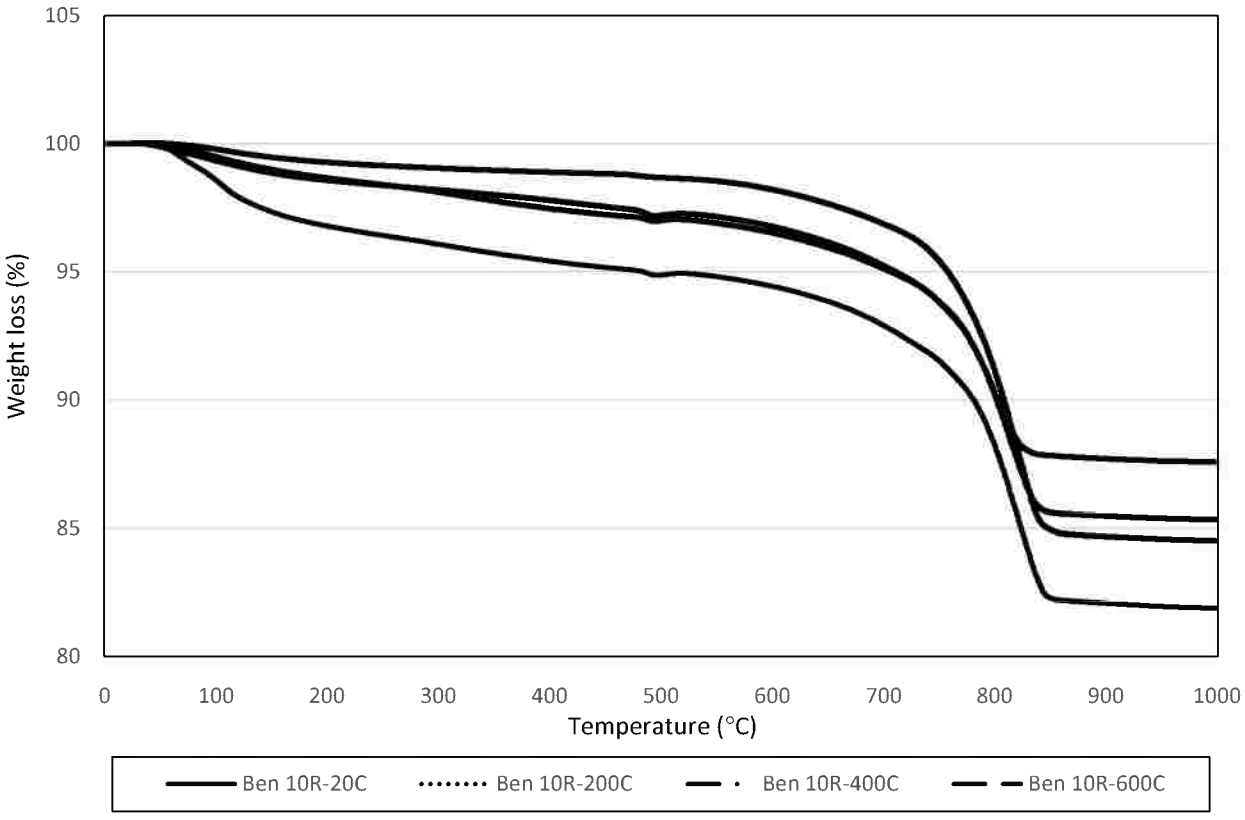

(a)

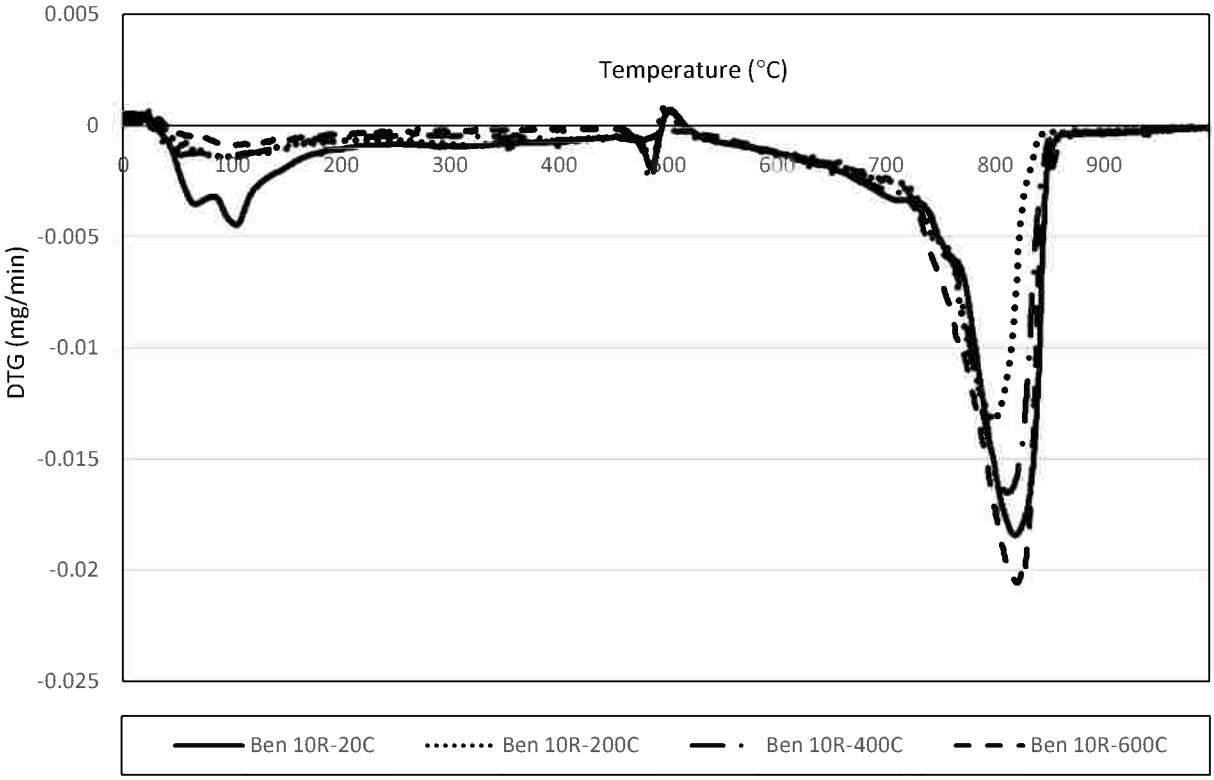

Fig. 4.34 - (TGA/DTG) curves of concrete with 10% bentonite as cement replacement by mass a) TGA b)DTG

4.2.6 Visual inspection.

Visual inspection was carried out on the100 mm cubes after being exposed to 200, 400 and 600ºC, which shows that as the temperature increase as the cracks increase. This observation for the specimens of concrete is critical because the dissociation of portlandite made the concrete practically useless after cooling. At the beginning all specimens tested did not show any occurrence of surface cracks at heating temperature of 200°C.

For concrete specimens containing 10% silicafume as cement replacement and as all studied mixtures, no surface cracks were observed at 200°C.From **Fig 4.35-b**, the specimens showed signs of occurrences of surface cracks when heated to 400°C. **Fig. 4.35-c** shows that mix with 10% silicafume has more surface cracks than control mix and the specimens became hollow at 600°C. This is because of the free water that has been transgressed at about 105°C, and then cement particles combine more tightly and vapor transgress becomes more difficult as reported by **[Min et al. 2004].**

a) 200°C b) 400°C c) 600°C

Fig. 4.35 - Maps of the cracks of concrete specimens with 10% silicafume as cement replacement.

For polypropylene fibers concrete,and as shown in **Fig. 4.36**, it can be reported that with the addition of PPF, the formation ofmicro-cracks is prevented and the scale of micro-cracks is reduced due to the crack-arresting effect, crack thinningeffect and crack-bridging effect of PPF as reported by **[Zhang et al. 2011 and , Hadipramana et al.2012]**. It should be noticed that the paths which the PPF leaves the concrete surface at 200°C.

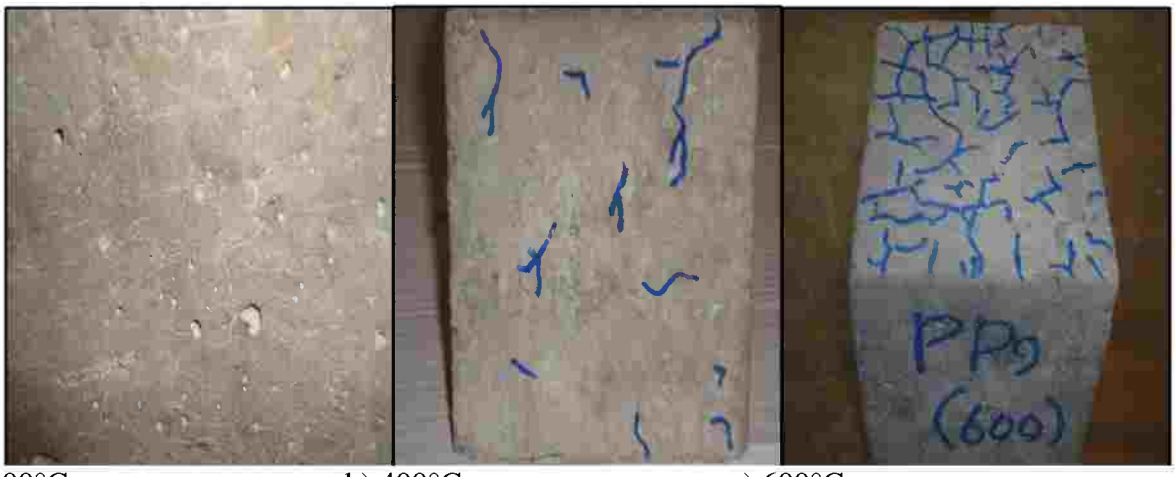

a)200°C b) 400°C c) 600°C

Fig. 4.36 - Maps of the cracks of concrete specimens containing 0.9 kg/m³ polypropylene fibers.

No evidence of surface cracks in M-(Sil+PPF) cubes at 200 and 400°C as clearly showninFig. 4.37. The effect of polypropylene fibers appears clearly if the 10% silicafume mix and 10%silicafume with 0.90kg/m³ polypropylene fibers mix have been compared together at

600°C as shown in **Fig. 4.37-c.** It is clear that the presence of polypropylene fibers in blended concrete reduce the growth of cracks. It is attributed to the fact that the polypropylene fibers melt and create channels through which the water vapor pressure built-up within blended concrete temperature rises is released. This release of the vapor pressure significantly reduces the spalling tendency of blended concrete under fire conditions.

a) 200°C b) 400°C c) 600°C

Fig. 4.37 -Maps of the cracks of concrete specimens containing 10% silicafume as cement replacement with 0.9 kg/m³ polypropylene fibers.

a)200°C b) 400°C c) 600°C

Fig. 4.38 -Maps of the cracks of concrete specimens containing 20 kg/m³ steel fibers.

For steel fiber concrete, a network of hair cracks appeared after heating to maximum temperatures at 600°C as seen in **Fig. 4.38**. It is concluded overall that a fiber reinforcing

concrete has higher strength and better performance in crack resistance than non-fiber concrete after exposure to high temperature.

The addition of LP as 10% and 15% cement replacement was investigated and presented in **Fig. 4.39**. The visual inspection shows that the addition of LP as cement replacement decreases the surface cracks of the cubes when compared to the control mix. The increasing of LP from 10% to 15% as a partial replacement of cement mass may reveal a slight increasing in the surface cracks at 400 and 600°C which is a sign of strength being diminished.

a) 200°C b) 400°Cc) 600°C

(1)

a) 200°C b) 400°C c) 600°C

(2)

Fig. 4.39 -Maps of the cracks of concrete specimens containing LP as a partial cement replacement 1) M-(LP 10R) 2) M-(LP 15R).

a) 200°C b) 400°C c) 600°C

(1)

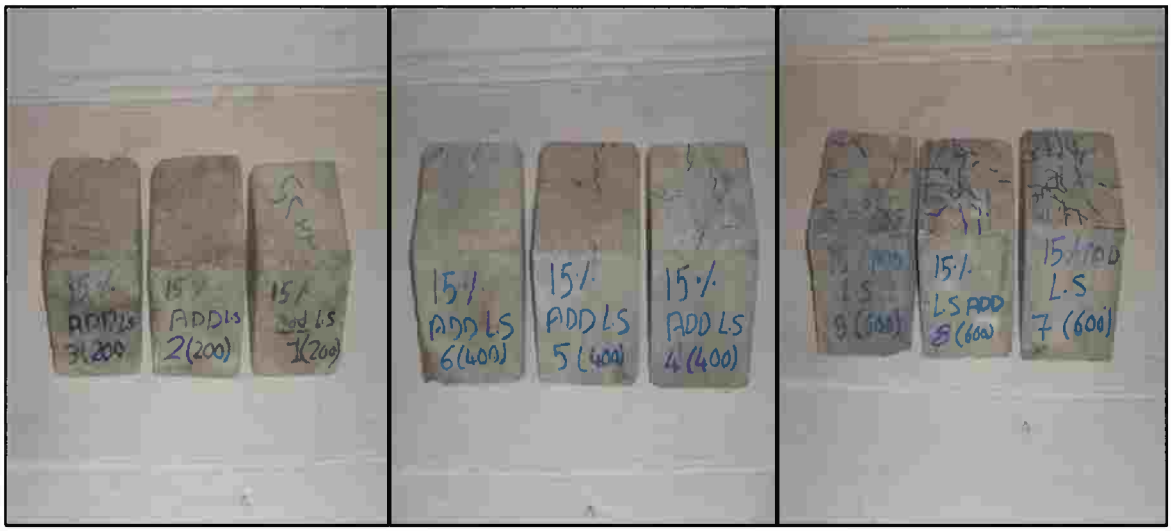

a) 200°C b) 400°C c) 600°C

(2)

Fig. 4.40 -Maps of the cracks of concrete specimens containing LP as an additive to cement content 1) M-(LP-10A) 2) M-(LP-15A).

The surface cracks of concrete cubes containing 10 and 15% of LP as an additive to cement content have been shown in **Fig. 4.40** It is also clear that the usage of LP as an additive to cement content up to 15% decreases the surface cracks considerably. M-(LP 15A) considers with the M-(Steel.F) the best mixtures that have the least surface cracks. This visual investigation sustains the results of the compressive strength.

The examination of bentonite concrete surface is very important to study the effect of bentonite on the properties of the conventional concrete. No visible cracks were obtained up to 400°C. At 600°C the concrete specimens have many surface cracks but still less than the control mix as noted in**Fig. 4-41**. This may be attributed to the fact thatbentonite has good high-temperature durability which means that the bonding properties are not destroyed easily especially at moderate temperature.

a) 600°C

Fig. 4.41 -Maps of the cracks of concrete specimens containing 10% bentonite as cement replacement at 600°C.

4.2.7 Temperature of the Rft , unexposed and exposed surface of reinforced slabs.

Evaluation of the behavior of the heat in concrete is very significant, for that it is important to measure the temperature of the exposed, unexposed surface and steel of the all slabs for different mixtures. The temperature was controlled during tests by taking the average temperature of two shielded thermocouples located 10 mm below the exposed surface of the concrete slabs. The temperature of the exposed surface of the slab to fire, the unexposed surface and the steel inside the slab were measured, for 2 hrsexposure and for 2 hrs air cooling regime.The data is presented in the following tables and figures for all the studied materials.

4.2.7.1Temperature of the Rft , unexposed and exposed surface of silicafume concrete slabs.

The measured temperatures that determine during the exposure of the Rft concrete slabs with 10% silicafume as cement replacement were reported.

Time	Rft.	Unex.	Ex.
10	20	20	20
20	86	61	600
30	120	92	600
40	141	109	600
50	149	120	600
60	159	127	600
70	168	133	600
80	174	138	600
90	188	144	600
100	196	151	600
110	202	158	600
120	209	161	600
130	214	164	600
140	203	159	389
150	185	154	178
160	155	134	148
170	124	113	117
180	111	103	105
190	98	93	94
200	89	84	84
210	79	74	75
220	73	70	69
230	67	65	64
240	64	61	59

0	Rft.	Unex.	Ex.
10	20	20	20
20	102	60	800
30	124	90	800
40	157	109	800
50	188	130	800
60	204	148	800
70	223	162	800
80	234	176	800
90	247	190	800
100	260	200	800
110	267	206	800
120	272	211	800
130	273	216	800
140	257	211	510
150	240	206	219
160	198	174	178
170	156	142	136
180	140	128	124
190	125	114	112
200	111	101	100
210	97	87	88
220	88	80	81
230	80	73	74
240	73	67	68

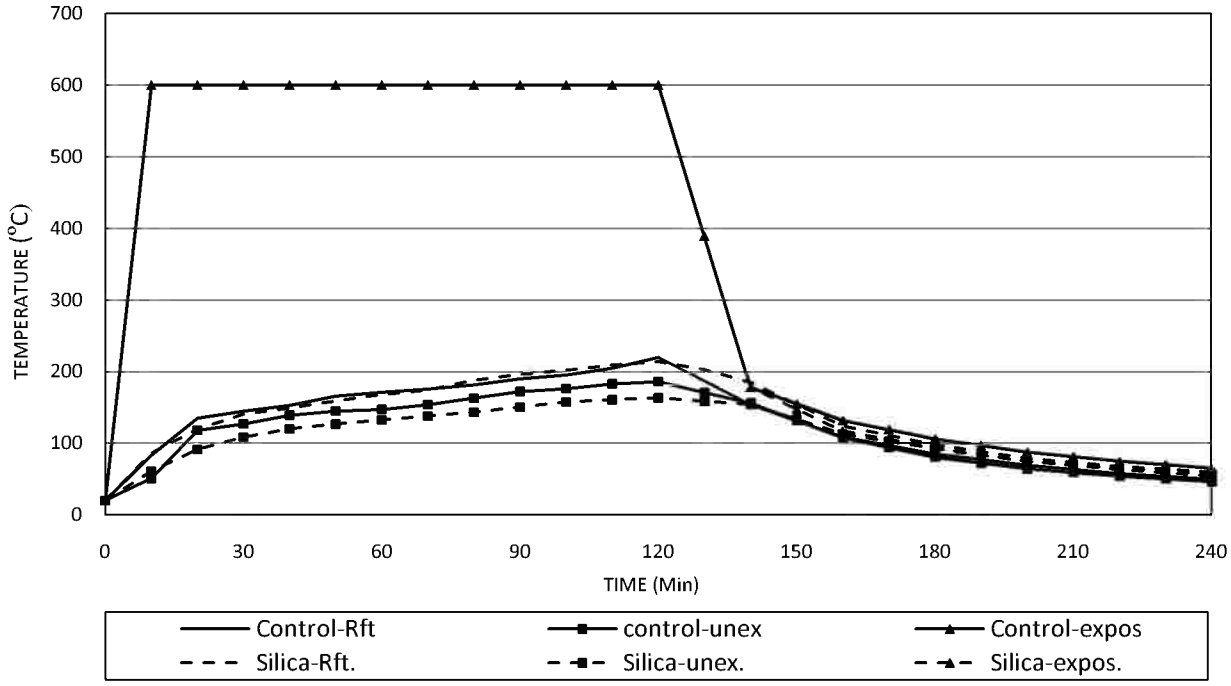

(a)

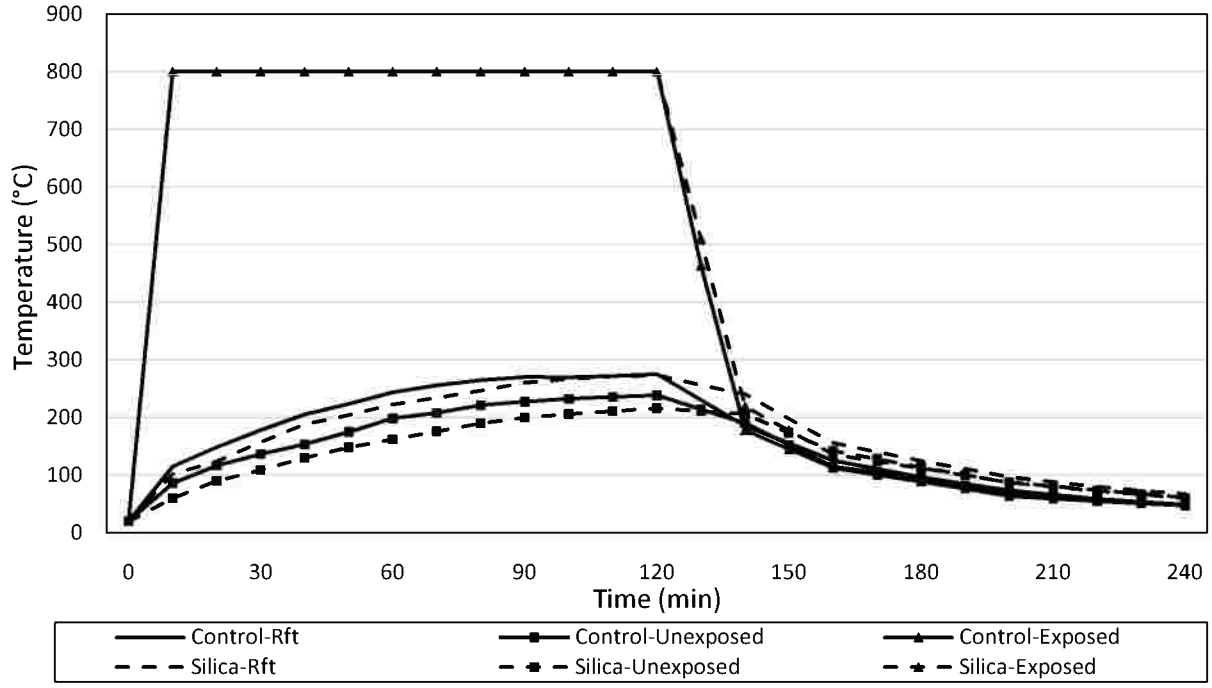

(b)

Fig. 4.42 -Temperature of Rft, unexposed and exposed surface of silicafume concrete slabs exposed to a) 600°C b)800°C.

4.2.7.2Temperature of Rft, unexposed and exposed surface of polypropylene fiber concrete slabs.

Time (min)	Rft (°C)	Unex. (°C)	Exp. (°C)
0	20	20	20
10	103	67	600
20	149	121	600
30	158	136	600
40	162	143	600
50	171	149	600
60	177	156	600
70	184	169	600
80	189	173	600
90	193	180	600
100	205	184	600
110	215	188	600
120	228	189	600
130	191	175	376
140	154	161	153
150	127	130	123
160	101	98	94
170	91	88	83
180	81	78	73
190	73	70.7	66
200	65	63	60
210	61	59	56
220	56	54	53
230	51	50	48
240	47	45	44

Time (min)	Rft (°C)	Unex. (°C)	Exp. (°C)
0	20	20	20
10	110	72	800
20	142	104	800
30	179	128	800
40	201	143	800
50	226	156	800
60	245	180	800
70	262	196	800
80	274	202	800
90	284	212	800
100	292	216	800
110	298	220	800
120	302	228	800
130	265	210	475
140	228	192	201
150	200	170	174
160	172	149	147
170	145	128	130
180	119	108	113
190	107	97	99
200	95	86	86
210	86	78	77
220	76	70	69
230	70	65	63
240	64	59	58

Time (min)	Rft (°C)	Unex. (°C)	Exp. (°C)
0	20	20	20
10	103	82	1200
20	196	127	1200
30	247	170	1200
40	303	220	1200
50	356	252	1200
60	391	283	1200
70	409	292	1200
80	424	298	1200
90	438	308	1200
100	448	313	1200
110	456	318	1200
120	459	321	1200
130	392	289	726
140	326	256	252
150	273	220	215
160	220	183	178
170	183	153	150
180	147	123	123
190	128	111	109
200	109	98	96
210	97	88	87
220	84	78	79
230	76	71	73
240	68	63	67

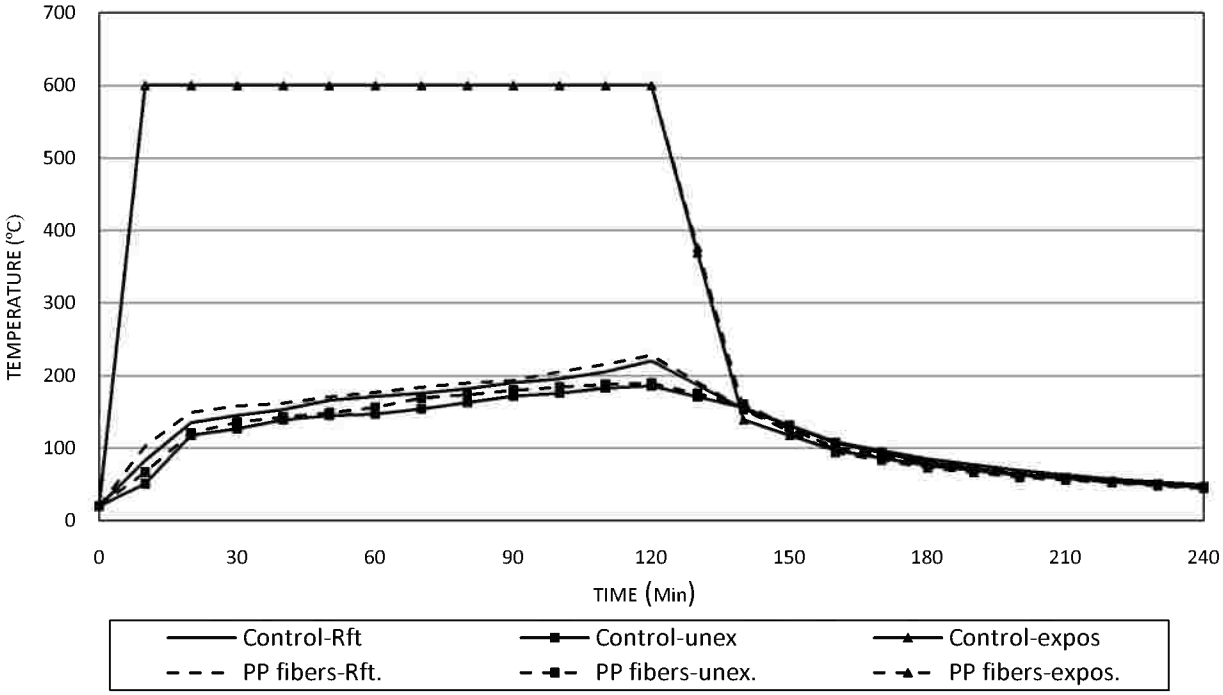
700
600
500
400
300
200
100
0
TEMPERATURE (°C)
0
30
60
90
120
150
180
210
240
TIME (Min)
Control-Rft
Control-unex
Control-expos
PP fibers-Rft.
PP fibers-unex.
PP fibers-expos.

(a)

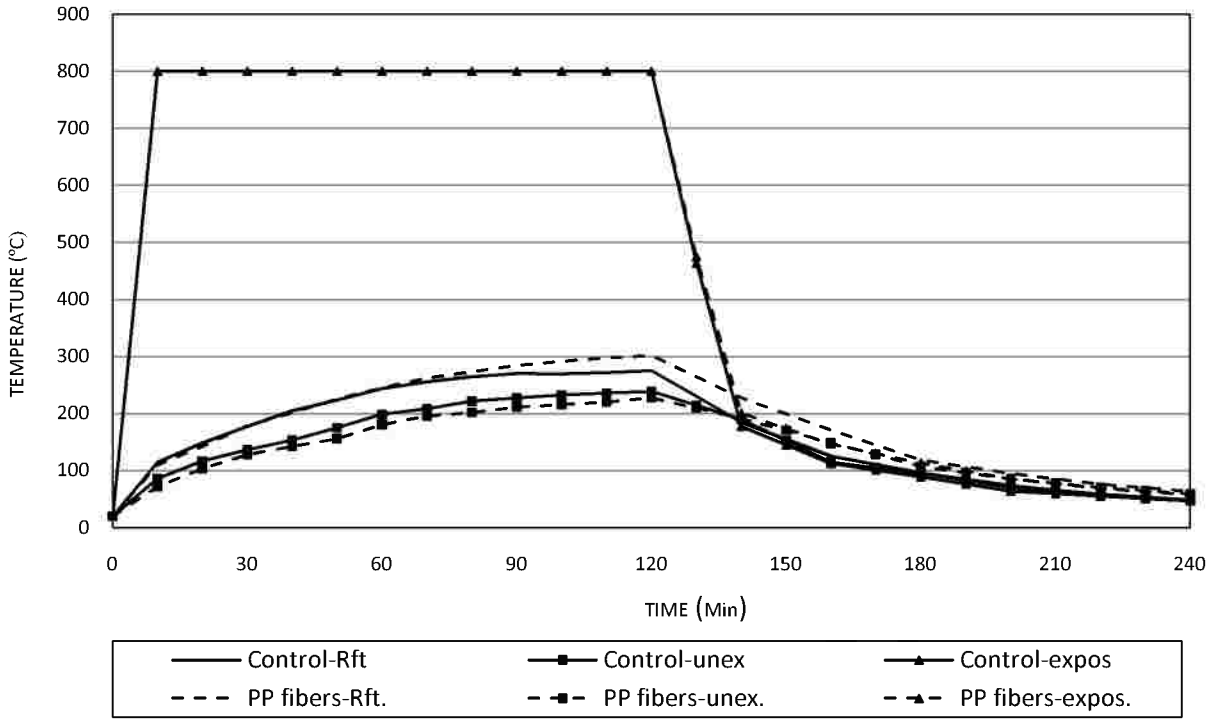
900
800
700
600
500
400
300
200
100
0
TEMPERATURE (°C)
0
30
60
90
120
150
180
210
240
TIME (Min)
Control-Rft
Control-unex
Control-expos
PP fibers-Rft.
PP fibers-unex.
PP fibers-expos.

b)

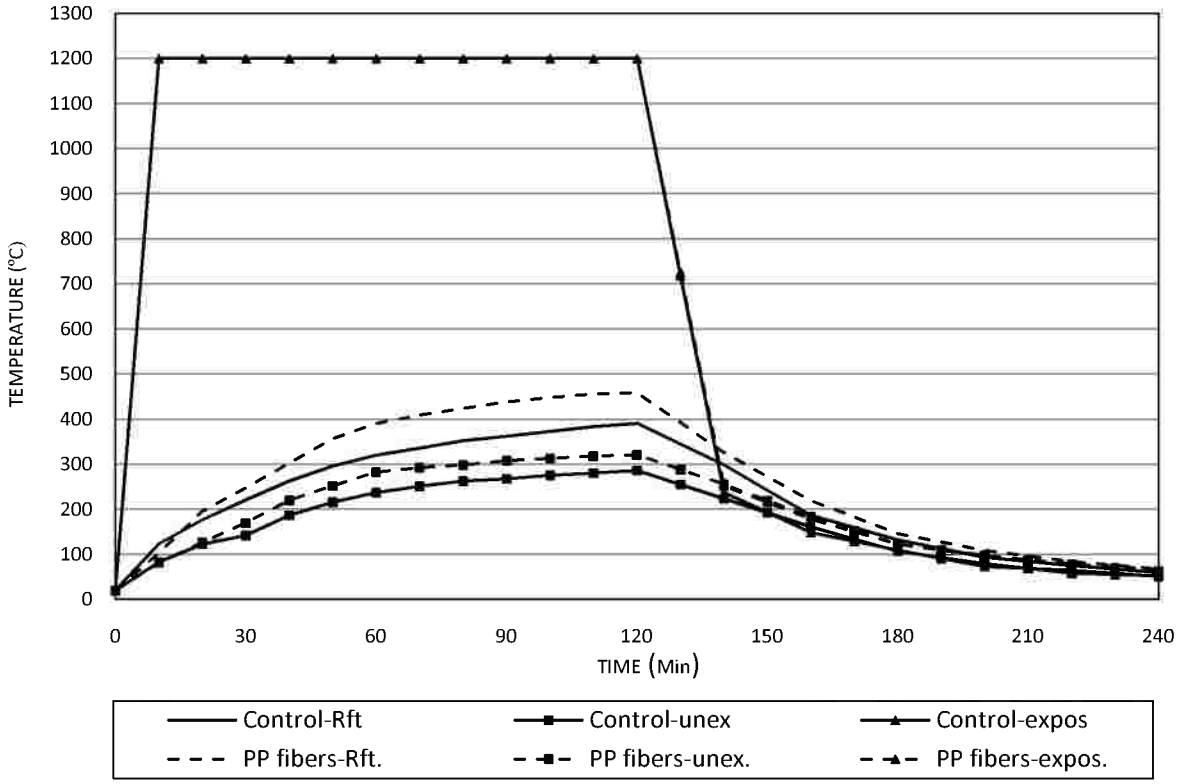

c)

Fig. 4.43 -Temperature of Rft, unexposed and exposed surface of 0.90kg/m³ polypropylene fiber concrete slabs when exposed to a) 600°C b) 800°C c)1200°C.

4.2.7.3 Temperature of Rft, unexposed and exposed surface of silicafume with polypropylene fiber concrete slabs.

Time (min)	Rft (°C)	Unex. (°C)	Exp. (°C)
0	20	20	20
10	113	68	600
20	122	100	600
30	139	114	600
40	147	123	600
50	152	125	600
60	160	131	600
70	164	134	600
80	169	136	600
90	174	140	600
100	178	143	600
110	182	148	600
120	185	151	600
130	155	136	360
140	126	121	119
150	113	107	106
160	100	93	93
170	91	87	84
180	81	80	75
190	75	73	69
200	69	66	64
210	65	62	60
220	60	59	57
230	56	55	53
240	52	51	50

Time (min)	Rft (°C)	Unex. (°C)	Exp. (°C)
0	20	20	20
10	93	63	800
20	138	104	800
30	160	120	800
40	183	135	800
50	204	148	800
60	220	166	800
70	236	183	800
80	249	195	800
90	257	204	800
100	262	212	800
110	269	217	800
120	272	221	800
130	230	201	476
140	188	182	152
150	155	150	128
160	122	118	103
170	109	104	94
180	97	90	85
190	86	81	77
200	76	72	69
210	70	66	64
220	64	61	59
230	58	56	54
240	53	51	50

Time (min)	Rft (°C)	Unex. (°C)	Exp. (°C)
0	20	20	20
10	189	126	1200
20	261	156	1200
30	313	190	1200
40	353	210	1200
50	398	230	1200
60	429	267	1200
70	450	280	1200
80	466	291	1200
90	479	293	1200
100	490	305	1200
110	495	307	1200
120	498	309	1200
130	420	278	722
140	341	248	244
150	288	210	209
160	236	173	173
170	215	160	160
180	195	147	147
190	176	135	133
200	157	123	119
210	121	99	94
220	85	76	69
230	68	67	63
240	52	58	56

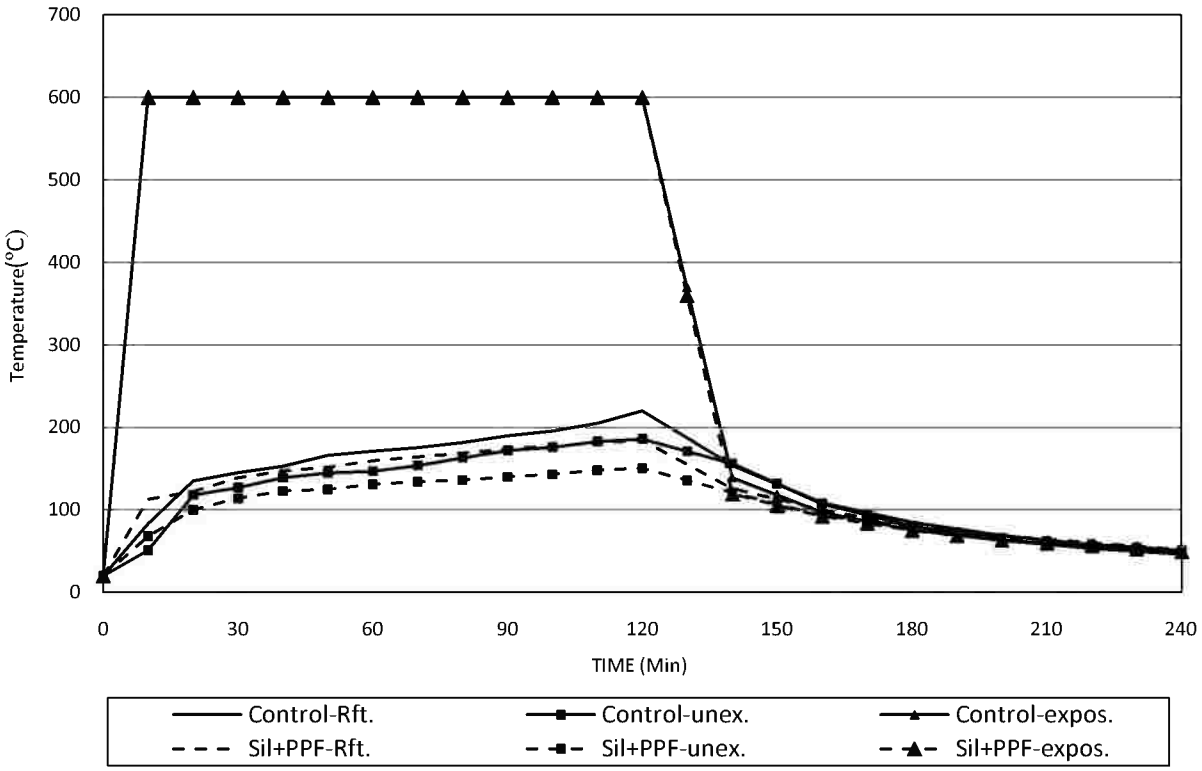
700
600
500
400
300
200
100
0
Temperature(°C)
0
30
60
90
120
150
180
210
240
TIME (Min)
Control-Rft.
Control-unex.
Control-expos.
Sil+PPF-Rft.
Sil+PPF-unex.
Sil+PPF-expos.

(a)

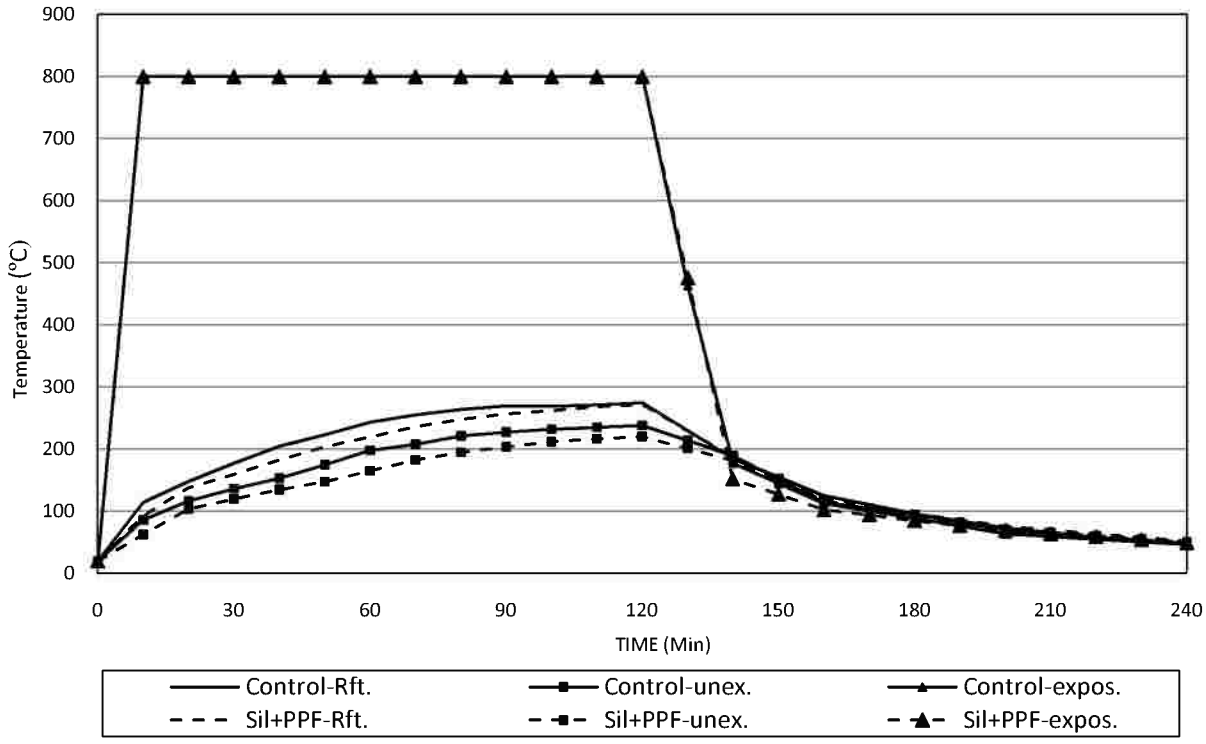
900
800
700
600
500
400
300
200
100
0
Temperature (°C)
0
30
60
90
120
150
180
210
240
TIME (Min)
Control-Rft.
Control-unex.
Control-expos.
Sil+PPF-Rft.
Sil+PPF-unex.
Sil+PPF-expos.

(b)

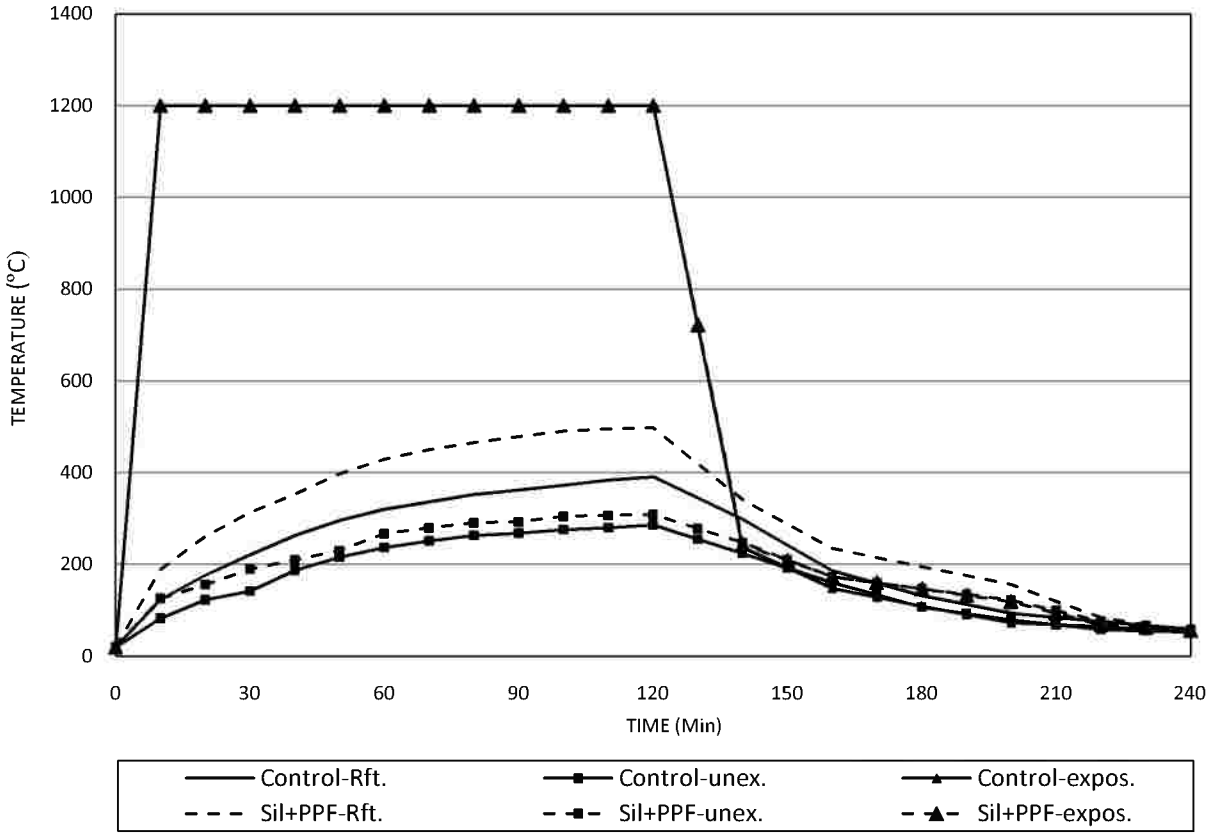

(C)

Fig. 4.44 -Temperature of Rft, unexposed and exposed surface of concrete slabs, with 10% silicafume as cement replacementand and 0.90kg/m^3 polypropylene fiber,when exposed to a) 600°C b) 800°C c)1200°C.

4.2.7.4Temperature of Rft, unexposed and exposed surface of steel fiber concrete slabs.

Time (min)	Rft (°C)	Unex. (°C)	Exp. (°C)
0	20	20	20
10	103	65	600
20	134	100	600
30	145	114	600
40	158	124	600
50	169	135	600
60	175	141	600
70	181	144	600
80	188	153	600
90	192	155	600
100	196	160	600
110	201	166	600
120	204	170	600
130	176	151	368
140	148	132	136
150	126	115	114
160	104	98	91
170	90	83	80
180	76	69	68
190	70	65	63
200	64	60	58
210	59	55	53
220	53	51	49
230	49	47	46
240	46	44	43

Time (min)	Rft (°C)	Unex. (°C)	Exp. (°C)
0	20	20	20
10	93	63	800
20	138	104	800
30	160	120	800
40	183	135	800
50	204	148	800
60	220	166	800
70	236	183	800
80	249	195	800
90	257	204	800
100	262	212	800
110	269	217	800
120	272	221	800
130	230	201	476
140	188	182	152
150	155	150	128
160	122	118	103
170	109	104	94
180	97	90	85
190	86	81	77
200	76	72	69
210	70	66	64
220	64	61	59
230	58	56	54
240	63	57	58

Time (min)	Rft (°C)	Unex. (°C)	Exp. (°C)
0	20	20	20
10	189	126	1200
20	261	156	1200
30	313	190	1200
40	353	210	1200
50	398	230	1200
60	429	267	1200
70	450	280	1200
80	466	291	1200
90	479	293	1200
100	490	305	1200
110	495	307	1200
120	498	309	1200
130	420	278	722
140	341	248	244
150	288	210	209
160	236	173	173
170	215	160	160
180	195	147	147
190	176	135	133
200	157	123	119
210	121	99	94
220	85	76	69
230	68	67	63
240	72	53	56

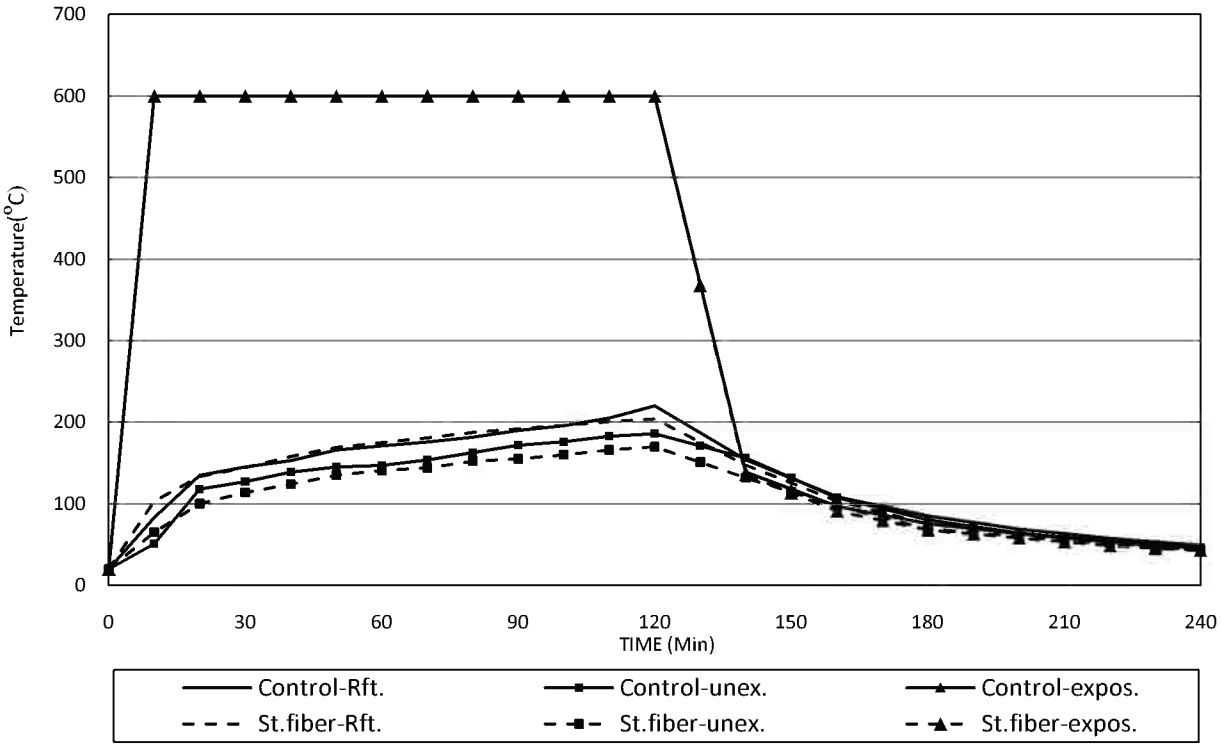
700
600
500
400
300
200
100
0
Temperature(°C)
0
30
60
90
120
150
180
210
240
TIME (Min)
Control-Rft.
Control-unex.
Control-expos.
St.fiber-Rft.
St.fiber-unex.
St.fiber-expos.

(a)

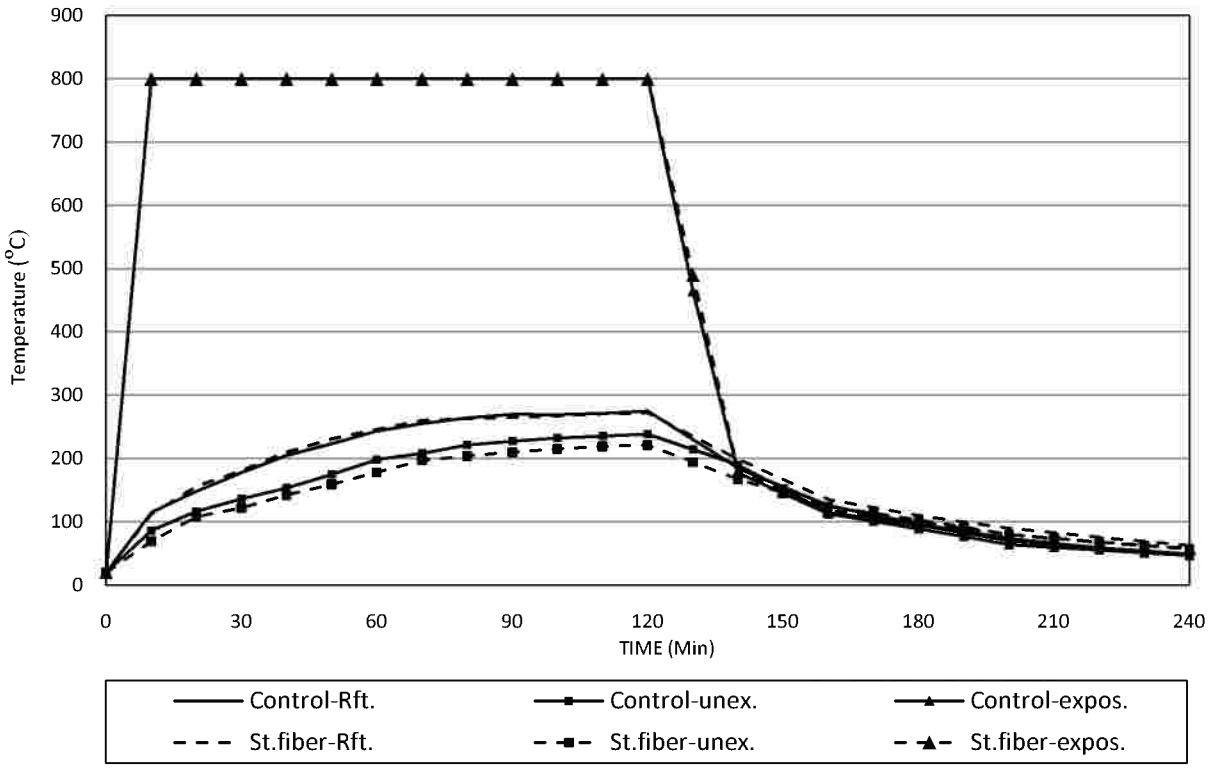
900
800
700
600
500
400
300
200
100
0
Temperature (°C)
0
30
60
90
120
150
180
210
240
TIME (Min)
Control-Rft.
Control-unex.
Control-expos.
St.fiber-Rft.
St.fiber-unex.
St.fiber-expos.

(b)

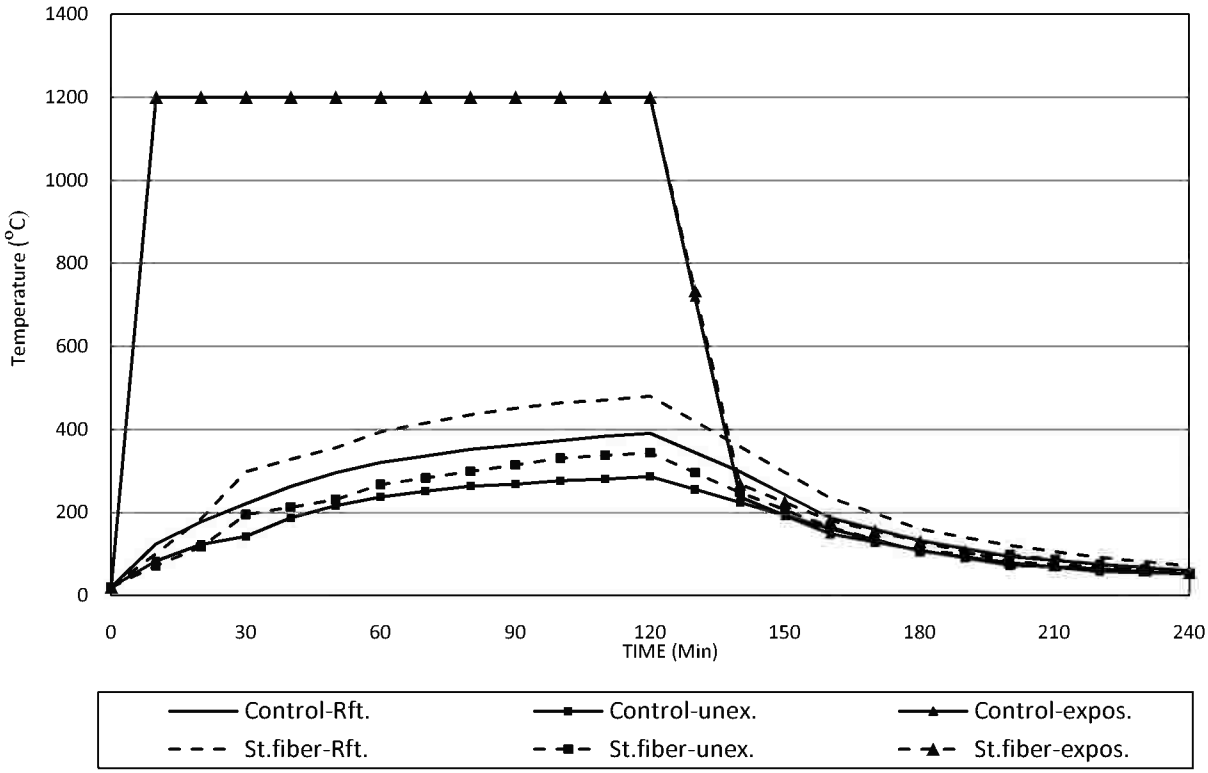

(d)

Fig. 4.45 -Temperature of Rft, unexposed and exposed surface of 20 kg/m³steel fiber concrete slabs when exposed to a) 600°C b) 800°C c)1200°C.

4.2.7.5Temperature of Rft, unexposed and exposed surface of limestone concrete slabs.

A- Temperature of Rft, unexposed and exposed surface of concrete slabs with 10% L.P as cement replacement.

Time (min)	Rft (°C)	Unex. (°C)	Exp. (°C)
0	20	20	20
10	116	60	600
20	142	91	600
30	161	109	600
40	172	120	600
50	180	123	600
60	189	127	600
70	195	138	600
80	198	145	600
90	206	150	600
100	217	158	600
110	218	170	600
120	221	173	600
130	177	148	358
140	134	123	115
150	117	108	101
160	99	92	87
170	87	81	77
180	75	70	67
190	67	63	60
200	58	56	53
210	53	51	49
220	48	47	45
230	45	43	42
240	43	40	39

Time (min)	Rft (°C)	Unex. (°C)	Exp. (°C)
0	20	20	20
10	125	91	800
20	150	108	800
30	191	133	800
40	224	149	800
50	255	163	800
60	284	185	800
70	297	207	800
80	304	222	800
90	310	230	800
100	314	233	800
110	318	236	800
120	325	242	800
130	278	222	496
140	232	202	191
150	197	174	163
160	162	146	134
170	135	122	112
180	109	98	89
190	97	89	82
200	86	80	75
210	78	73	70
220	71	66	64
230	64	59	58
240	56	52	52

Time (min)	Rft (°C)	Unex. (°C)	Exp. (°C)
0	20	20	20
10	109	80	1200
20	169	108	1200
30	236	146	1200
40	298	195	1200
50	360	242	1200
60	390	260	1200
70	422	280	1200
80	435	284	1200
90	448	288	1200
100	456	303	1200
110	467	306	1200
120	471	309	1200
130	409	281	727
140	347	253	254
150	293	218	217
160	239	182	180
170	201	159	156
180	164	135	131
190	137	116	113
200	110	97	94
210	99	88	86
220	88	78	77
230	79	72	71
240	71	66	65

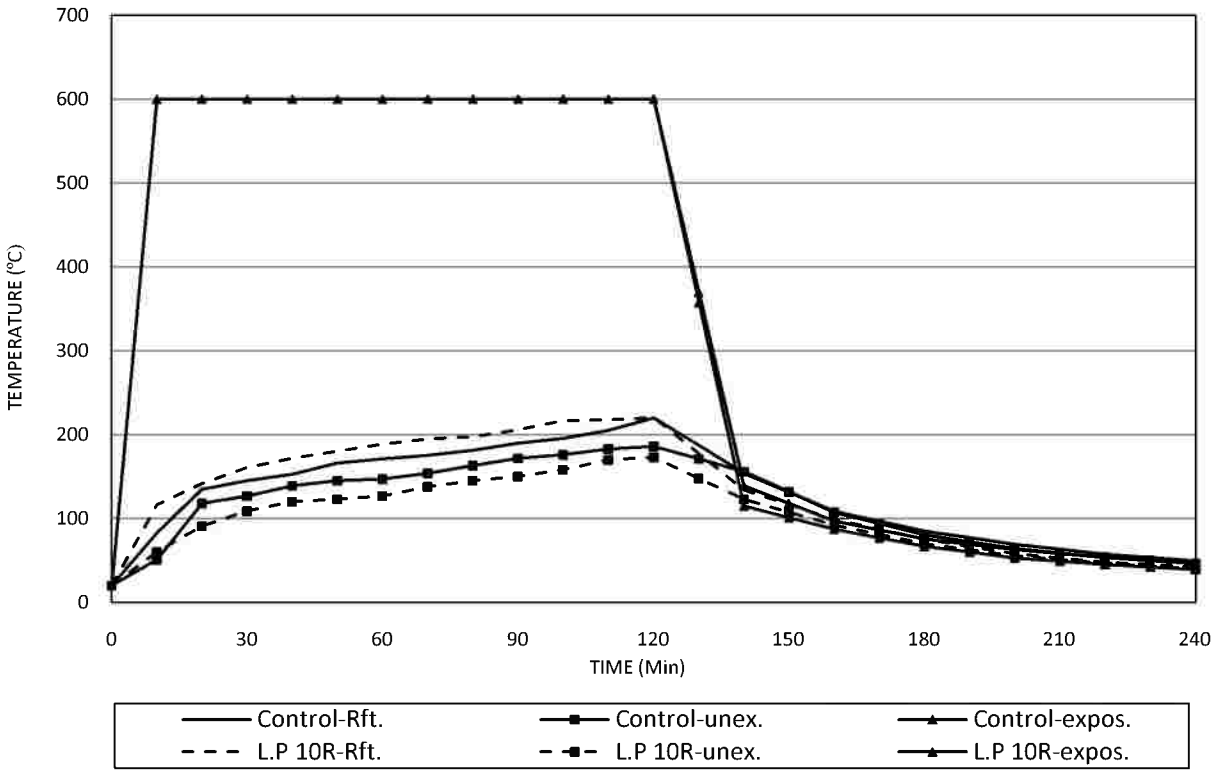
TEMPERATURE (°C)
700
600
500
400
300
200
100
0
0
30
60
90
120
150
180
210
240
TIME (Min)
Control-Rft.
Control-unex.
Control-expos.
L.P 10R-Rft.
L.P 10R-unex.
L.P 10R-expos.

(a)

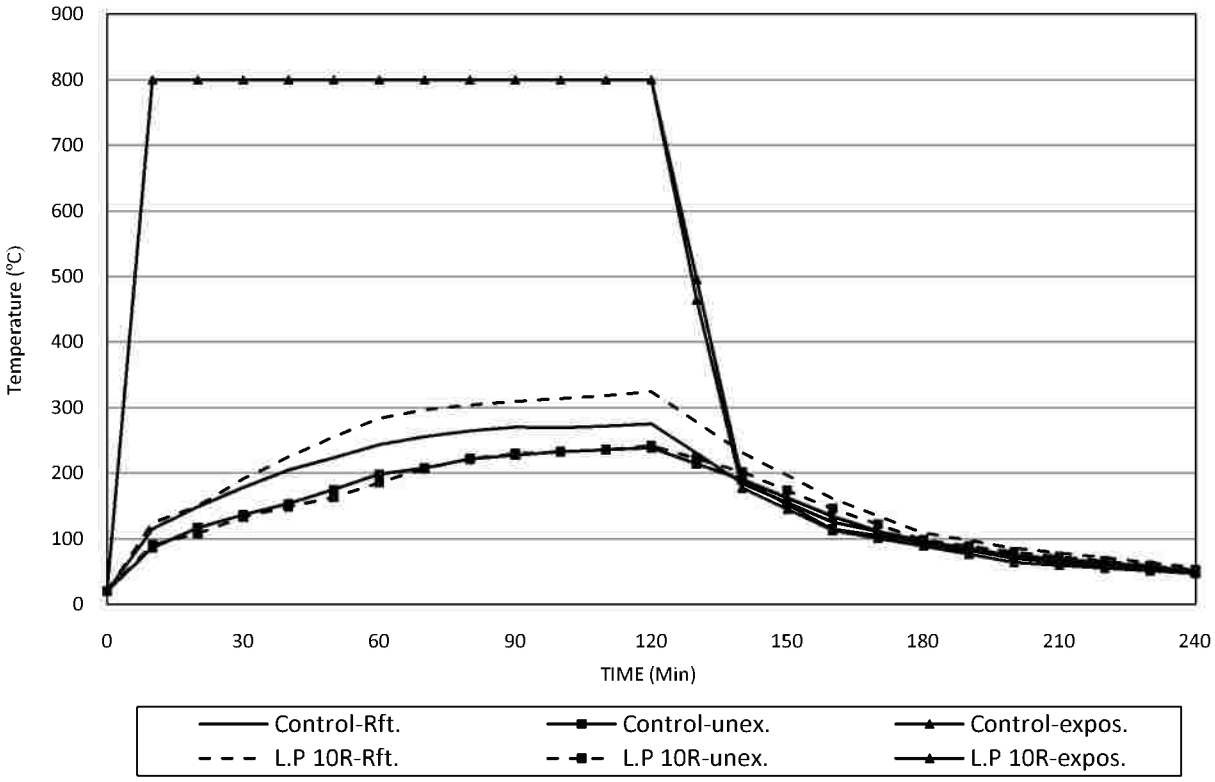
Temperature (°C)
900
800
700
600
500
400
300
200
100
0
0
30
60
90
120
150
180
210
240
TIME (Min)
Control-Rft.
Control-unex.
Control-expos.
L.P 10R-Rft.
L.P 10R-unex.
L.P 10R-expos.

(b)

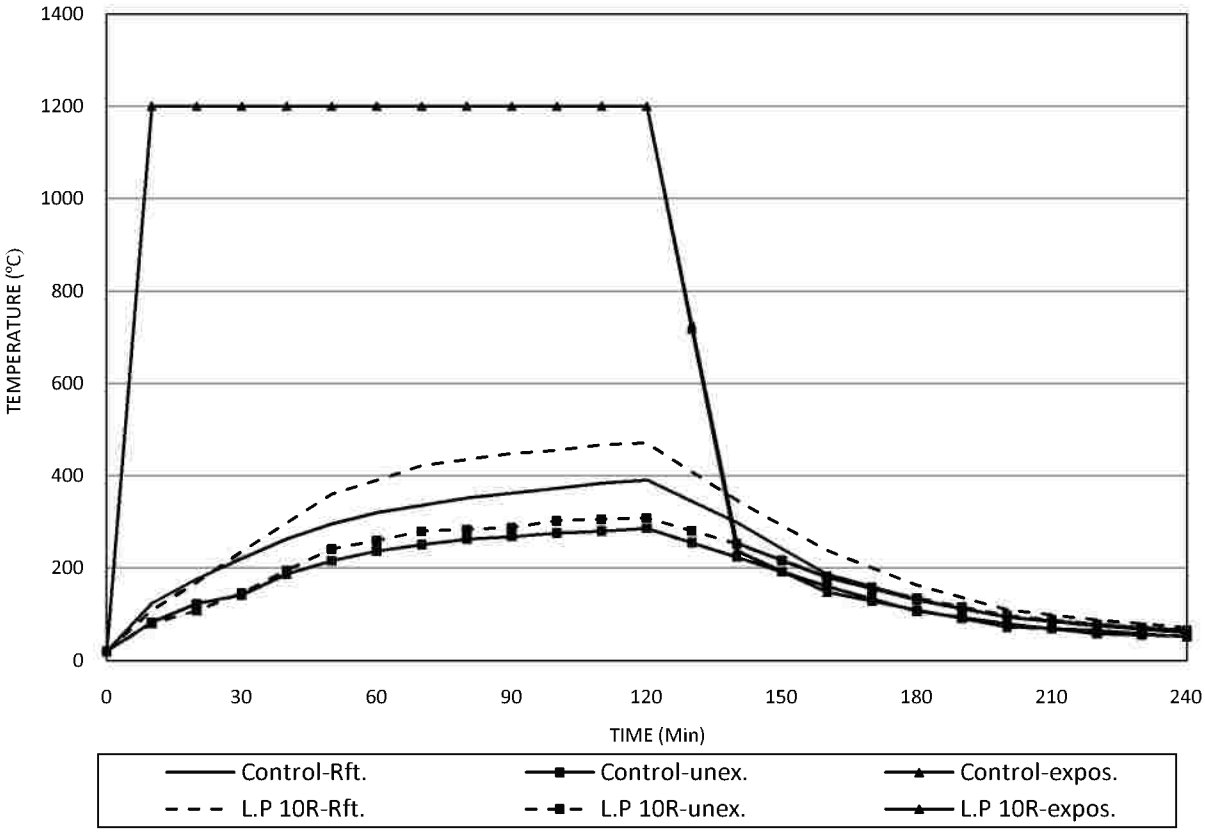

(c)

Fig. 4.46 -Temperature of Rft, unexposed and exposed surface of concrete slabs,with 10% L.P as cement replacement,when exposed to a) 600°C b) 800°C c)1200°C.

B-Temperature of Rft, unexposed and exposed surface of concrete slabs with 15% L.P as cement replacement.

Time (min)	Rft (°C)	Unex. (°C)	Exp. (°C)
0	20	20	20
10	106	78	600
20	127	100	600
30	147	123	600
40	162	138	600
50	168	148	600
60	178	168	600
70	192	185	600
80	214	202	600
90	216	205	600
100	219	209	600
110	223	212	600
120	226	217	600
130	214	213	402
140	202	210	203
150	173	177	169
160	145	143	135
170	126	126	118
180	108	109	101
190	100	100	96
200	92	91	90
210	84	82	82
220	77	73	74
230	71	68	68
240	65	64	62

Time (min)	Rft (°C)	Unex. (°C)	Exp. (°C)
0	20	20	20
10	112	88	800
20	136	110	800
30	156	135	800
40	188	155	800
50	217	173	800
60	242	205	800
70	254	220	800
80	268	233	800
90	278	240	800
100	288	250	800
110	294	253	800
120	299	259	800
130	259	234	493
140	218	208	185
150	186	181	158
160	154	153	130
170	134	133	115
180	114	113	99
190	101	99	87
200	87	84	76
210	78	74	68
220	68	65	61
230	62	59	56
240	57	54	51

Time (min)	Rft (°C)	Unex. (°C)	Exp. (°C)
0	20	20	20
10	116	70	1200
20	202	121	1200
30	258	159	1200
40	310	204	1200
50	366	265	1200
60	388	270	1200
70	411	275	1200
80	426	302	1200
90	440	310	1200
100	447	313	1200
110	456	315	1200
120	463	319	1200
130	420	298	745
140	376	276	289
150	307	231	240
160	237	185	191
170	198	155	162
180	158	125	132
190	137	109	115
200	116	93	98
210	103	84	88
220	90	75	77
230	82	69	71
240	75	63	65

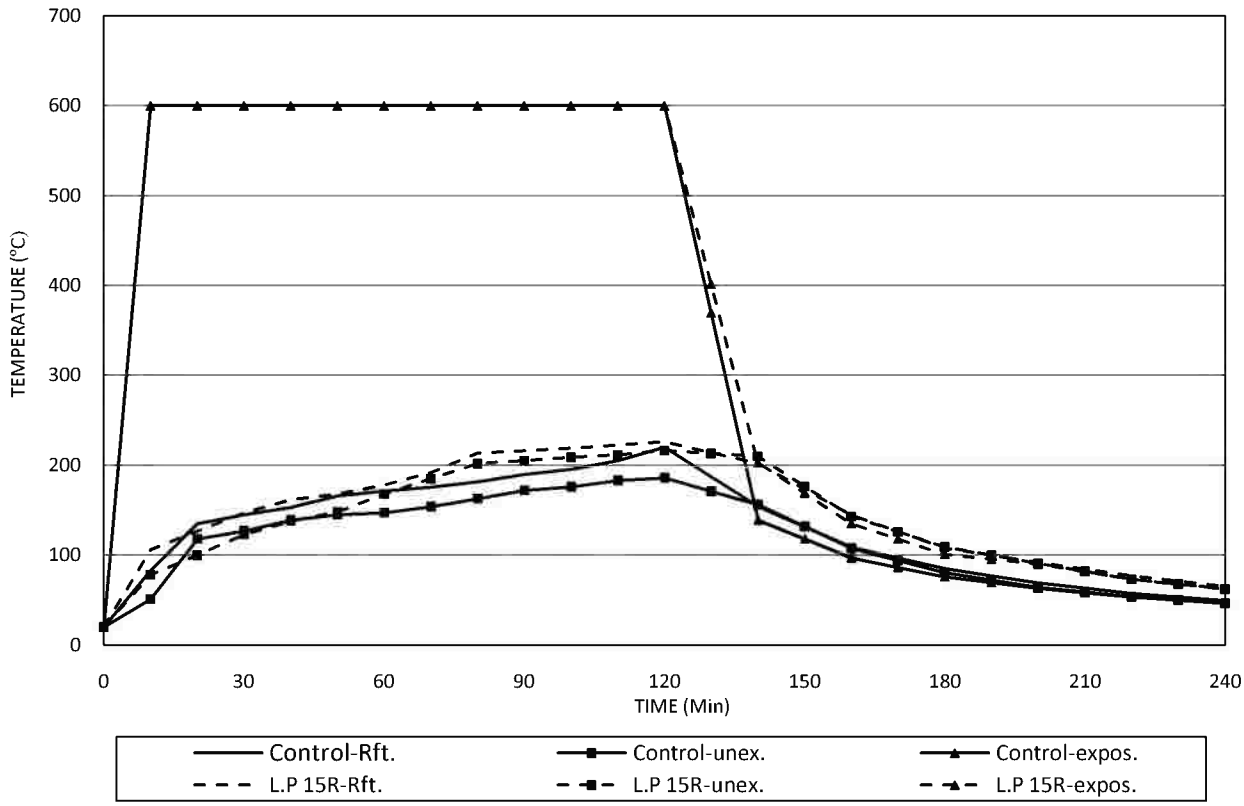
700
600
500
400
300
200
100
0
TEMPERATURE (°C)
0
30
60
90
120
150
180
210
240
TIME (Min)
Control-Rft.
Control-unex.
Control-expos.
L.P 15R-Rft.
L.P 15R-unex.
L.P 15R-expos.

(a)

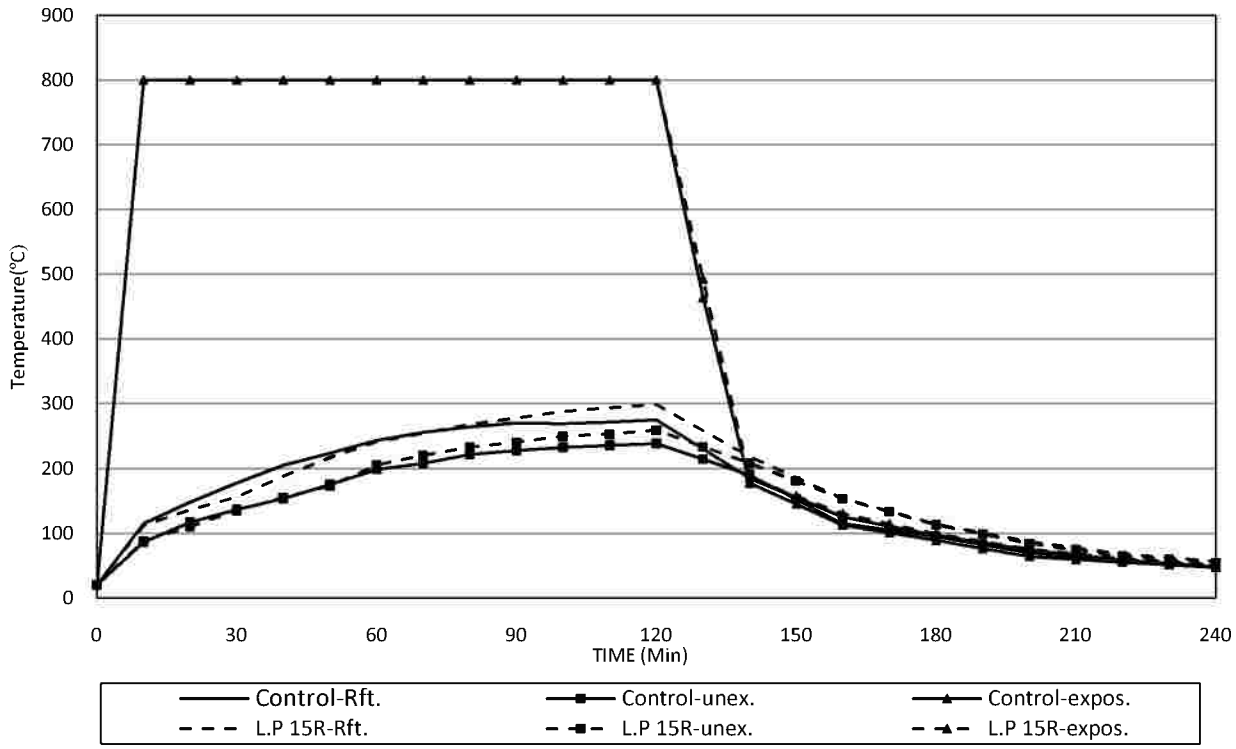
900
800
700
600
500
400
300
200
100
0
Temperature(°C)
0
30
60
90
120
150
180
210
240
TIME (Min)
Control-Rft.
Control-unex.
Control-expos.
L.P 15R-Rft.
L.P 15R-unex.
L.P 15R-expos.

(b)

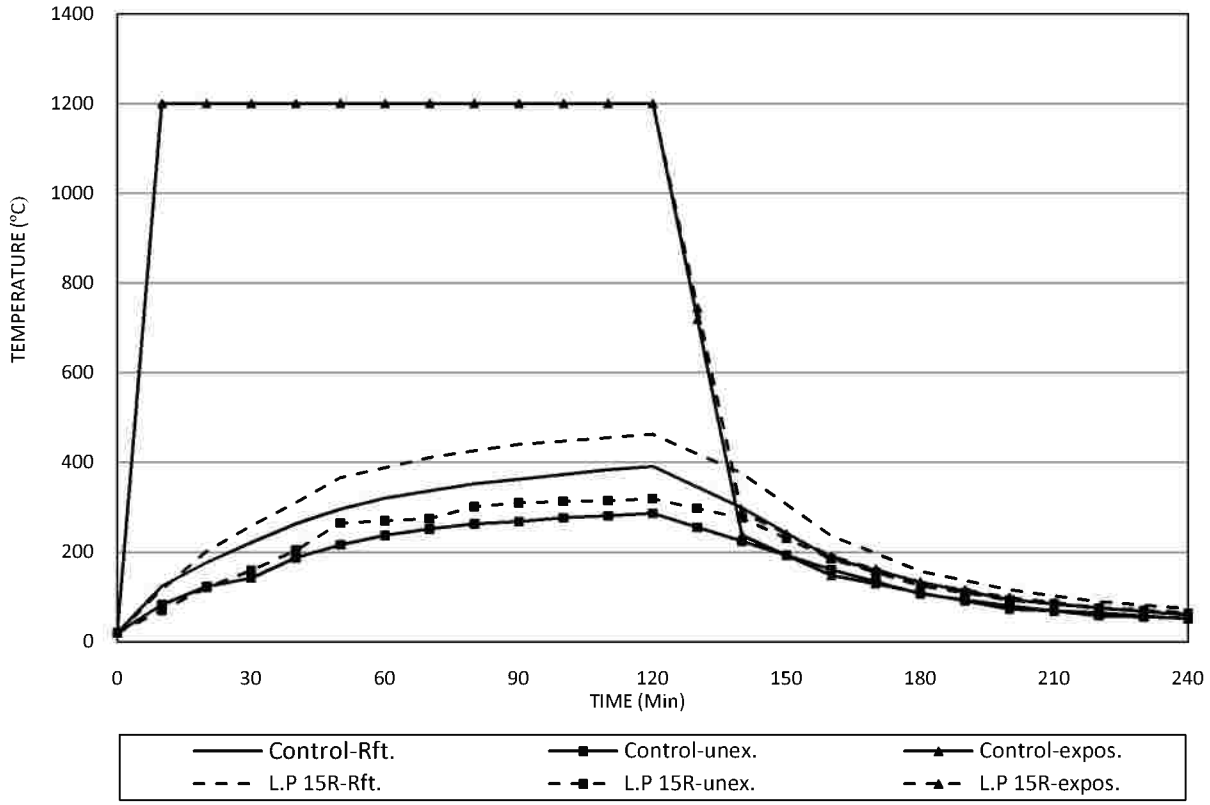

(c)

Fig. 4.47 -Temperature of Rft, unexposed and exposed surface of concrete slabs,with 15% L.P as cement replacement,when exposed to a) 600°C b) 800°C c)1200°C.

C-Temperature of Rft, unexposed and exposed surface of concrete slabs with 10% L.P as cement additive.

Time (min)	Rft (°C)	Unex. (°C)	Exp. (°C)
0	20	20	20
10	106	50	600
20	140	120	600
30	162	128	600
40	168	138	600
50	175	144	600
60	191	149	600
70	202	155	600
80	210	166	600
90	214	175	600
100	216	178	600
110	220	185	600
120	225	188	600
130	197	175	403
140	160	159	207
150	130	134	175
160	100	110	143
170	93	97	124
180	85	83	105
190	75	75	97
200	65	67	89
210	60	64	81
220	55	56	73
230	50	53	68
240	45	47	44

Time (min)	Rft (°C)	Unex. (°C)	Exp. (°C)
0	20	20	20
10	118	85	800
20	153	117	800
30	181	137	800
40	209	156	800
50	241	180	800
60	257	198	800
70	273	214	800
80	284	227	800
90	289	234	800
100	291	238	800
110	292	242	800
120	293	245	800
130	260	224	499
140	227	202	198
150	188	171	162
160	150	139	126
170	133	123	113
180	115	106	100
190	100	93	87
200	85	79	73
210	75	71	67
220	65	62	61
230	60	57	56
240	56	52	51

Time (min)	Rft (°C)	Unex. (°C)	Exp. (°C)
0	20	20	20
10	116	70	1200
20	202	121	1200
30	258	159	1200
40	310	204	1200
50	366	265	1200
60	388	270	1200
70	411	275	1200
80	426	302	1200
90	440	310	1200
100	447	313	1200
110	456	315	1200
120	463	319	1200
130	420	298	745
140	376	276	289
150	307	231	240
160	237	185	191
170	198	155	162
180	158	125	132
190	137	109	115
200	116	93	98
210	103	84	88
220	90	75	77
230	82	69	71
240	75	63	65

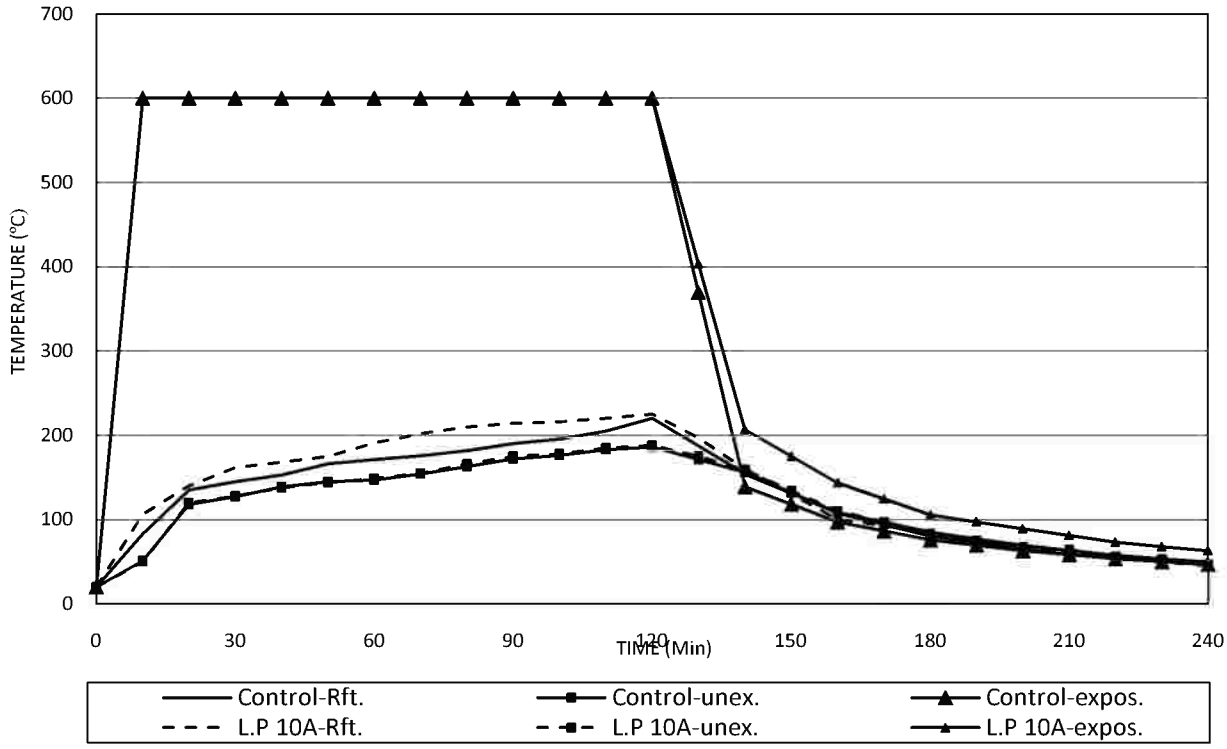

(a)

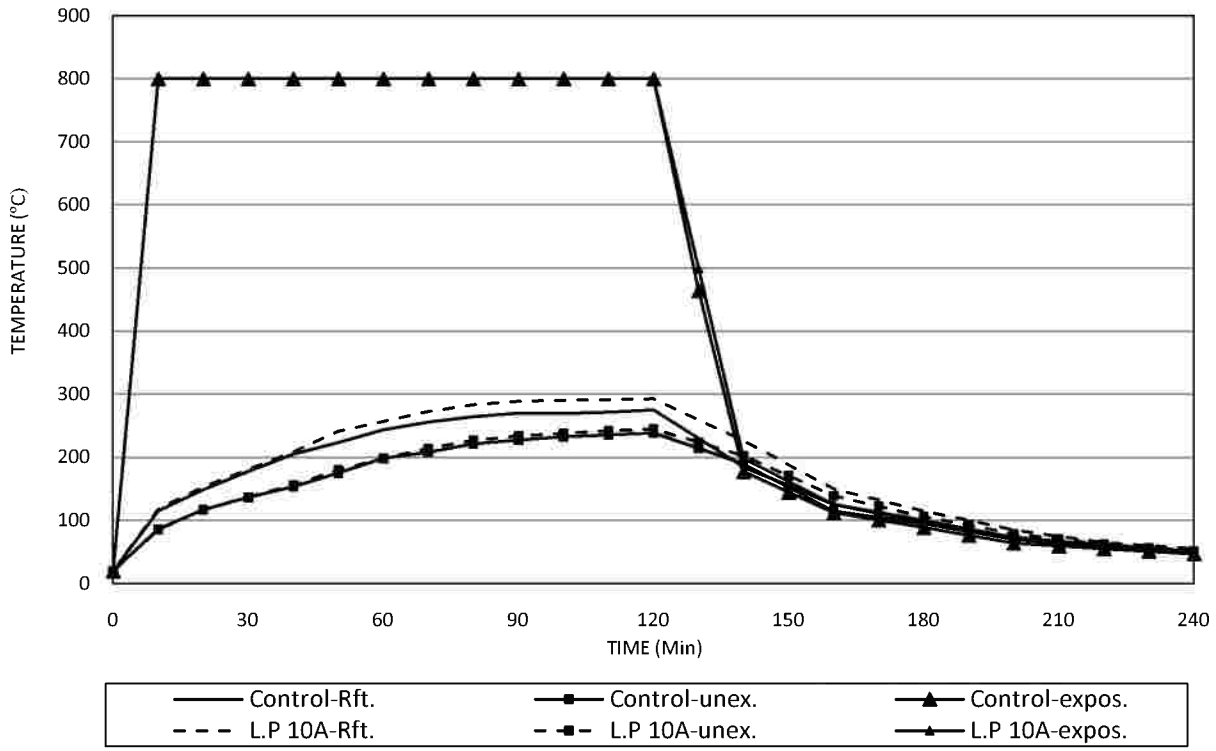

(b)

Fig. 4.48 -Temperature of Rft, unexposed and exposed surface of concrete slabs,with 10% L.P as cement additive,when exposed to a) 600°C b) 800°C c)1200°C.

D- Temperature of Rft, unexposed and exposed surface of concrete slabs with 15% L.P as cement additive.

Time (min)	Rft (°C)	Unex. (°C)	Exp. (°C)
0	20	20	20
10	108	65	600
20	135	107	600
30	156	118	600
40	180	128	600
50	194	140	600
60	200	146	600
70	203	155	600
80	208	159	600
90	213	167	600
100	217	171	600
110	221	175	600
120	222	179	600
130	188	162	369
140	154	145	137
150	130	124	115
160	106	102	92
170	92	88	80
180	77	74	69
190	72	68	64
200	66	63	60
210	61	58	57
220	56	54	54
230	52	50	53
240	49	47	51

Time (min)	Rft (°C)	Unex. (°C)	Exp. (°C)
0	20	20	20
10	112	68	800
20	146	100	800
30	173	122	800
40	204	144	800
50	233	161	800
60	258	183	800
70	269	194	800
80	283	213	800
90	290	220	800
100	295	227	800
110	300	230	800
120	302	237	800
130	254	208	484
140	206	179	168
150	175	155	141
160	144	130	114
170	125	115	102
180	105	100	89
190	93	88	80
200	81	75	71
210	73	69	65
220	65	62	59
230	59	57	55
240	54	53	50

Time (min)	Rft (°C)	Unex. (°C)	Exp. (°C)
0	20	20	20
10	138	84	1200
20	212	113	1200
30	260	143	1200
40	307	170	1200
50	358	241	1200
60	388	250	1200
70	405	261	1200
80	423	272	1200
90	434	286	1200
100	445	300	1200
110	457	309	1200
120	470	320	1200
130	423	298	749
140	375	276	299
150	316	231	253
160	256	185	207
170	216	158	174
180	175	130	142
190	155	118	129
200	135	105	116
210	119	93	103
220	103	80	90
230	92	73	81
240	80	65	72

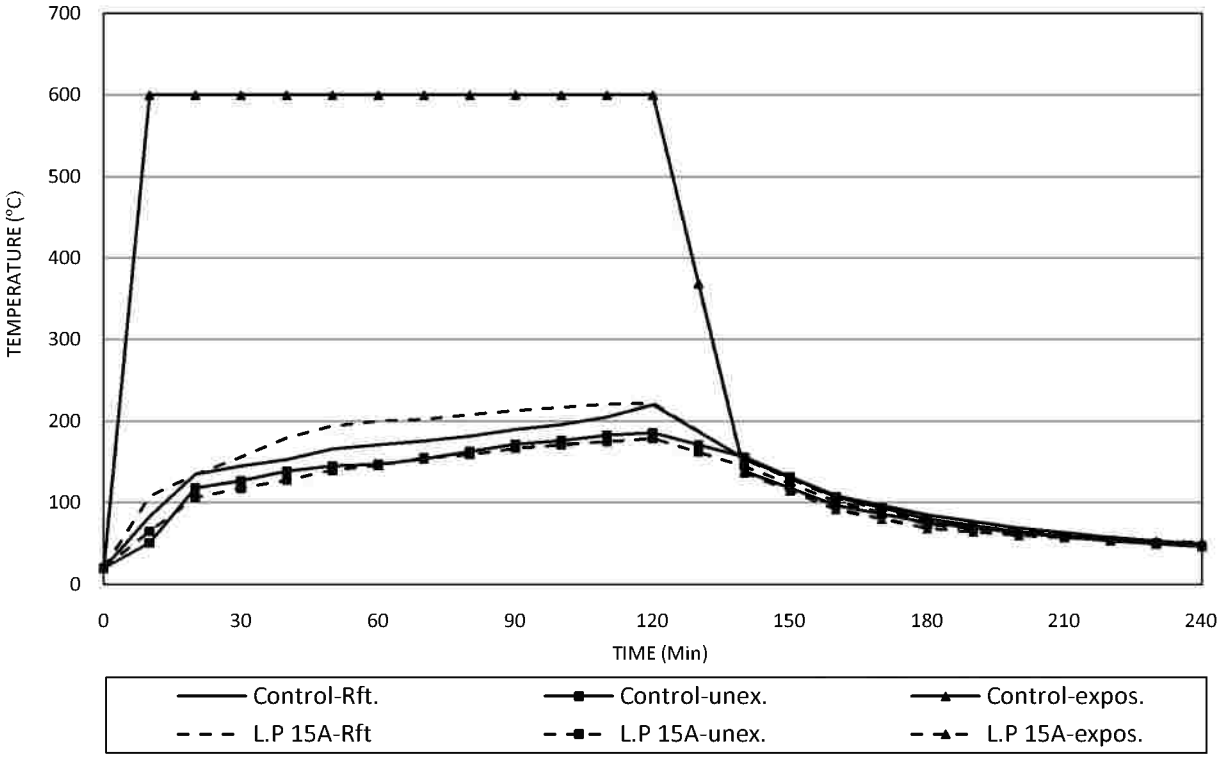
700
600
500
400
300
200
100
0
TEMPERATURE (°C)
0
30
60
90
120
150
180
210
240
TIME (Min)
Control-Rft.
Control-unex.
Control-expos.
L.P 15A-Rft
L.P 15A-unex.
L.P 15A-expos.

(a)

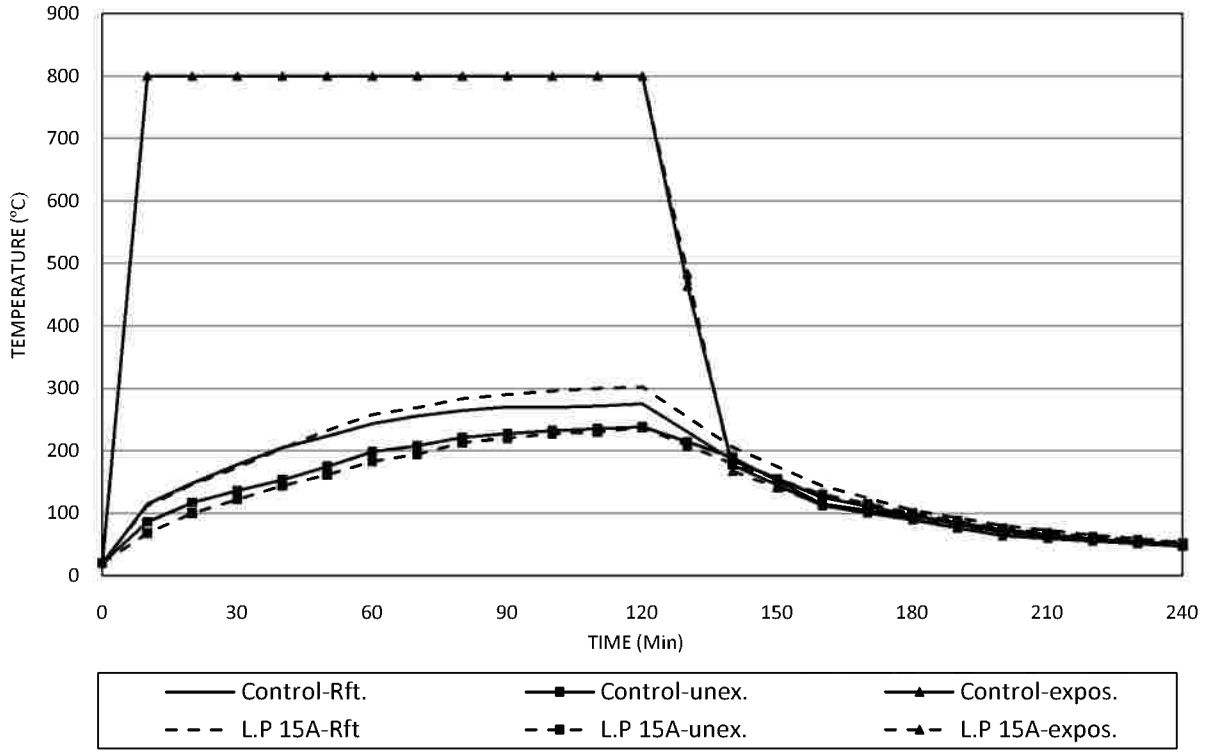
900
800
700
600
500
400
300
200
100
0
TEMPERATURE (°C)
0
30
60
90
120
150
180
210
240
TIME (Min)
Control-Rft.
Control-unex.
Control-expos.
L.P 15A-Rft
L.P 15A-unex.
L.P 15A-expos.

(b)

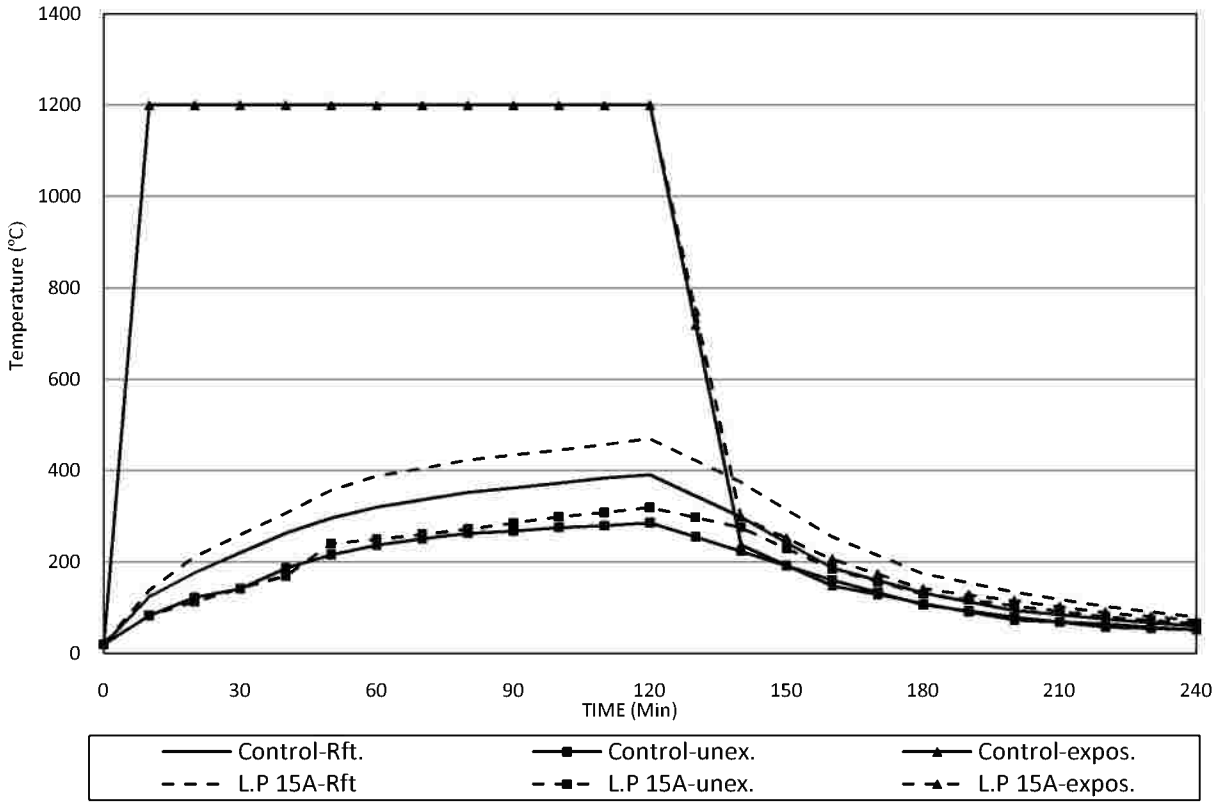

(c)

Fig. 4.49 -Temperature of Rft, unexposed and exposed surface of concrete slabs,with 15% L.P as cement additive,when exposed to a) 600°C b) 800°C c)1200°C.

4.2.7.6Temperature of Rft, unexposed and exposed surface of concrete slabs with 10% bentonite as cement replacement.

The reinforced concrete slabsresemble 10% bentonite as a partial replacement of cement mass were exposed to different degrees of temperature at 600, 800 and 1200°C. The temperatures of Rft, unexposed and exposed surface of the slabs have been tabluted in **Table 4.11**and respectively and plotted in **Figs. 4.50(a, b, c)** consecutively. It can beseen from **Figs. 4.50(a, b, c)** that the temperature of Rft, unexposed and exposed surface of the bentonite slabs at each experimental temperatureis more than the measured temperature of control mix slabs. The Rft temperature was increased when compared to the control mix by about 9, 15 and 20% at 600, 800 and 1200°C respectively, which means that the difference in Rft temperature for M-(Ben 10R) and M-C increases with the increasing of the exposed temperatureas. This aggressive effect in protecting Rft from elevated temperature may be attributed to the more fissuresof bentonite that makes large cracks at high temperature. As confirmation to this resul, the temperature of unexposed surfaces of the bentonite concrete slabs were more than the counterpart of control mix by about 5, 3 and 14% at 600, 800 and 1200°C respectively.

Table 4.11 Temperature of Rft, unexposed and exposed surface of reinforced concrete slabs with 10% bentonite as cement replacement.

Time (min)	Rft (°C)	Unex. (°C)	Exp. (°C)
0	20	20	20
10	110	76	600
20	132	93	600
30	145	100	600
40	175	126	600
50	191	137	600
60	204	148	600
70	210	158	600
80	220	166	600
90	225	175	600
100	230	184	600
110	236	192	600
120	239	196	600
130	211	177	379
140	182	157	158
150	164	145	143
160	146	132	128
170	129	119	113
180	111	105	98
190	101	97	90
200	91	89	82
210	86	84	77
220	80	79	71
230	74	73	66
240	68	66	60

Time (min)	Rft (°C)	Unex. (°C)	Exp. (°C)
0	20	20	20
10	119	88	800
20	141	105	800
30	181	124	800
40	208	143	800
50	238	167	800
60	266	192	800
70	279	200	800
80	291	218	800
90	303	224	800
100	308	228	800
110	313	238	800
120	318	246	800
130	265	216	486
140	212	185	171
150	181	159	146
160	151	132	121
170	126	112	104
180	100	91	87
190	90	82	78
200	80	72	69
210	73	67	65
220	66	62	60
230	59	56	55
240	52	50	49

Time (min)	Rft (°C)	Unex. (°C)	Exp. (°C)
0	20	20	20
10	142	92	1200
20	184	117	1200
30	248	149	1200
40	328	219	1200
50	363	247	1200
60	395	265	1200
70	427	283	1200
80	437	297	1200
90	447	310	1200
100	458	319	1200
110	465	322	1200
120	470	325	1200
130	372	268	704
140	274	210	208
150	235	184	183
160	196	157	157
170	168	136	138
180	140	114	118
190	121	98	102
200	102	81	86
210	89	73	76
220	76	64	65
230	69	59	60
240	62	53	55

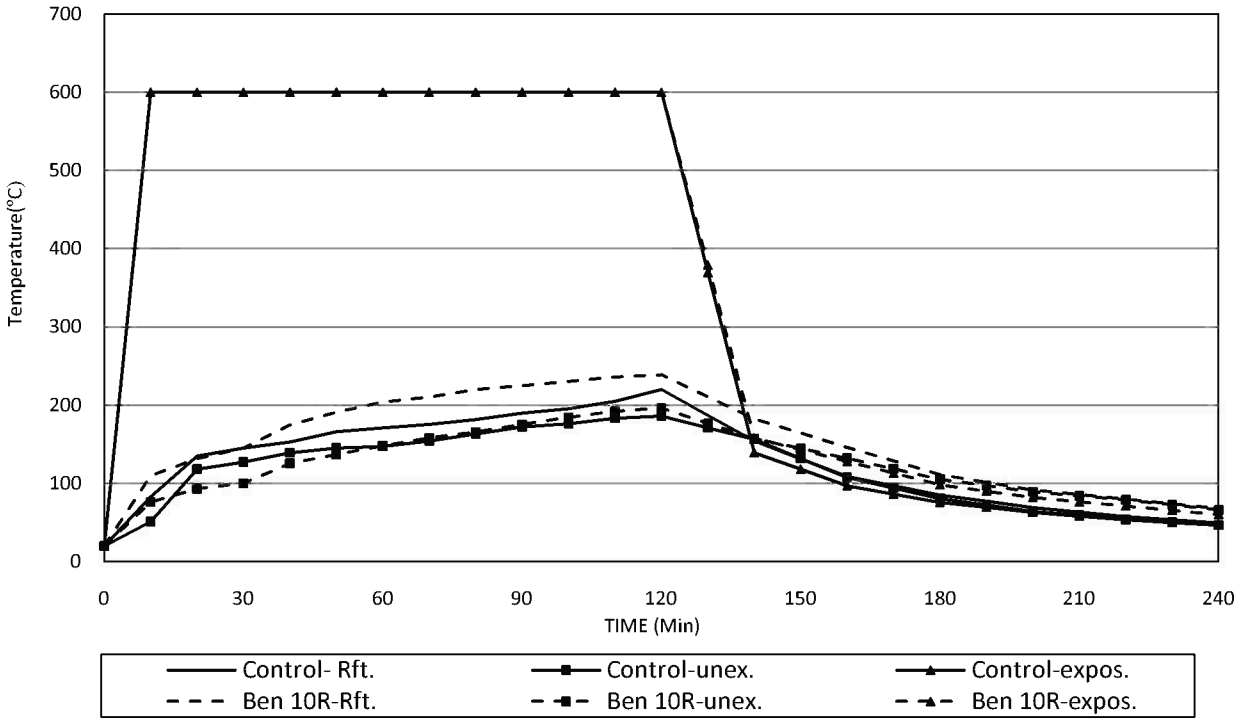
700
600
500
400
300
200
100
0
Temperature(°C)
0
30
60
90
120
150
180
210
240
TIME (Min)
Control- Rft.
Control-unex.
Control-expos.
Ben 10R-Rft.
Ben 10R-unex.
Ben 10R-expos.

(a)

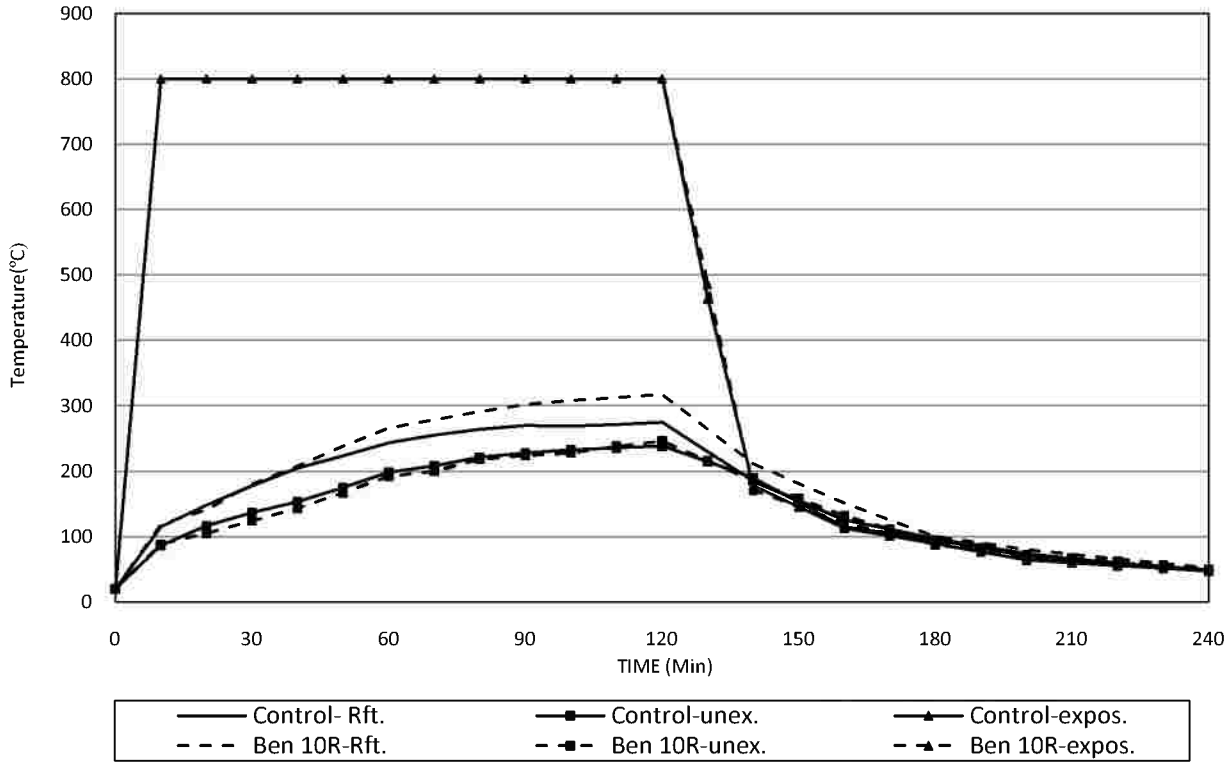
900
800
700
600
500
400
300
200
100
0
Temperature(°C)
0
30
60
90
120
150
180
210
240
TIME (Min)
Control- Rft.
Control-unex.
Control-expos.
Ben 10R-Rft.
Ben 10R-unex.
Ben 10R-expos.

(b)

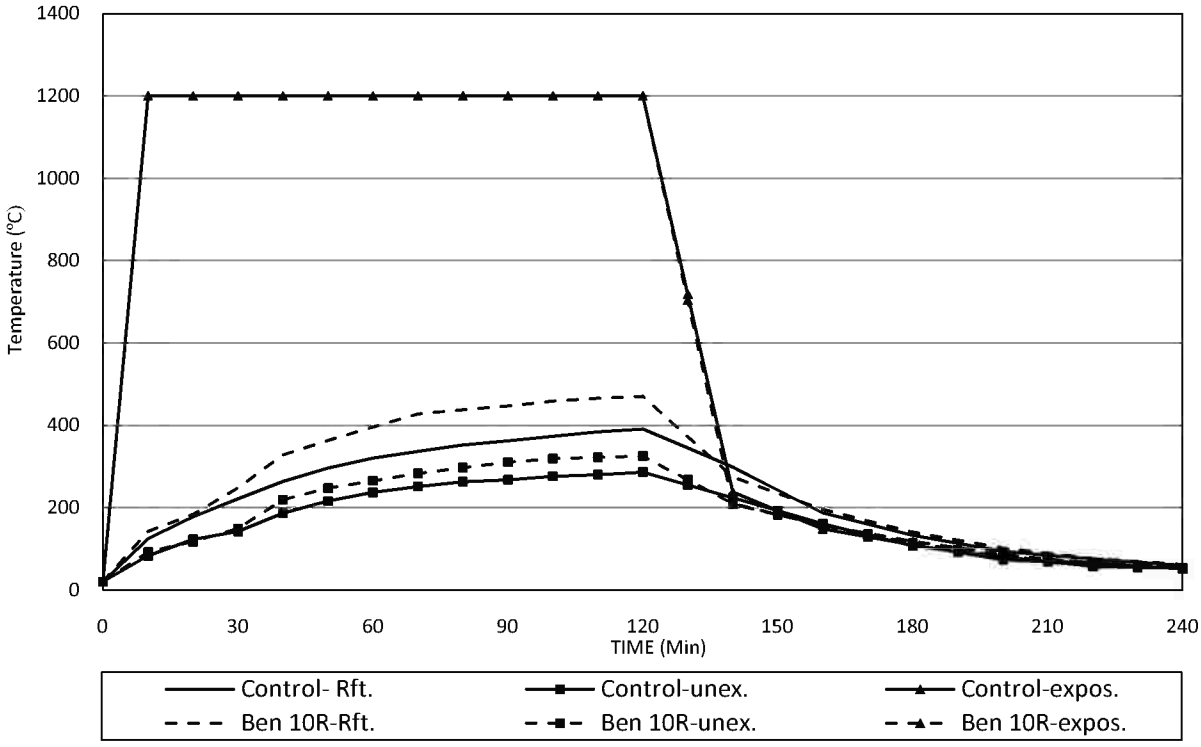

(c)

Fig. 4.50-Temperature of Rft, unexposed and exposed surface of concrete slabs,with 10% bentonite as cement replacement,when exposed to a) 600°C b) 800°C c)1200°C.

From the previous tables and charts, the reinforcement and the unexposed surface temperatures, after 2 hrs exposure, were taken as a criterion to study the effect of silicafume, PPF, steel.F, L.P and bentonite on the enhancementof the fire endurance and protect the Rft and the concrete from the fire.The relative temperature of unexposed surface and reinforcement temperature were recorded in **Tables 4.12** and **4.13** at 600°C and 800°C respectively. From **Figs. 4.51** to**Fig. 4.54** it can be noted that after exposure to 600 and 800°C for 2 hrs, the unexposed surface and steel temperatures inside the slabs in M-Silica, M-(Silica+ PPF), M-(Steel.F) and M-(L.P.15A) are less than that of the unexposed surface and steel temperatures of the control slabs. On the other hand the trend of the time- temperature relation of M-PPF, M-(L.P.10R),M-(L.P.15R), M-(L.P.10A) and M-(Ben.10R) shows a slight negative effect in protecting the reinforcement from fire.

Table 4.12 -Relative temperaturesof steel and unexposed surfaceof slabs after being exposed to 600ºC for 2 hr.

Mixdesignation	Relative unexposed surface temp. (%)	Relative steel temperature (%)
M-Control	100	100
M-Silica	88	97
M-PPF	102	104
M-(Silica+ PPF)	81	84
M-(Steel.F)	91	93
M-(L.P.10R)	103	100
M-(L.P.15R)	116	103
M-(L.P.10A)	101	102
M-(L.P.15A)	96	101
M-(Ben.10R)	105	109

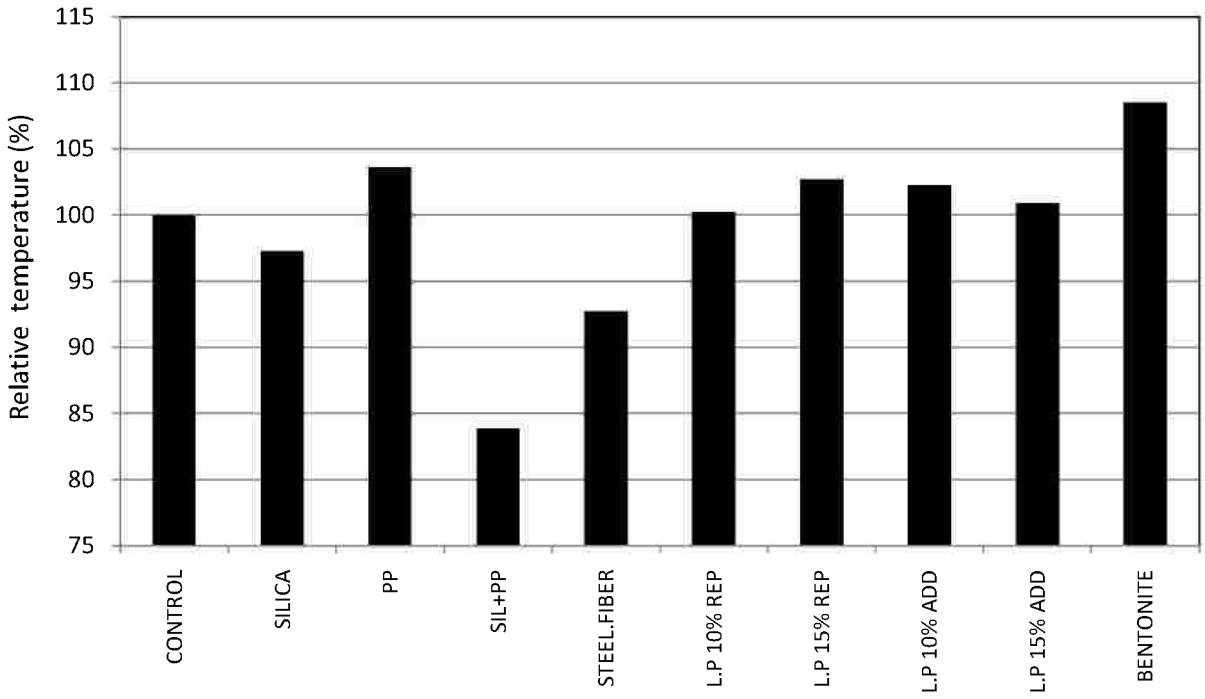

Fig. 4.51 - Relative steel temperatures inside slabs exposure to 600ºC for 2 hrs.

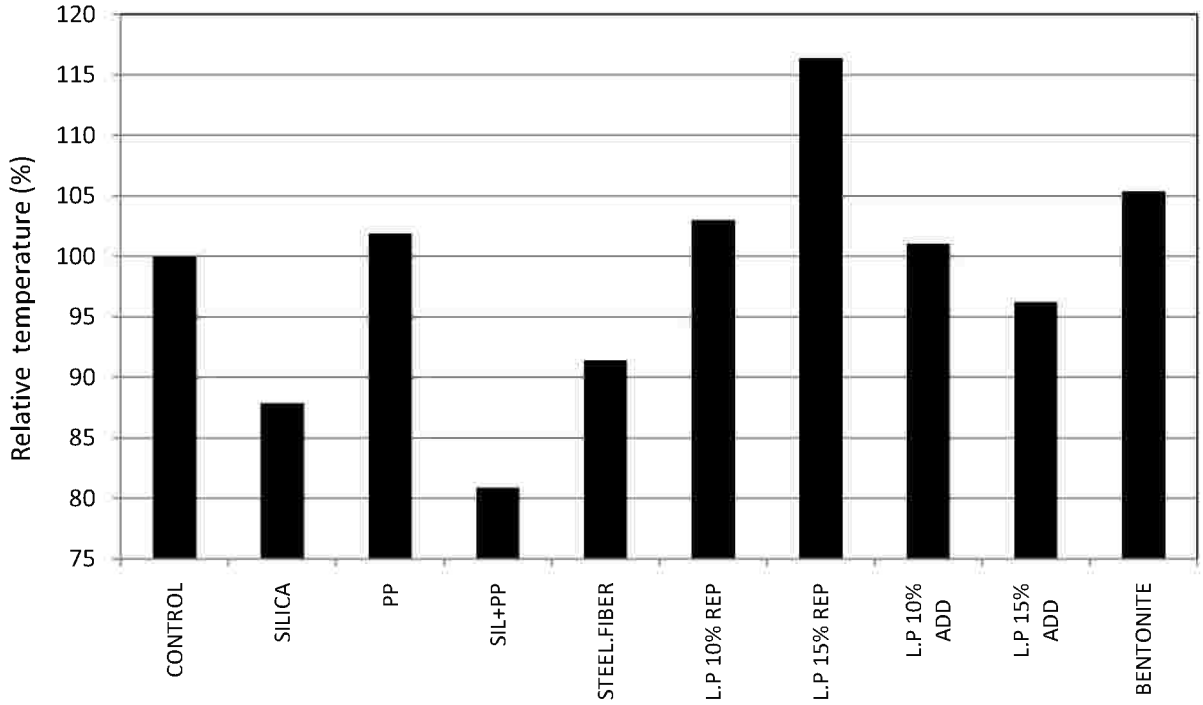

Fig. 4.52- Relativeunexposed surface temperaturesof slabs exposure to 600ºC for 2 hr.

Table 4.13: Relative temperaturesof steel and unexposed surfaceof slabs after being exposed to 800ºC for 2 hrs.

Mixdesignation	Relative unexposed surface temp. (%)	Relative steel temperature (%)
M-Control	100	100
M-Silica	90	99
M-PPF	95	110
M-(Silica+ PPF)	92	99
M-(Steel.F)	92	99
M-(L.P.10R)	101	118
M-(L.P.15R)	108	109
M-(L.P.10A)	103	107
M-(L.P.15A)	99	110
M-(Ben.10R)	103	115

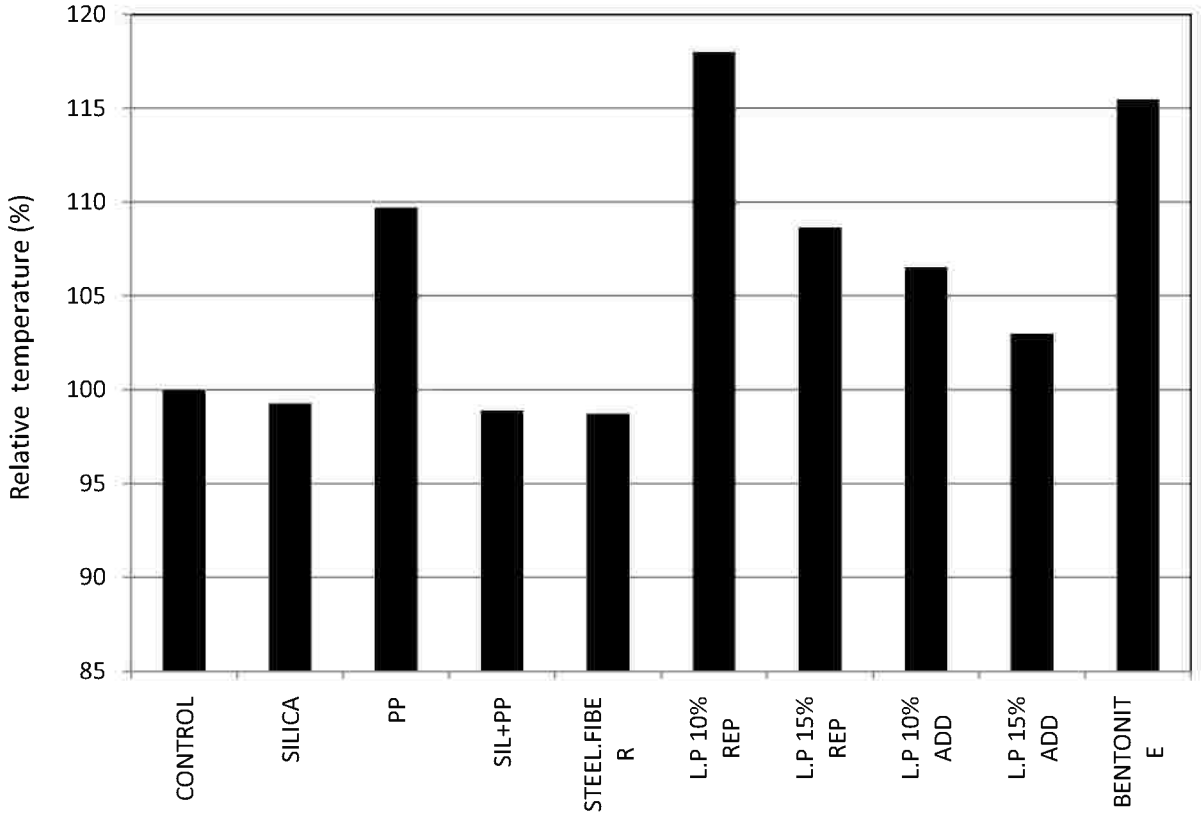

Fig. 4.53 - Relative steel temperatures inside slabs when exposed to 800ºC for 2 hrs.

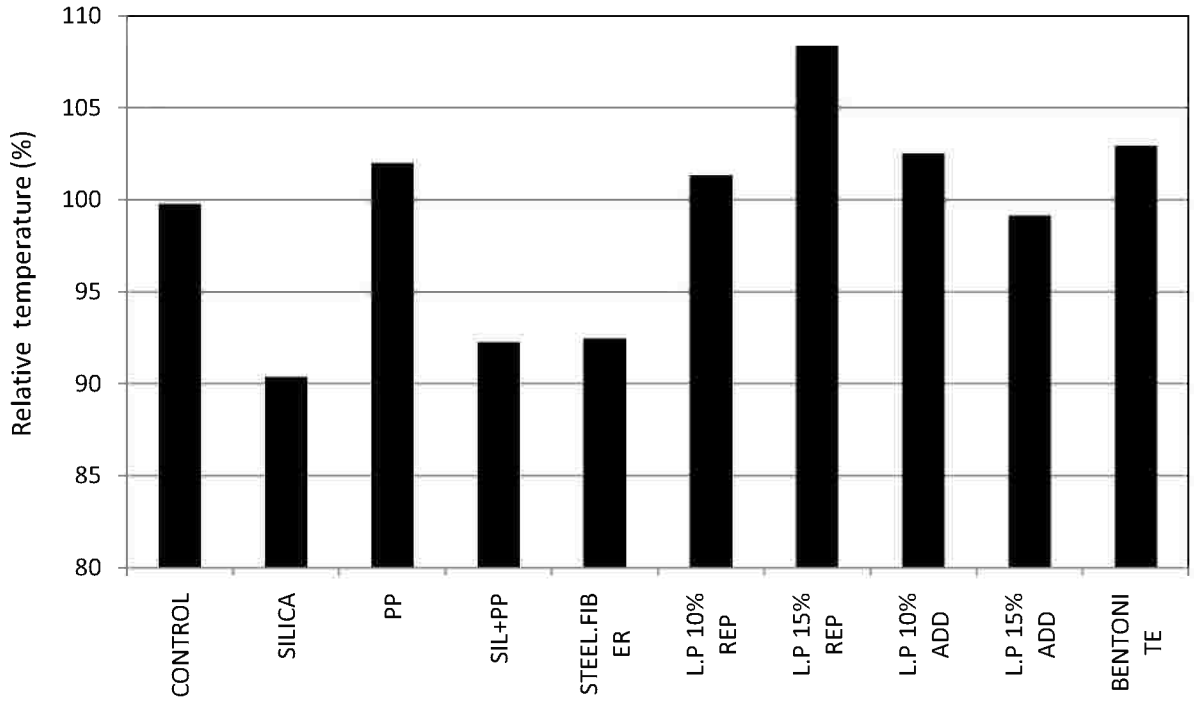

Fig. 4.54 - Relative unexposed surface temperaturesof slabs when exposed to 800ºC for 2 hrs.

It can be noted from **Table 4.14**that after 2 hrs of air cooling, the difference in reinforcement temperature inside the exposed slabs at 600 and 800ºC is rather small. Also it appears that the unexposed surface temperature is slightly more than the exposed surface after 2 hrs of air cooling. This may be attributed to the heat transportation from exposed (with higher temperature) to unexposed surface (lower temperature) after heating.

Table 4.14: The temperature of exposed and unexposed surface of the concrete slabs after 2hrs of air cooling regime.

Mixdesignation	Exposed surface	Unexposed surface
M-Control	47	46
M-Silica	61	59
M-PPF	45	44
M-(Silica+ PPF)	51	50
M-(Steel.F)	44	43
M-(L.P.10R)	40	39
M-(L.P.15R)	64	62
M-(L.P.10A)	47	44
M-(L.P.15A)	47	51
M-(Ben.10R)	66	60

4.3 Phase 3: Results of experiments carried out on mortars (as a plastering for concrete).

The aim of this part that isreported here is studying the interaction of the CEM I with some materials like ceramic powder, melamine powder, brick clay powder and bentonite based on a series of short term experiments (28 days) under elevated temperatures. The changes in the chemical and physical properties of the modified mortars are measured through the analysis of some parameters.

4.3.1 Compressive strength.

Many authors **[Georgali et al., 2005; Serdar et al., 2008; Fu et al., 2004;Fares et al., 2009]** agree on the fact that strength decreases with increasingthe temperature of the exposure.When exposed to high temperatures, mortar suffers damage which consistsof cracking and significant physicochemical changes that influence mechanicalbehavior. So the compressive strength of all studied mortars was observed as following.

4.3.1.1 Compressive strength test results of the conventional (reference) mortar.

The compressive strength of the traditional mortar which containscement content 400 kg/m³, 0.40 w/c ratio and cement : sand = 1:2.75 was graphically presented in **Fig. 4.55**which shows that the residual compressive strength was reduced with the increase in the elevated temperature. The compressive strength is reduced by about 20, 25 and 60% if exposed to 200, 400 and 600°C. The major reduction in the residual compressive strength of the traditional mortars is considerable at 600°C.

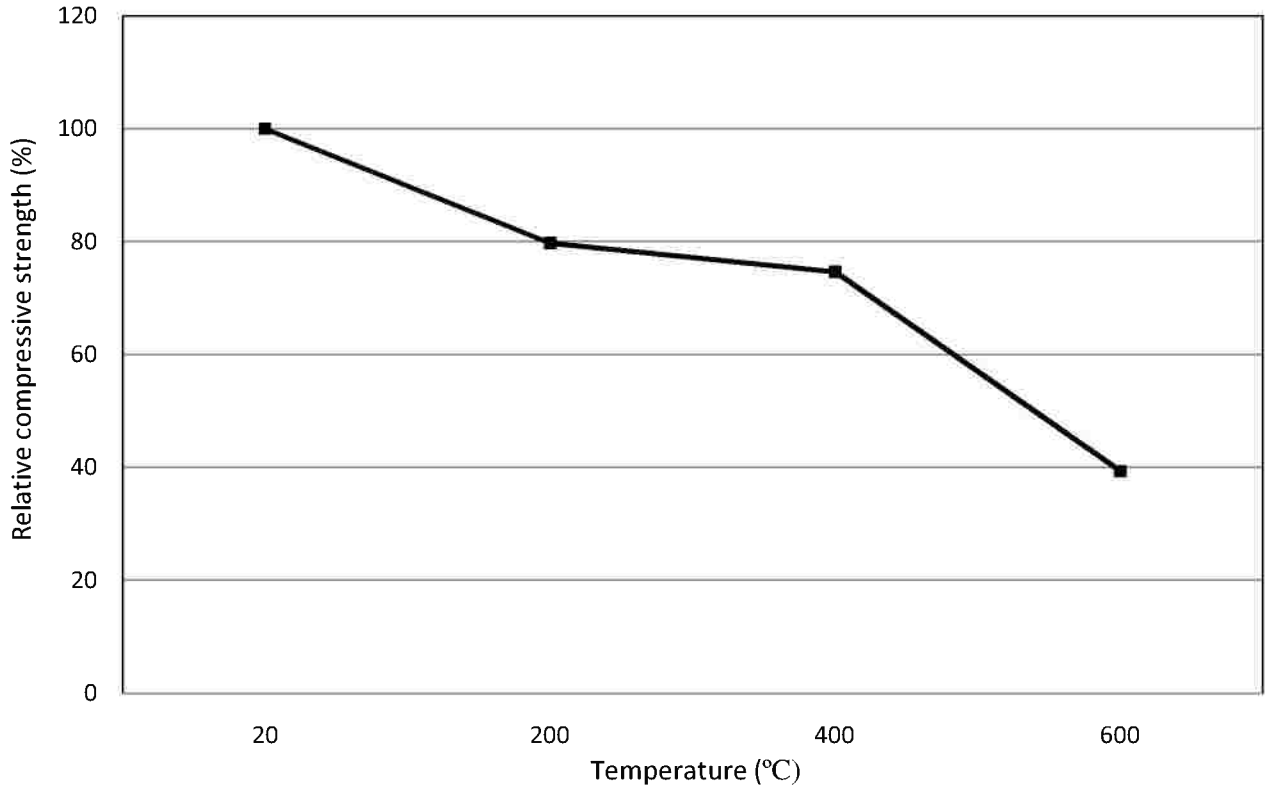

Fig. 4.55 - Relative compressive strength of conventional mortar at room temperature and after exposed to 200, 400 and 600°C.

4.3.1.2 Compressive strength test results of the limestone Portlandcement mortar.

Al-Amreya limestone portlandcement was used and the relative compressive strength was observed as shown in **Fig. 4.56**. It is clear that the usage of limestone cement instead of CEM I increase the residual compressive strength at elevated temperature up to 600°C. Limestone Portland cement increases the compressive strength by about 10, 30, 6 and 11% if compared withreference mortar at 20, 200, 400 and 600°C respectively.

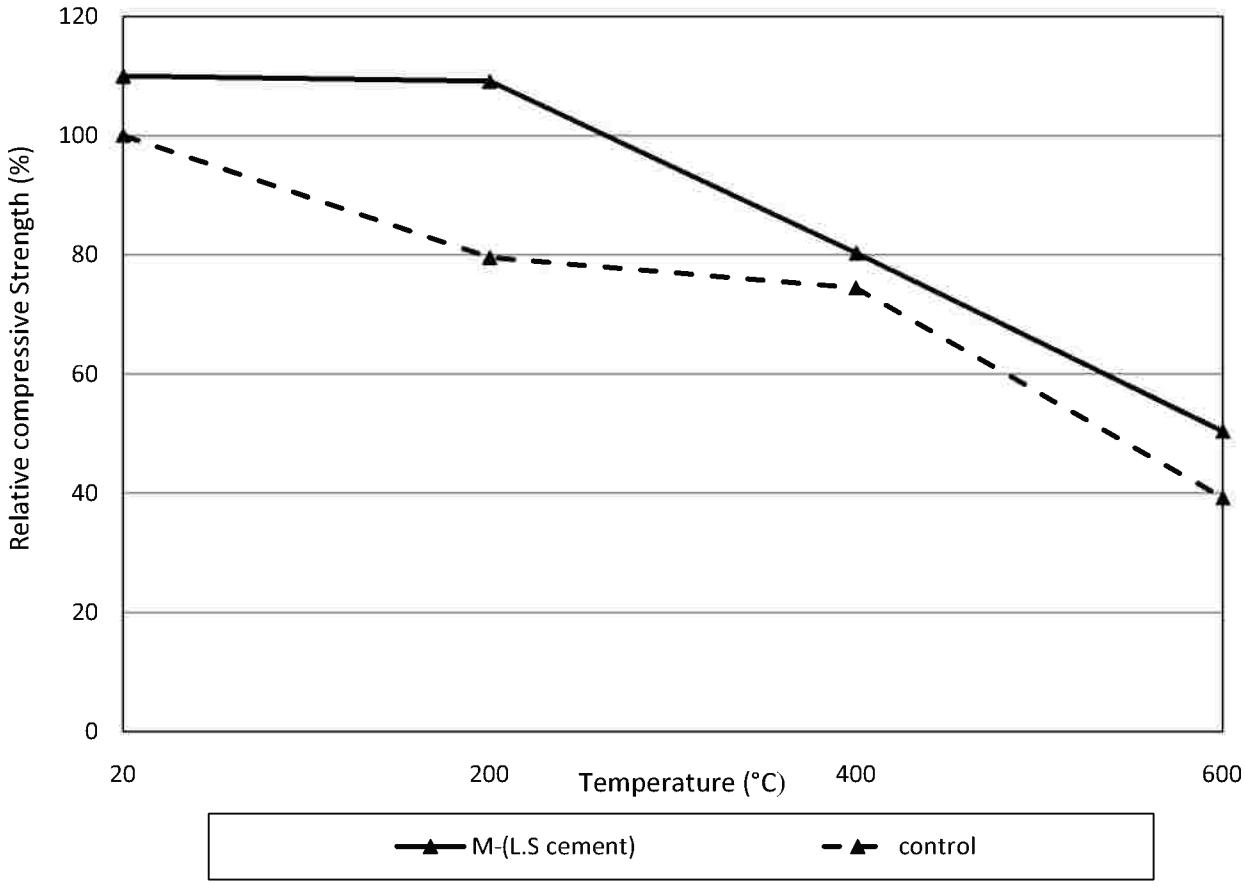

Fig. 4.56 - Relative compressive strength of limestone Portland cement mortar at roomtemperature and after exposed to 200, 400 and 600°C.

4.3.1.3 Compressive strength test results of the mortar with 10 and 20% ceramic powder.

This paper investigates the usage of ceramic powder in the partial replacement of Portland cement to produce mortars. In order to study the behavior of the mortars, mixtures with 10% and 20% of cement replacement content were prepared. Compressive test results are presented in **Table 4.15**and graphically presented in **Fig. 4.57** and have shown a9, 23, 14 and 2% strength increase for the 10% replacement mortar at 20, 200, 400 and 600°C respectively.For the 20% replacement ceramic powder mortara 4, 23 and 2% strength reduction was observed at 20, 400 and 600°C, just a slight increase in residual compressive strength was appointed at 200°C. The conclusion was made that the partial replacement of cement by the ceramic powder admixture at the levels studied causesan improvement in residual compressive strength at 10% replacement as a result to presence of large amount of quartz phase in the ceramic powder and the main crystalline component of the ceramic sample evidently is calcite ($CaCO_3$). Asignificant reduction in the mixture at 20% replacement has been considered.

Table 4.15: Relative compressive strength of control mortar, 10 and 20% ceramic powder as cement replacement

Mix designation	Relative compressive strength (%)			
	Temperature (°C)			
	20	200	400	600
Control mortar	100	79.5	74.4	39.2
Ceramic-10R	108.7	102.6	88.5	40.9
Ceramic-20R	95.9	83.4	51.2	37.1

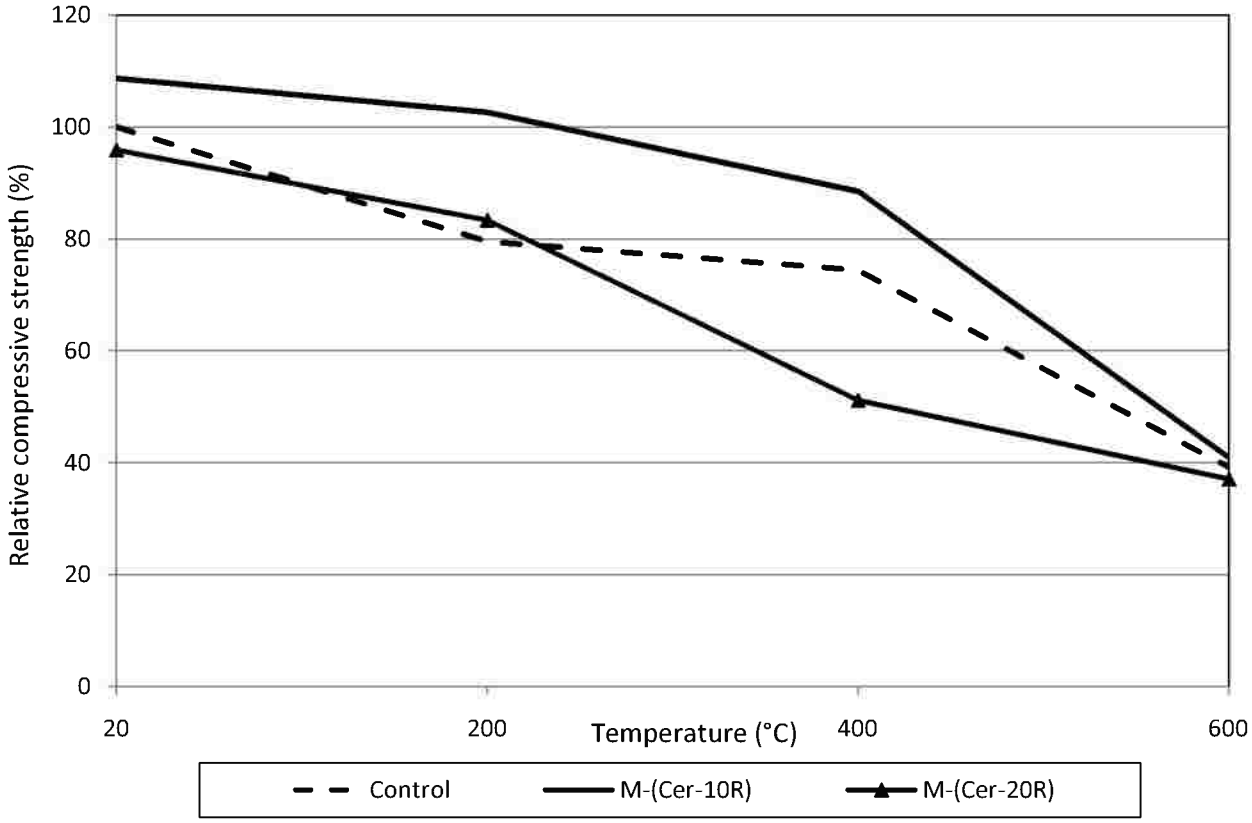

Fig. 4.57 - Relative compressive strength ofmortarcontaining 10 and 20% ceramic powder as a partial cement replacement.

4.3.1.4 Compressive strength test results of the mortar with 10 and 20% melamine powder mortar.

Our presentation develops the study of cement mortars manufactured with melamine powder taken from the industrial production of particle boards, characterizing all of their properties and comparing them with traditional cement mortars. The objective is to determine in

what way the addition of melamine powder will modify traditional mortar, once these materials have been subjected to a polymerization process under pressure and under increased temperature, in order to assess the possibility of using these new materials for applications in the construction industry. The behavior of melamine powder mortar in the hardened state is studied, determining their mechanical properties under compression and compared with those obtained from the reference mortar. Dosages were prepared for a reference mortar and a further two series of mortars with 10 and 20% of melamine powder as cement replacement together with cement, sand and water. The relative compressive strength resultswere seen in **Fig. 4.58** show that the use of melamine powder can be used to manufacture mortars with properties that are better than the traditional mortars. Use of melamine powder as a 10% cement replacement increases the compressive strength of the conventional mortar by about 8, 22, 25 and 17% at 20, 200, 400 and 600°C respectively, while 20% melamine powder mortar increases the compressive strength by a approximately 6, 20 and 14% at 20, 200 and 400°C but shows about 7% reduction in the residual compressive strength at 600°C. So it can be said that the 10% melamine powder mixture has a better results than 20% melamine powder mixture. Melamine powder takes role in neutralizing the surface charges on the cement particles and enhancing water tied up in the cement agglomerations and thereafter reducing the viscosity of the paste and concrete. It promotes dispersing of cement particles and reduces water requirements without affecting the workability, thus resulting high-strength concrete, lower permeability and approves resistance to high temperature and aggressive environments.

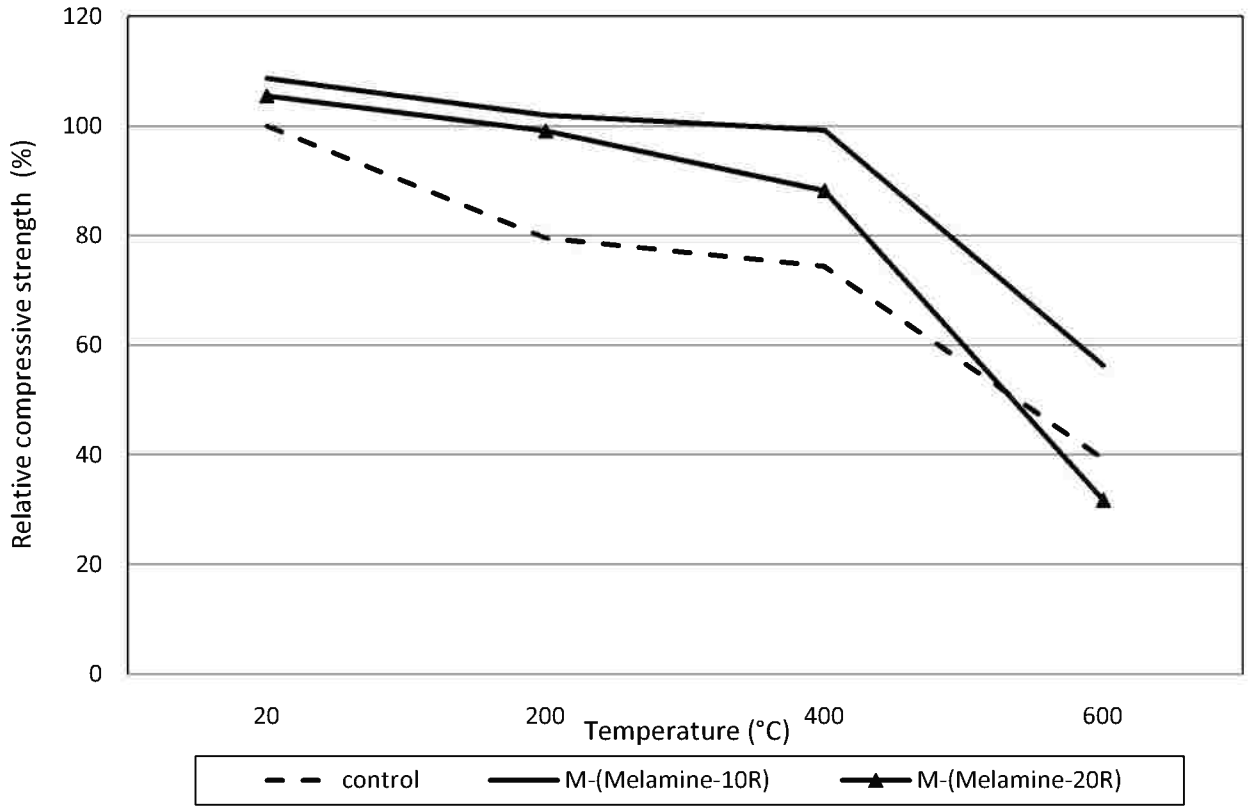

Fig. 4.58- Relative compressive strength of mortar containing 10 and 20% melamine powder asa partial cement replacement.

4.3.1.5 Compressive strength test results of the mortar with 10 and 20% brick clay powder mortars.

In concrete, the economy, technical aspect of concrete, environmental and energyconsumption are important. Reduction of Portland cement without reducing the performance of concrete is veryimportant for huge projects that need a lot of cement. Today, pozzolan and cementitiousmaterials play an important role in concrete. Wastes of industries and constructions whichhave pozzolanic or cementitious property, not only can reduce environmental pollution andenergy consumption of construction industry, but also make it cheap. For this reason the use of brick clay powder as cement replacement was studied. Many obvious researches demonstrate that the bricks powder show pozzolanic properties

The results of the compressive strength of specimens with and withoutbrick clay powder as cement replacement are plotted in **Fig. 4.59.** Results illustrate that at room temperature the compressive strength was observed to decrease, as the proportion of waste brick powder in theconcrete produced increase. In the sample with 10 percent brick clay powder, there was a decrease of 6% percent incompressive strength. In sample with 20% brick clay, there was a decrease of 15% in thecompressive strength. The cause of the reduction in compressive strength

was due to thehigh finess- high absorption of water and the large amount of the brick clay powder,which leads to the lack of hydration action and the presence of air voids in cement mortarstructure**[Toledo et al. 2007].** At 200, 400 and 600° C the performance of brick clay mortars were enhanced where, both 10 and 20 % brick clay mortars show a slight,or it can be said the same relative compressive strength, compared with reference mortar.

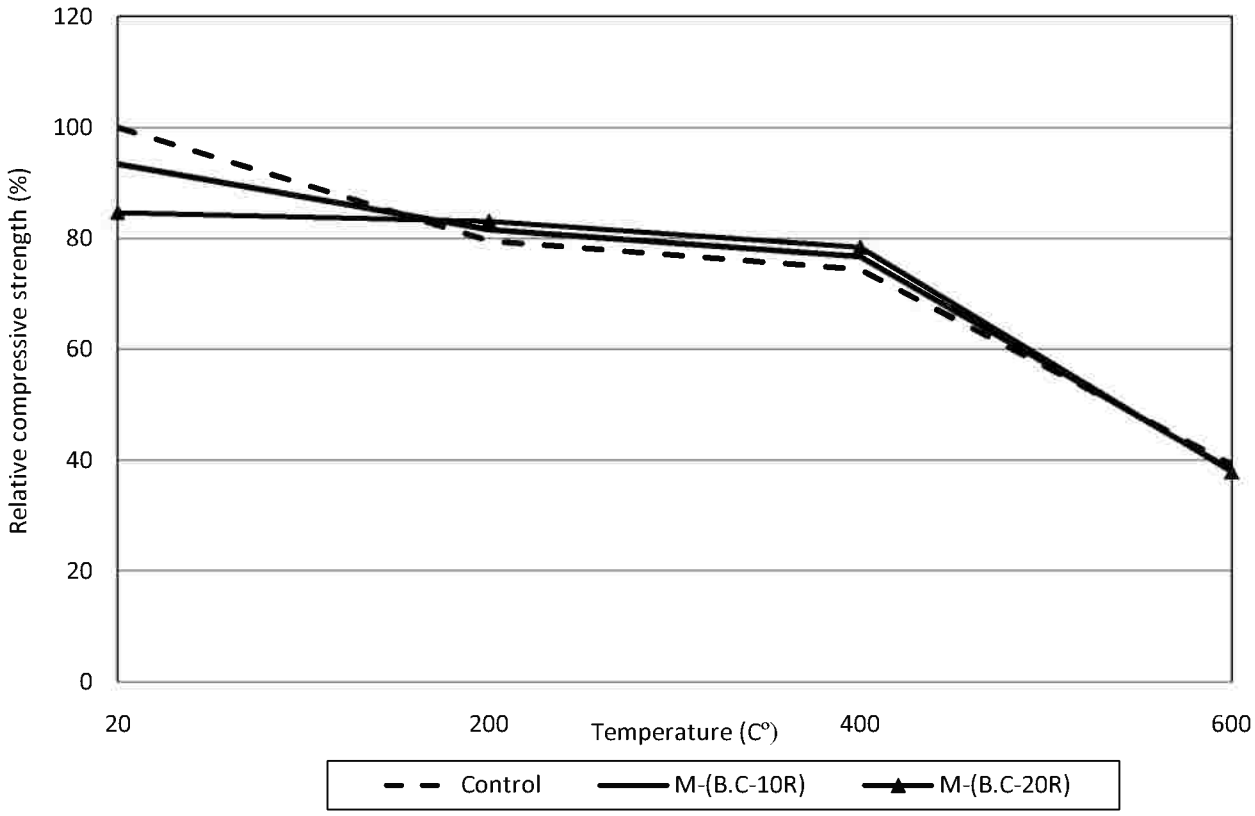

Fig. 4.59 - Relative compressive strength of mortar containing 10 and 20% brick clay powder as a partial cement replacement.

4.3.1.6 Compressive strength test results of the mortar with 10 and 20% bentonite mortar.

The compressive strength test results of 10 and 20% bentonite as cement replacement were plotted as shown in **Fig. 4.60**. The using of bentonite as a cement replacement increases the residual compressive strength of the mortars at all studied elevated temperatures; this may be due to the fact that the bentonitehas a large content of silica and alumina.

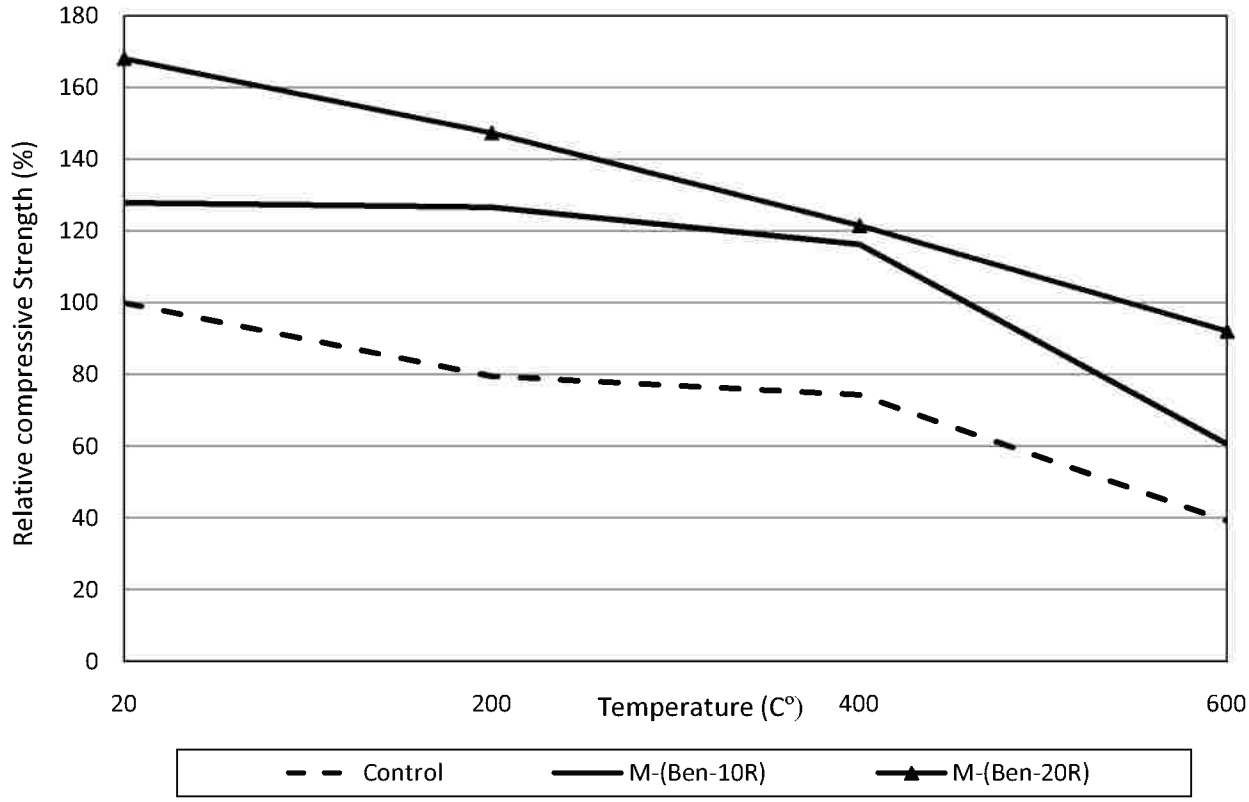

Fig. 4.60 - Relative compressive strength of mortar containing 10 and 20% bentonite as a partial cement replacement.

A visual inspection was carried out for 10 and 20% bentonite mortars after exposure to 600°C.It is clear that the difference between the two mortars, where the 20% bentonite mortar has less surface cracks compared to 10% bentonite mortar, which supports the previous compressive strength results.

Fig. 4.61–Mortar specimens with 10 and 20% bentonite as a cement replacement at 600°C.

4.3.2 Using the modified mortars as anexternal cover for conventional concrete cubes.

An important part of this study is to evaluate the effect of the modified mortars which contain limestone cement, ceramic powder, melamine powder, brick clay powder and bentonite in preventing the traditional concrete from elevated temperature. For this aim cubes with 100 mm side length were covered by 25 mm of the obvious different modified mortars from all sides and exposed to 600°C for 2 hr. After exposure, the cover was removed and the traditional concrete cubes were tested to obtain their compressive strength. As the compressive strength of the traditional concrete cube increases as the additive material is considered to be more effective.

At the beginning, the conventional plastering shows enhancement in the residual compressive strength of the concrete cubes by about 20%, where the residual compressive strength of the concrete cube without and with conventional plastering was 20.2 and 24.4 MPa after exposure to 600°C.

The relative compressive strength of the conventional concrete cubes after the removal of the modified mortars cover after being exposed to 600°C for 2 hrs was plotted in **Fig. 4.62**. On one hand, from this graph it can be concluded that the limestone cement, 10% ceramic powder, 10%melamine powder mortars have a slight good effect on protecting the traditional concrete cubes from the elevated temperature. On contrary the 20% ceramic powder, 20% melamine powder, 20% brick clay powder and 10% bentonite mortars have an adverse effect on protecting the conventional concrete cubes from the elevated temperature that appears from that these concrete cubes have a compressive strength less than the concrete cubes which are covered by reference mortar, while the traditional concrete cubes which were covered by 20% bentonite have nearly the same compressive strength of the concrete cubes that were covering by ordinary Portland cement. The relative compressive strength of the modified mortars after being exposed to 600°C for 2 hrs was presented in **Fig. 4.63**, the aim of this chart is to support the results obtained later. The comparison between **Fig. 4.62** and **Fig. 4.63** shows harmony in their results and the results obtained from **Fig. 4.63** sustain the results obtained from **Fig. 4.62**.

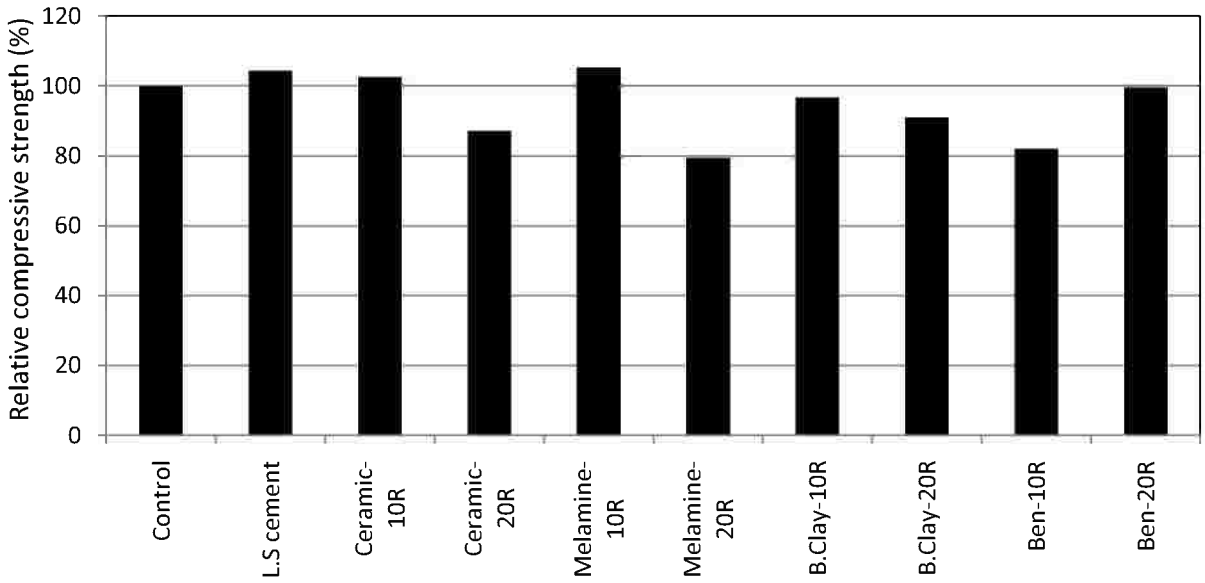

Fig. 4.62 – Relative compressive strength of the conventional concrete cubes after the removal of the modified mortars cover after being exposed to 600°C for 2 hr.

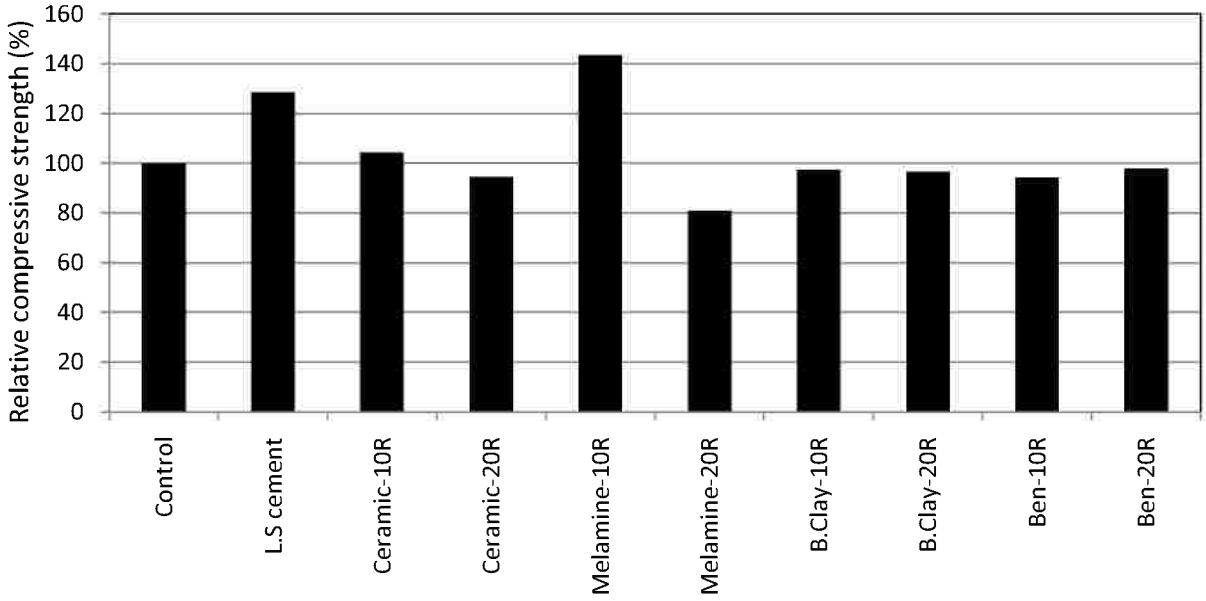

Fig. 4.63 – Relative compressive strength of the modified mortars after being exposed to600°C for 2 hr.

Also the temperature of the steel reinforcement inside the small scale slabs that are covered by modified mortar were recorded and plotted in **Fig. 4.64**. From this figure it can be noted that the modified mortars that contain limestone cement, 10% ceramic powder and 10% melamine powder as a cement replacement can protect the reinforcement inside the slabs from the elevated temperature and reduce it by about 1.3, 3.8 and 1.7%. On the other hand, all the other mixtures don' t show an applicable behavior about protecting the reinforcement from the

elevated temperature. The results of the compressive strength of both the conventional concrete cubes after the removal of the modified mortars cover and the modified mortars after exposed to 600°C for 2 hrs are compatible with the measured temperature of the reinforcement inside the small scale slabs depending on the exposure of temperature increases as the residual compressive strength decrease.

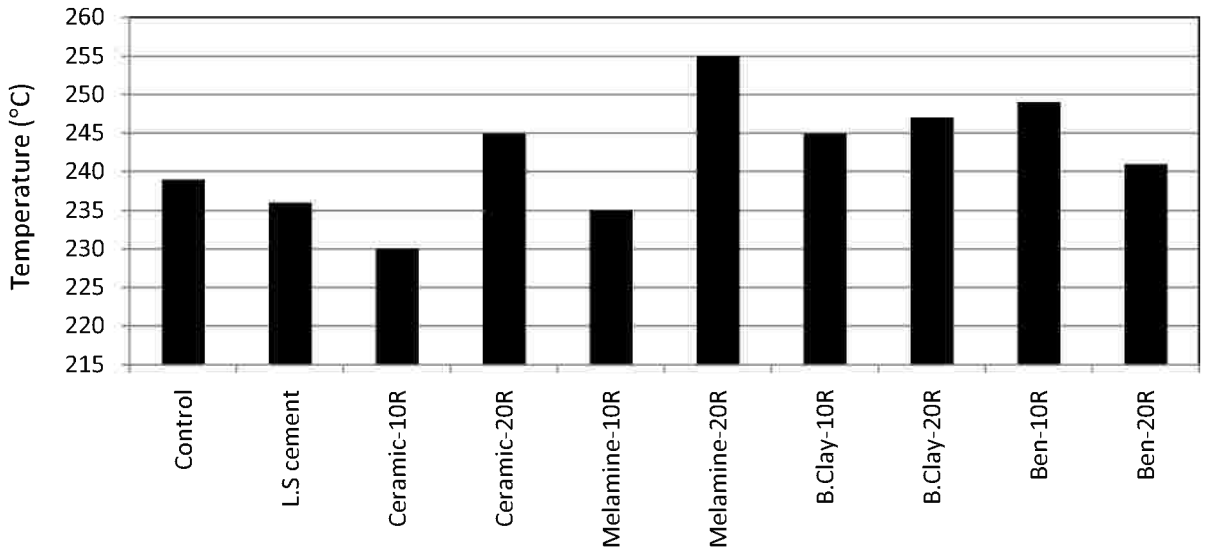

Fig. 4.64 – Temperature of the reinforcement inside the covered small scale concrete slabs by modified mortars afterbeing exposed to 1200°C for 2 hr.

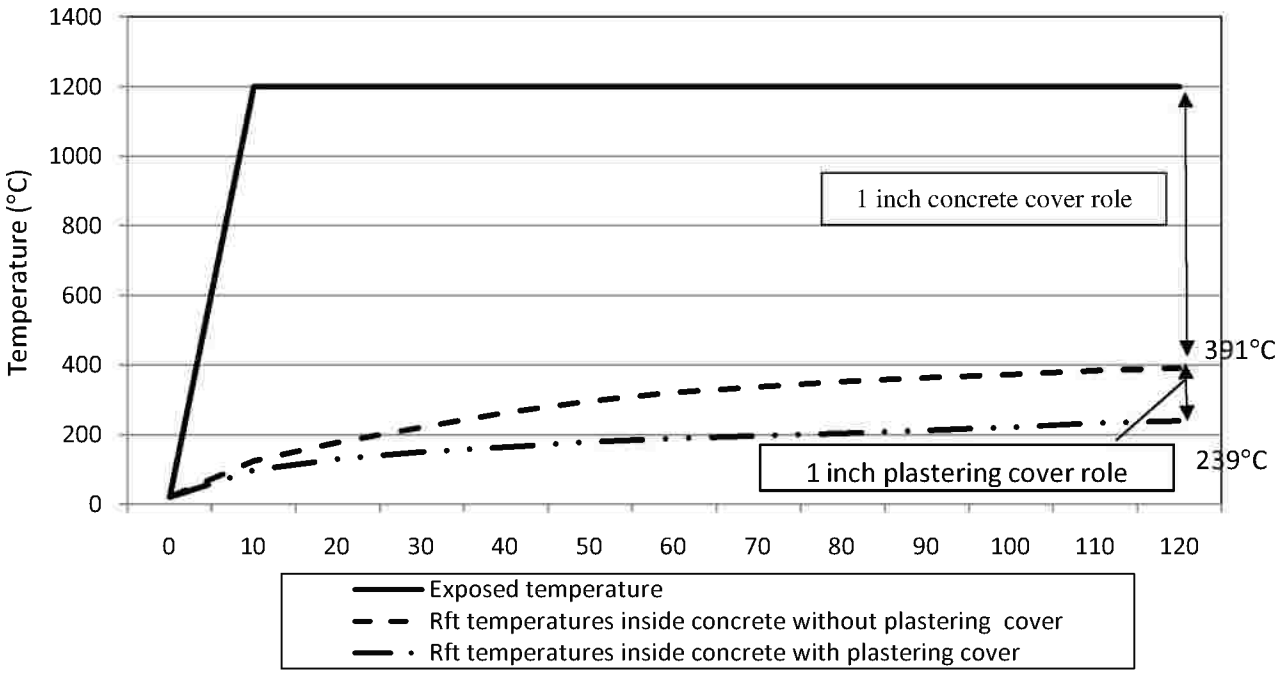

Fig. 4.64-a –The role of the 1-inch conventional mortar on protecting the reinforcement.

It can be noted from **Fig. 4.64-a**, the role of the 1 inch conventional mortar, as a plastering, on preventing the reinforcement inside the concrete slabs from the elevated temperatures. It is evident that just 1-inch concrete cover thicknesswith 1-inch traditional plastering allows only the arrival of 20% of the exposed temperature to the reinforcement.

4.3.3 Thermogravemtric analysis (TGA/DTG).

4.3.3.1 Control mix.

Table 4.16: TGA weight loss for unheated control mix.

Temperature (°C)	200	600	800	1000
Wt.loss (%)	3.8	6.4	9.5	9.8

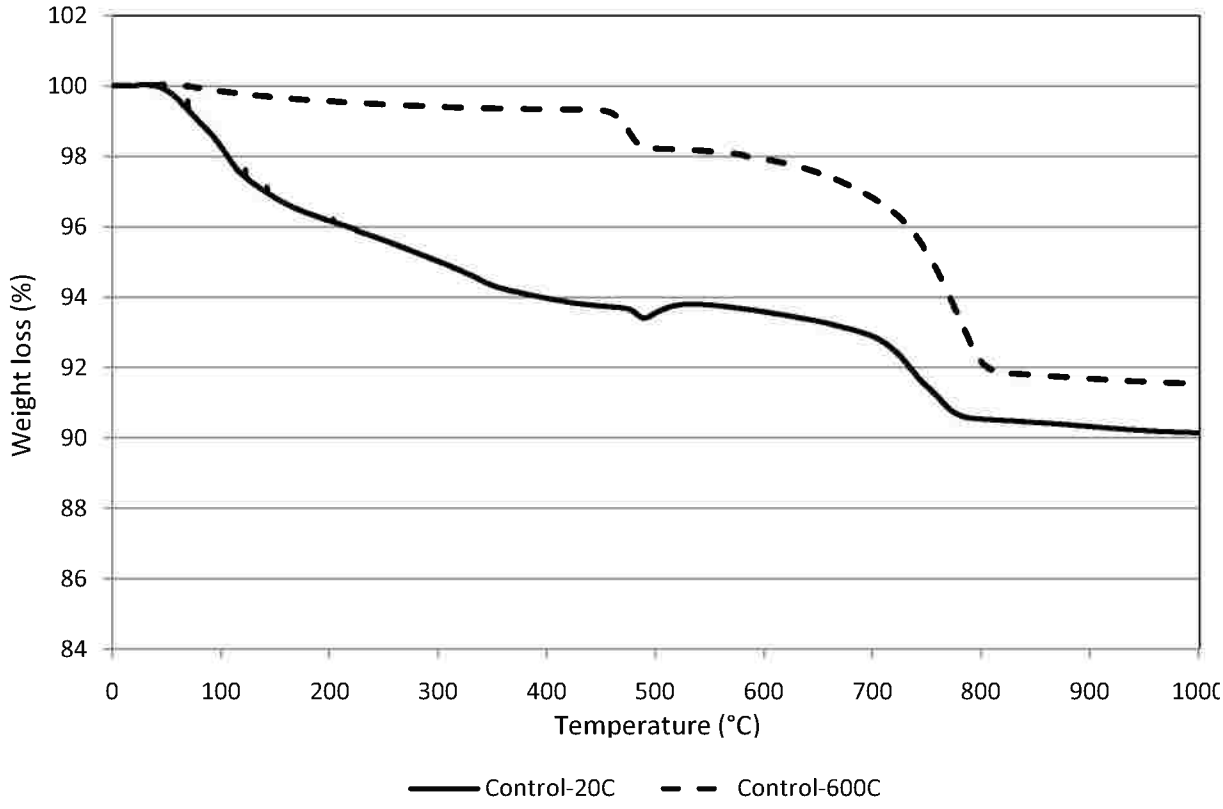

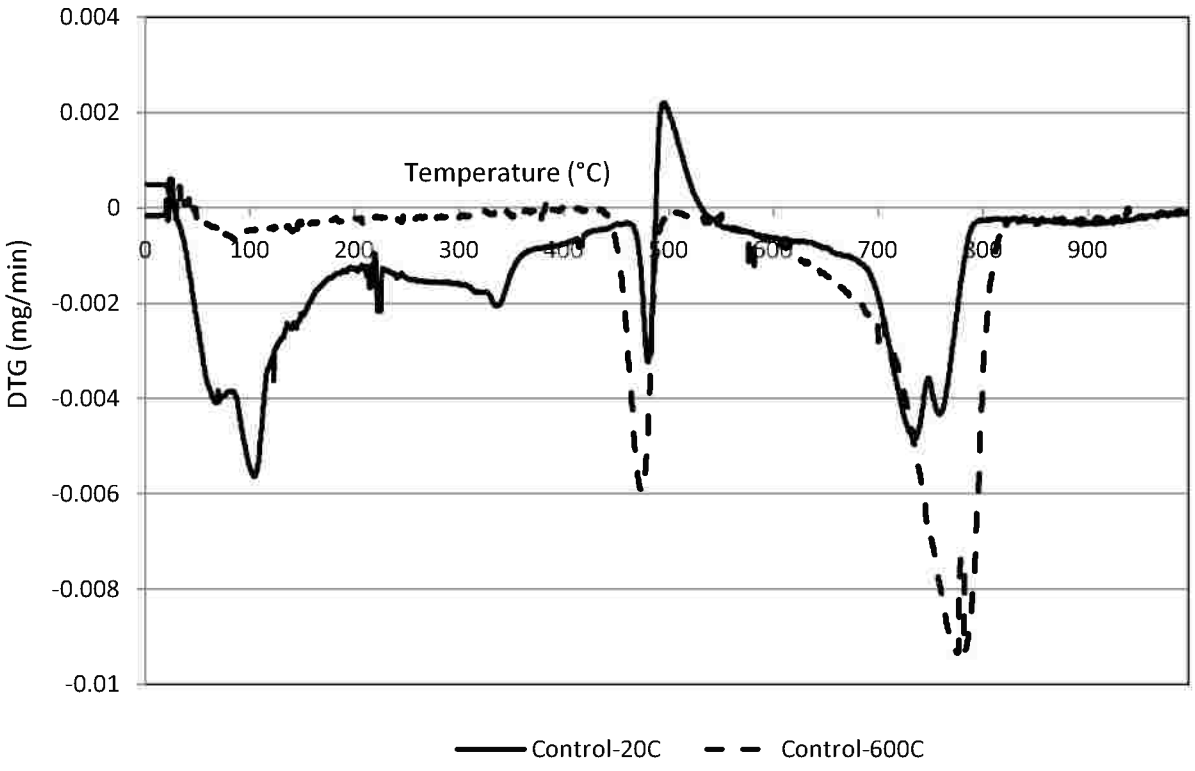

Fig. 4.65 – (TGA/DTG) curves of CEM I cement mortar (control mortar) a) TGA b) DTG

4.3.3.2 Limestone portlandcement mortar.

TGA/DTG for limestone Portland cement mortarwas investigated. It can be noted from **Fig. 4.66**and **Table 4.17**that the three regions of phase decomposition are visible. The first region corresponds to the evaporation offree water, C-S-H ,AFm and AFt decomposition. The mass loss for these phases overlaps, which makes quantification difficult. The second peak is at about 480°C which refers to the decomposition of portlandite.

The decomposition pattern for limestone cement mortar shows the main peak with its maximum at 750°C due to decomposition of calcium carbonate. Also it can be seen that for unheated sample the total weight loss was about 8%, the main weight loss was found between 600 and 800°C due to $CaCO_3$ decomposition which represent a high quantity of limestone cement. The weight loss up to 200°C was less than the weight loss of the control sample this may due to some chemical changes happen as a result for presence of limestone such as, there is no monosulfate observed. With limestone addition the decrease in ettringite formation could be attributed to carboaluminatephases formation.Also through comparing the TGA curves of limestone portland cement with control mix, it can be seen that dehydrationof CH at 450°C is less intensive in carbonated cement pastes, which indicatesthe CH consumption due to carbonation. The peak intensitiesaround 750 °C in the reference hydration cement pastes are weak andrepresent initial

carbon content in as-received cement or due to atmosphericcarbonation. Contrarily, the peaks around 750 °C in the limestone portland cement are strong. These peaks confirm the formation of strongcrystalline calcium carbonates.

Table 4.17: TGA weight loss for unheated and preheated limestone portland cement mix at600°C.

Temperature (°C)	200	600	800	1000
Weight loss (%)	2.6	4.6	7.8	8.1

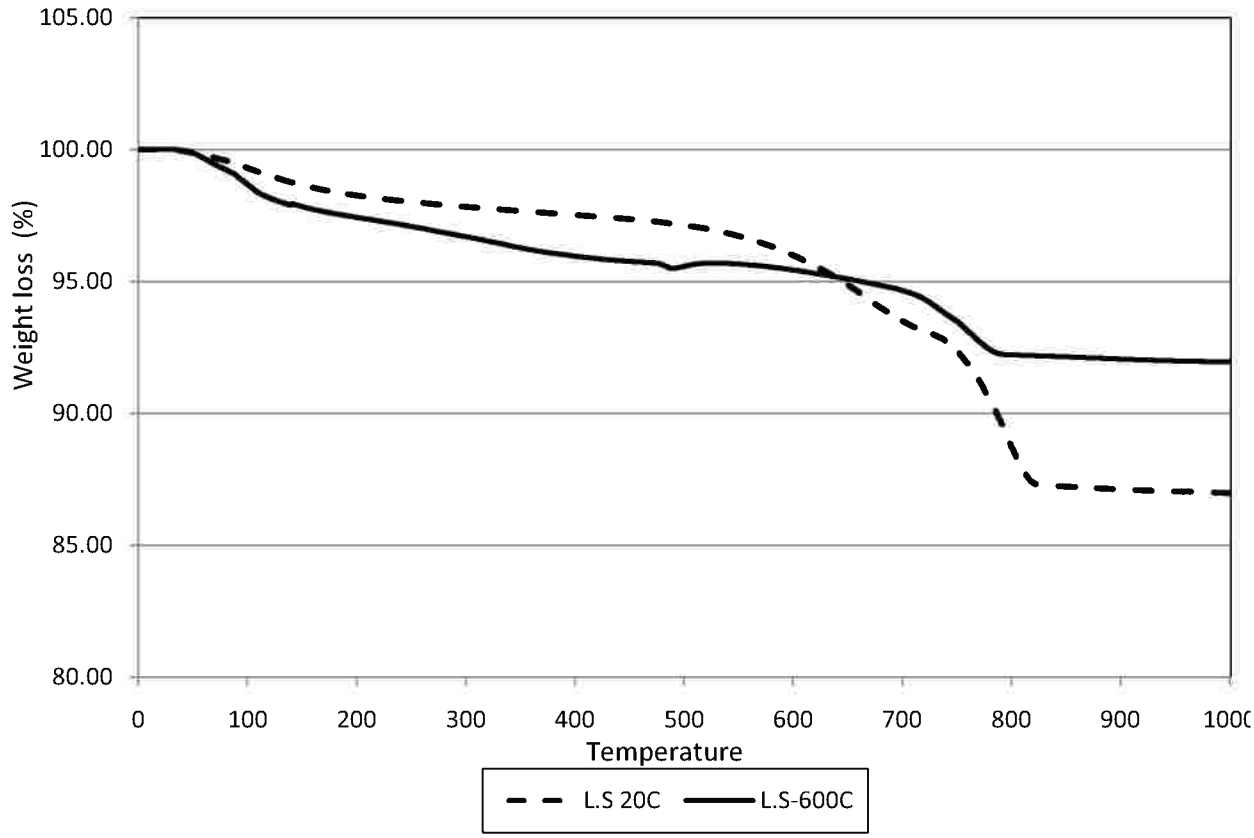

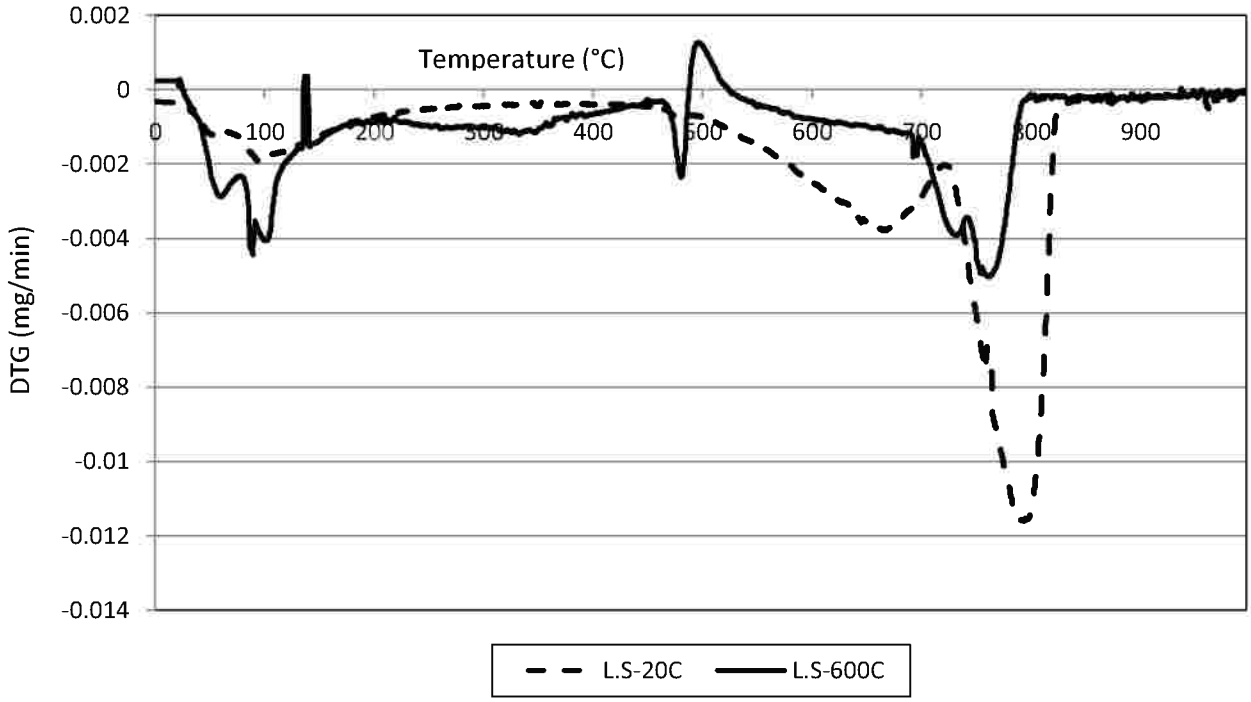

Fig. 4.66 – (TGA/DTG) curves of limestone portlandcement mortar a) TGA b) DTG.

4.3.3.3 CEM 1 with bentonite mortar.

The results of TGA/DTG of 20% bentonite as a partial replacement of cement content were graphically in **Fig. 4.67**. Three peaks were observed from DTG curve, the first was at about 90°C. The second peak was at about 490°C as indication of portlandite decomposition and the third peak was clearly about 730°C. For the preheated sample at 600°C these peaks were slightly shifted. From **Fig. 4.67-a**, the total weight loss of unheated 20% bentonite mortar shows a total weight loss more than that of the control mortar, this may be due to the high silica and alumina content in the bentonite which decomposes in the range of the first peak, this is clear in the weight loss up to 200°C which is consider the major weight loss stage as presented in **Table 4.18**The preheated bentonite mortar at 600°C shows a weight loss less than the unheated sample at all the elevated degree of TGA/DTG temperature.

Table 4.18: Weight loss for unheated and preheated 20% bentonite mortar according to TGA/DTG.

Temperature (°C)	200	600	800	1000
Weight loss (%) -20°C	6.0	9.4	13.1	13.4
Weight loss (%) -600°C	1.2	1.9	6.1	6.4

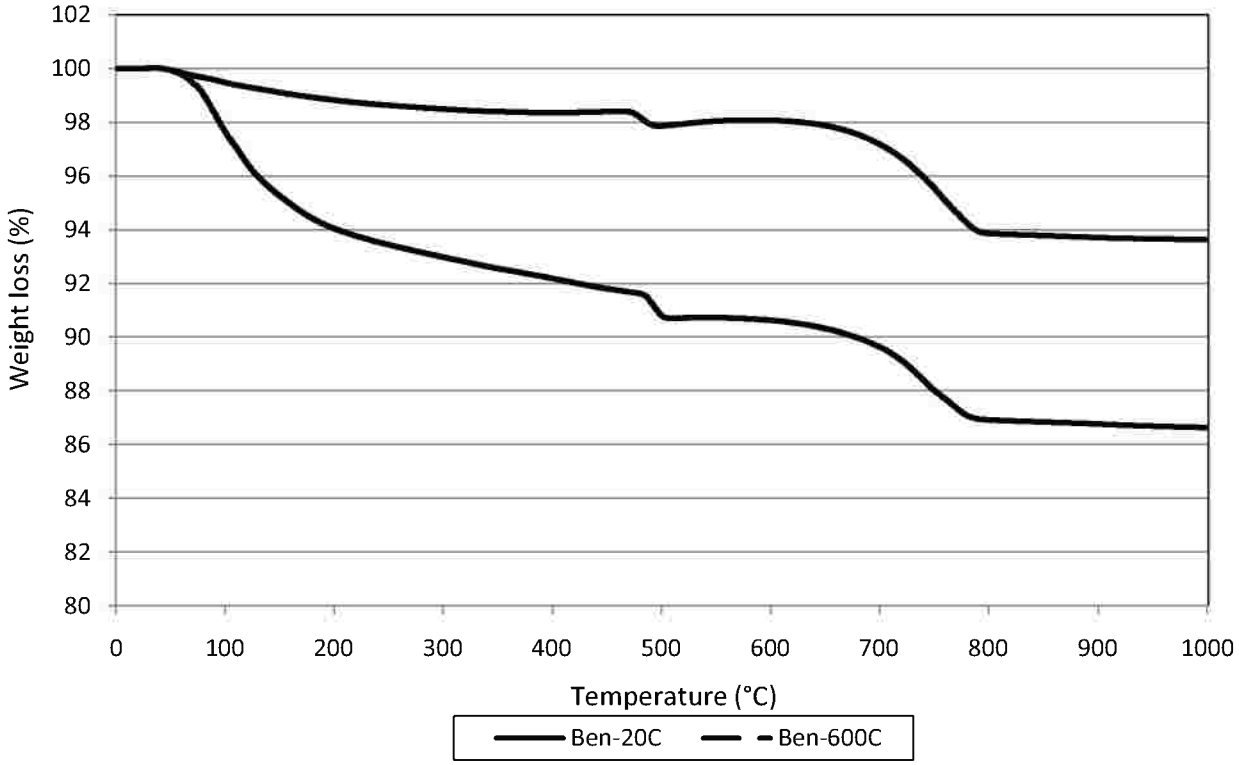

(a)

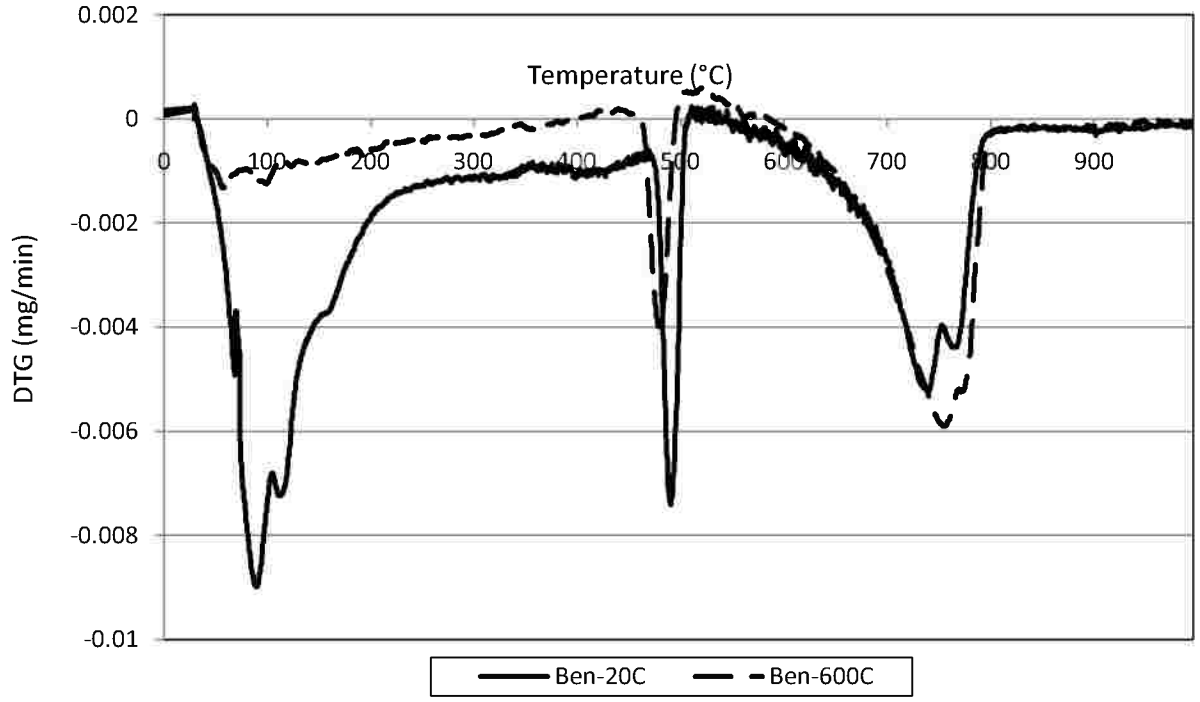

(b)

Fig. 4.67 – (TGA/DTG) curves of 20% bentonitemortar a) TGA b) DTG

4.3.3.4 CEM 1 with ceramic powder mortar.

The unheated and preheated 10% ceramic powder mortar as cement replacement was investigated by TGA/DTG and presented in **Table 4.19**. Also three main peaks were found for

unheated sample. The first peak has been found in **Fig. 4.68-b** which shows a broad peak with two maxima at 85 and 113°C. The firstis due to water evaporation and the second maxima corresponds to the decomposition of Aft and a further weight loss between 100 to 200°C due to decomposition of C_3A,C_3S, C-S-H gel and Aft. The second peak was at about 480°C due to the decomposition of $Ca(OH)_2$. At last, the third peak is at about 790°C as indication of $CaCo_3$decomposition. For the preheated sample at 600°C and after the (TGA/DTG) the peaks were slightly shifted and the first peak completely disappeared. From DTG curve it can be noted that the total weight loss is considerably high and more than the weight loss of reference mortar. This may be due to the high content of lime that is presented in the ceramic powder as investigated from EDAX.

Table 4.19: Weight loss for unheated and preheated 10% ceramic mortar according to TGA/DTG.

Temperature (°C)	200	600	800	1000
Weight loss (%) -20°C	7.9	11.5	18.8	21.1
Weight loss (%) -600°C	0.7	1.1	6.5	10.0

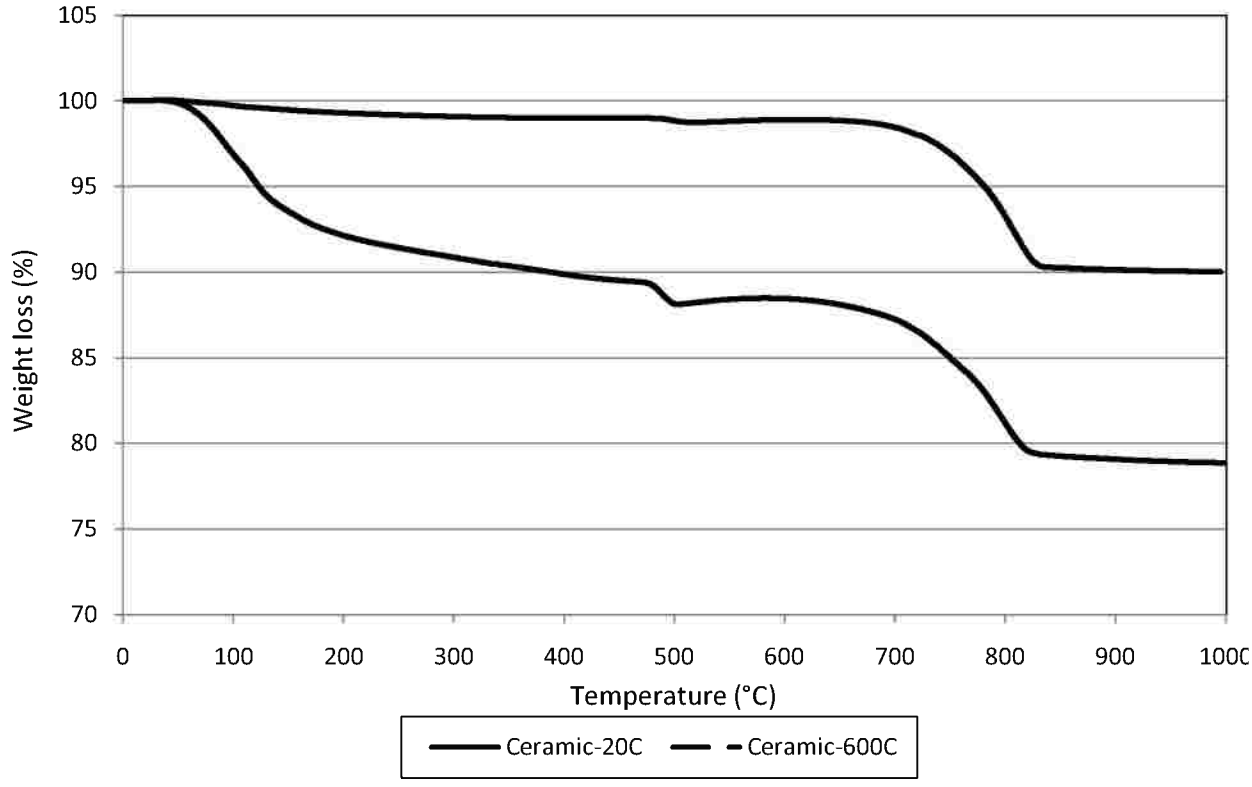

(a)

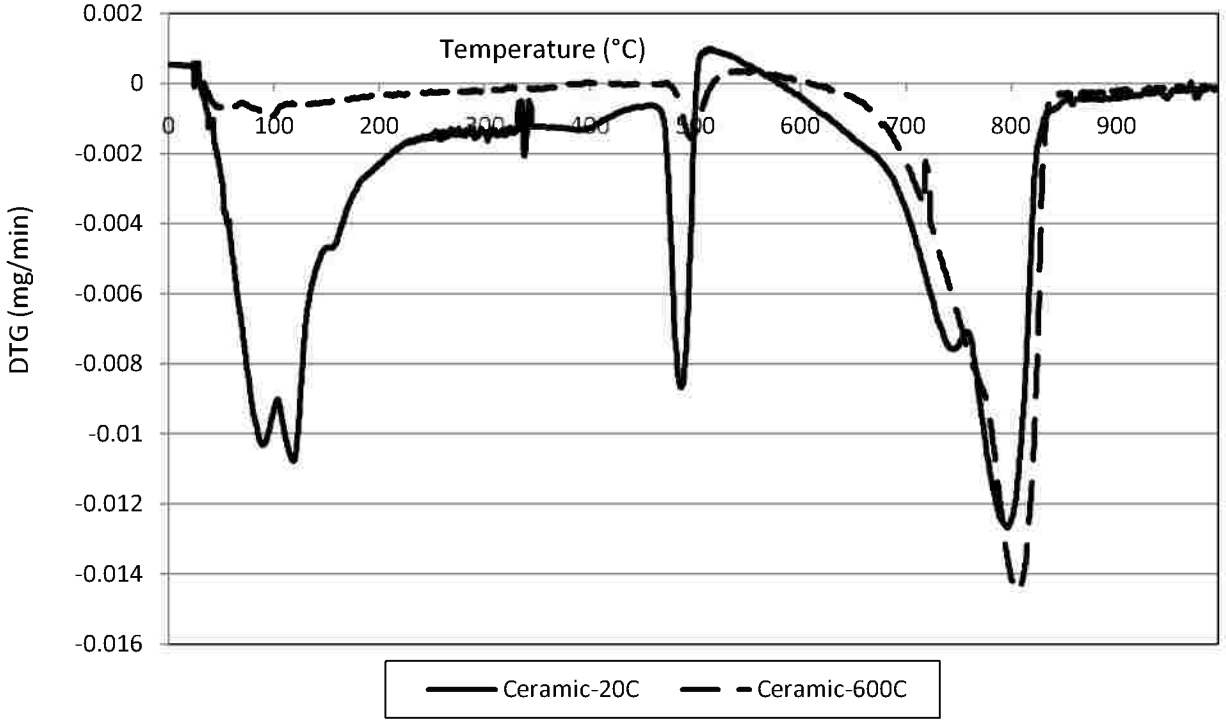

(b)

Fig. 4.68 – (TGA/DTG) curves of 10% ceramic powdermortar a) TGA b) DTG

4.3.3.5 CEM 1 with melamine powder mortar.

Thermal analysis of melamine and the total weight loss have been shown in**Table 4.20** and**Fig. 4.69**. At 250ºC melamine sample undergoes structural changes and as temperature approaches 100ºC the compound loses weight sharply. The DTG curve of unheated sample shows four peaks, the first peak was at about 105°C due to free water evaporation. The thermograms show that hydrated C_3A exhibits a small endothermal effect with a peak at about 325° C that is considered to be the second peak. The third peak appears at 495°C and the last peak considerably appears with two maxima at 755 and 795°C respectively.The fourth weight loss stepcan be attributed to the decomposition of $CaCO_3$. The total weight loss of the unheated 10% melamine powder specimen was more than the weight loss of the control specimen. This may be as a result of that the melamine powder has a high range of CaO, which means more hydration products decomposesat 800°C. Because of the difference in the amount of decomposed $Ca(OH)_2$ before test, the weight loss of the preheated specimens at 600°C is less than the weight loss of the unheated specimen resulting from TGA instrument.

Table 4.20: Weight loss for unheated and preheated 10% melamine mortar according to TGA/DTG.

Temperature (°C)	200	600	800	1000
Weight loss (%) -20°C	4.3	8.7	15.2	17.2
Weight loss (%) -600°C	0.9	1.7	7.9	9.8

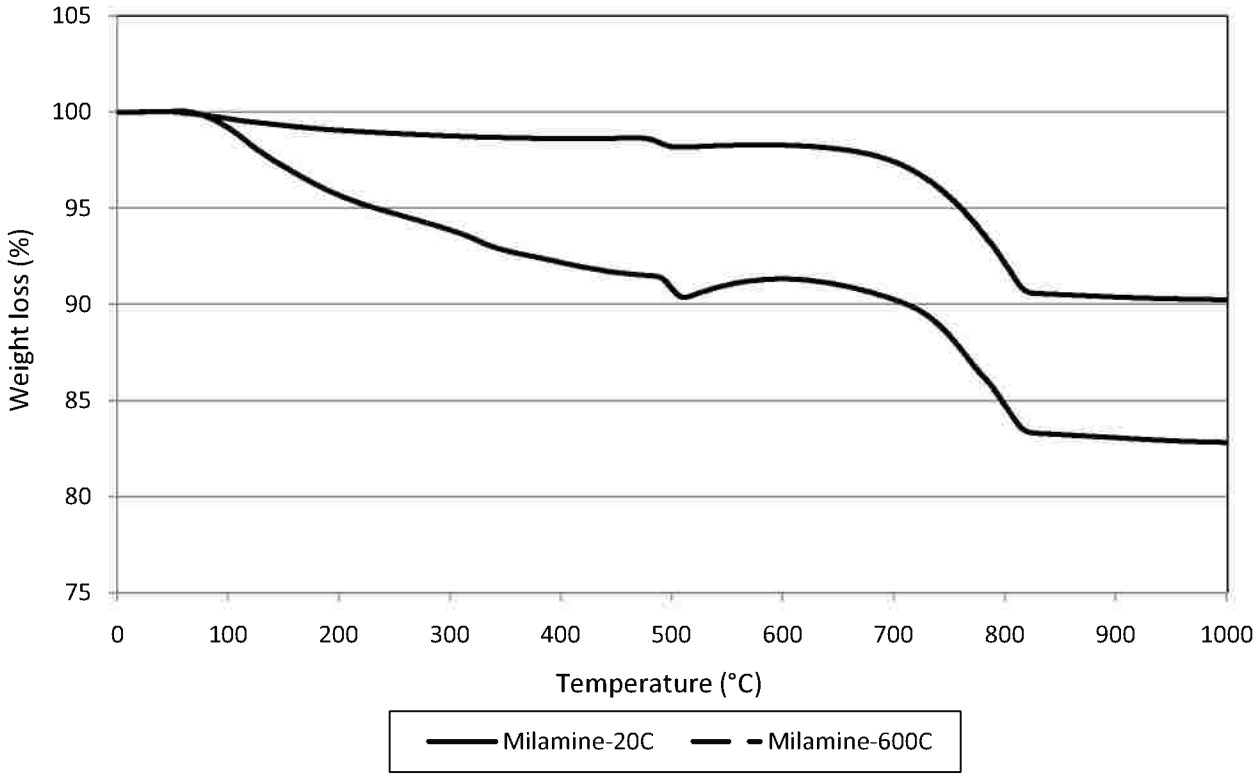

(a)

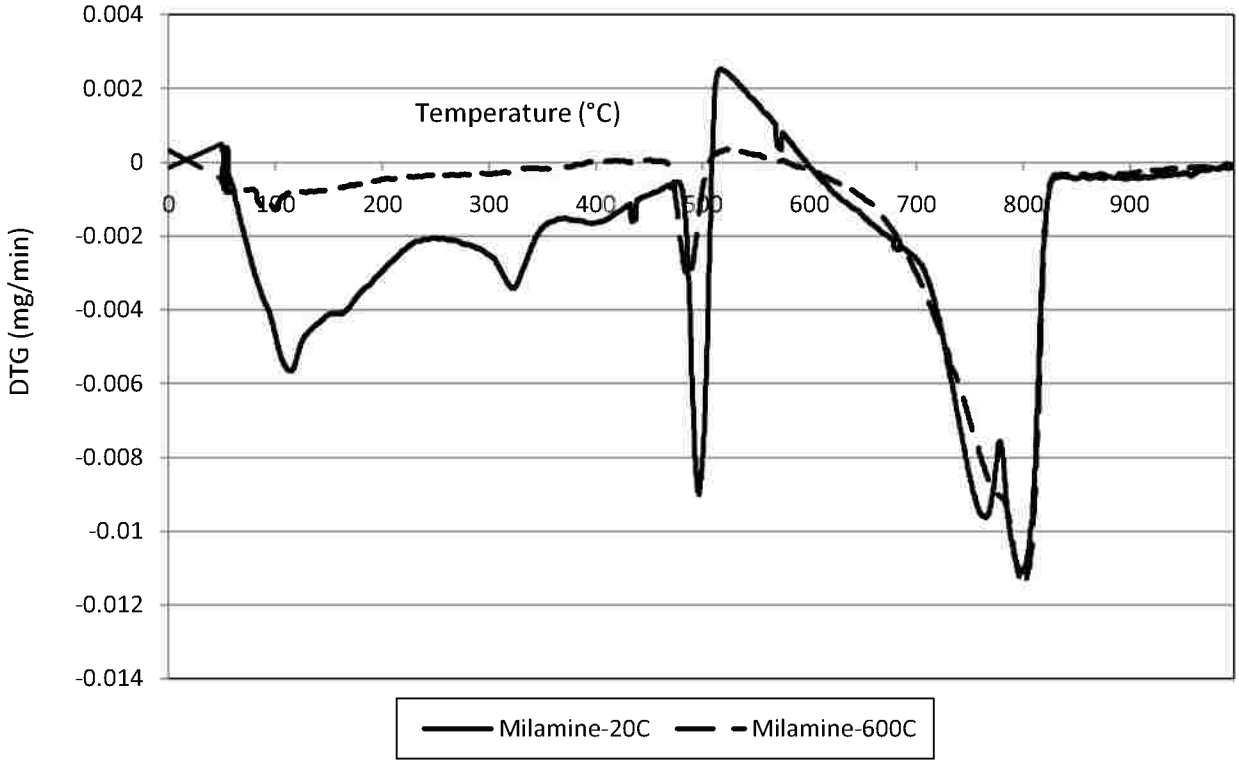

(b)

Fig. 4.69 – (TGA/DTG) curves of 10% melamine powdermortar a) TGA b) DTG.

4.3.4 Weight loss of the studied mortars.

The spalling of the all studied mortars was investigated as a function of weight loss as shown **Fig. 4.70**. All the studied mixtures forfeit their weight more than the control mix at 200, 400 and 600°C except the matrix containing 20% of brick clay as cement replacement of mass. An important observation is that, with the increasing percentage of bentonite, melamine, ceramic and brick clay from 10% to 20% as cement replacementsthere is a decrease in relative weight loss of the specimens as illustrated from **Fig 4.70.**

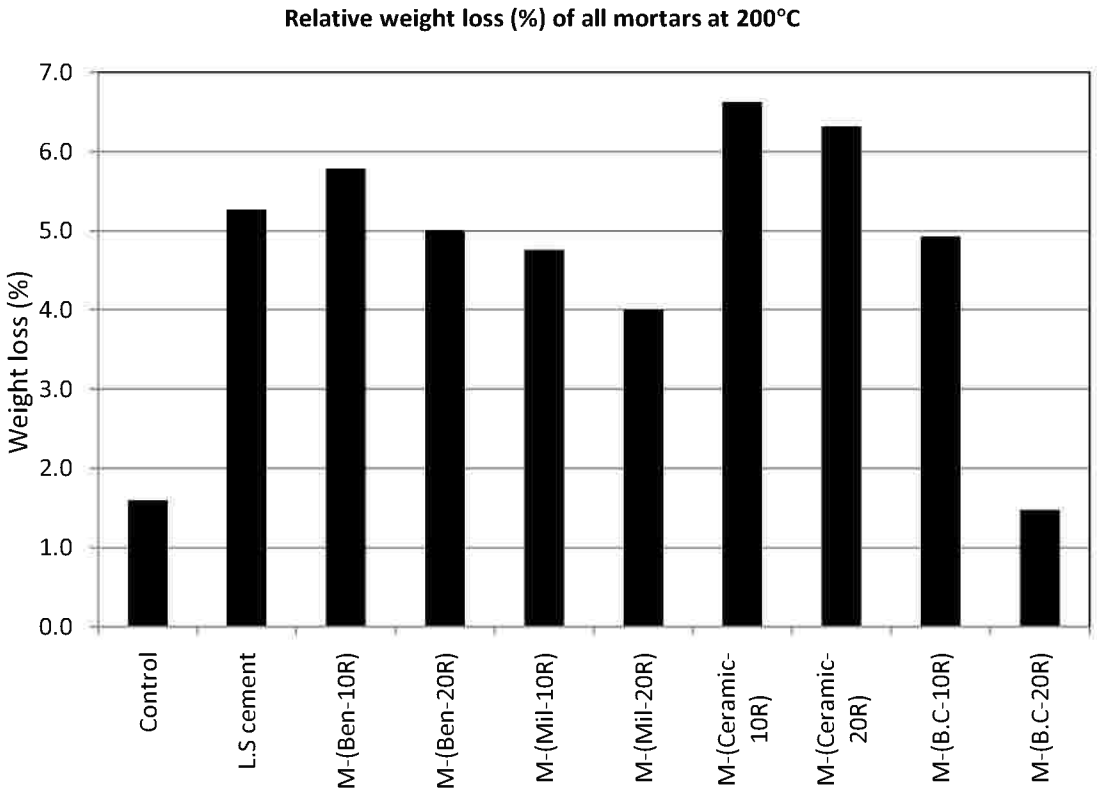
Relative weight loss (%) of all mortars at 200°C
Weight loss (%)
7.0
6.0
5.0
4.0
3.0
2.0
1.0
0.0
Control
L.S cement
M-(Ben-10R)
M-(Ben-20R)
M-(Mil-10R)
M-(Mil-20R)
M-(Ceramic-10R)
M-(Ceramic-20R)
M-(B.C-10R)
M-(B.C-20R)

(a)

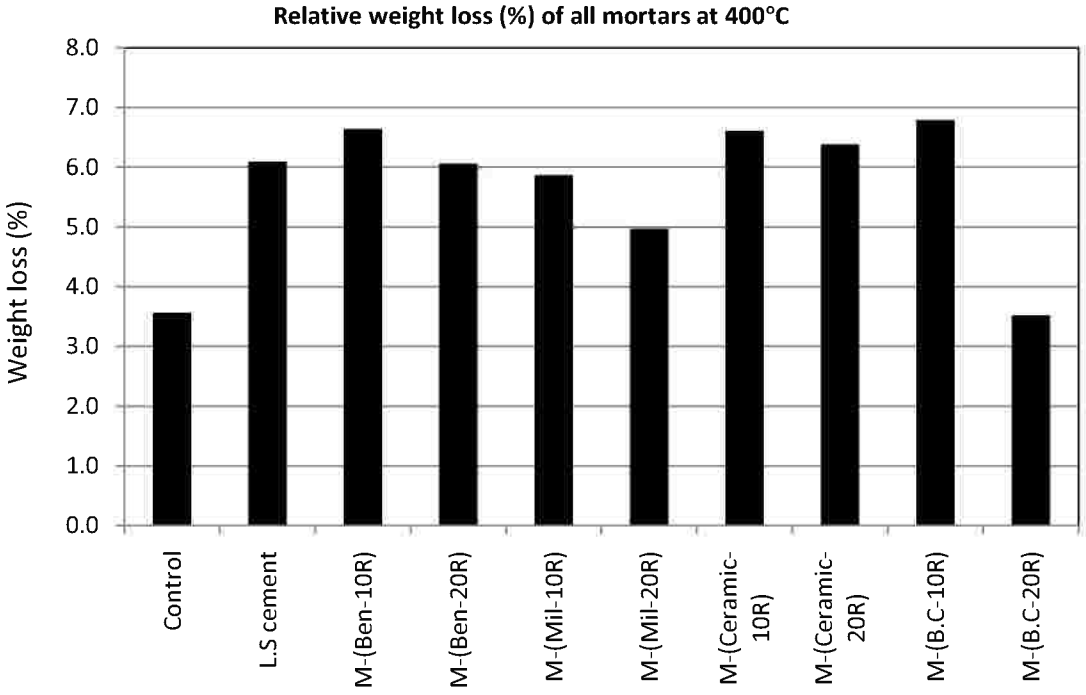
Relative weight loss (%) of all mortars at 400°C
Weight loss (%)
8.0
7.0
6.0
5.0
4.0
3.0
2.0
1.0
0.0
Control
L.S cement
M-(Ben-10R)
M-(Ben-20R)
M-(Mil-10R)
M-(Mil-20R)
M-(Ceramic-10R)
M-(Ceramic-20R)
M-(B.C-10R)
M-(B.C-20R)

(b)

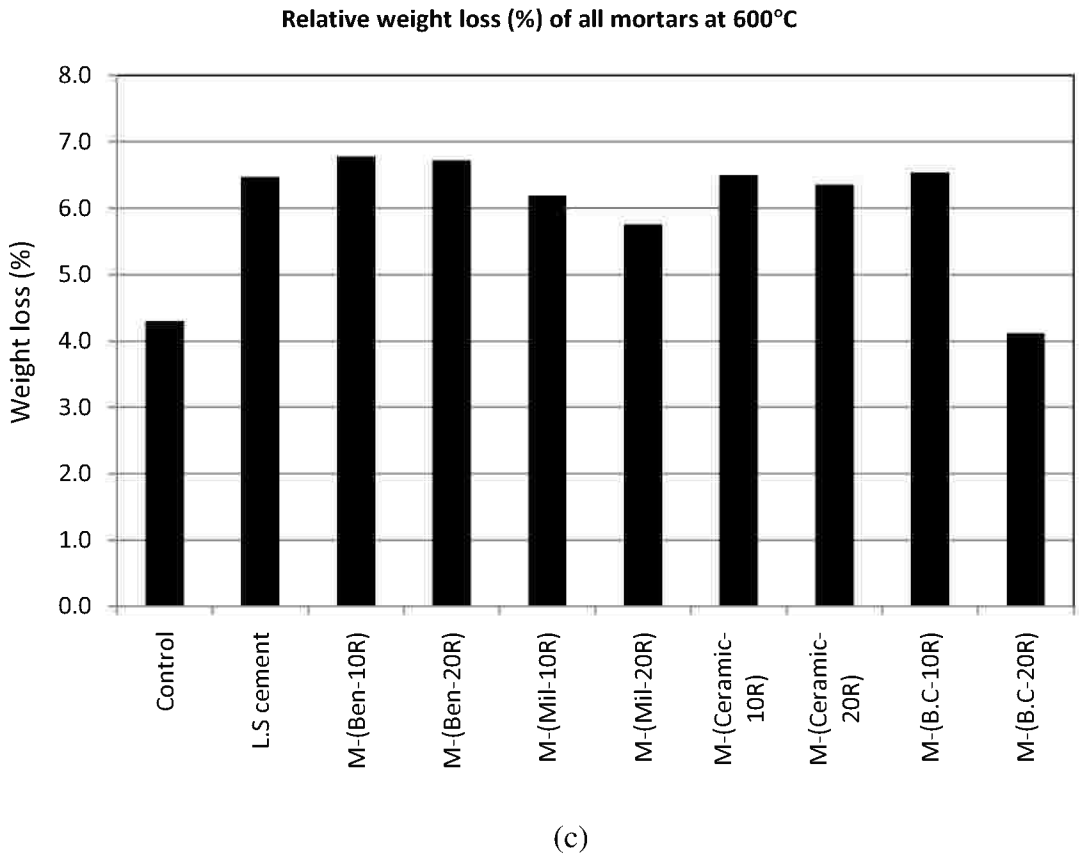

(c)

Fig. 4.70 – Weight loss of the all cube mixtures at a) 200 b) 400 c) 600°C.

4.3.5 Scanning electron microscope (SEM).

Scanning electron microscope was carried out to gain more information about the microstructure of the advanced mortars and study the effect of the additive materials on the properties of conventional concrete. At the beginning the raw materials of bentonite, ceramic powder, melamine powder and brick clay powder were investigated by SEM. The SEM was done on M-(C), M-(L.S), M-(Ben-20R), M-(Cer-20R), M-(Mila-20R) and M-(B.C-20R) at room temperature and after exposure to temperature degree of 600°C.

4.3.5.1 Limestone Portland cement mortar.

The scanning electron microscope was done on the limestone cement mortars at 20 and 600°C as shown in **Fig. 4.71**. At 20°C the SEM micrographs of limestone cementpaste shows a plenty of C-S-H and C-H. The microstructure obtained at higher temperature(600°C) displayed the presence of small micro-cracks and disunion between the cement matrix and the fine

aggregate as shownin **Fig. 4.71- b**. Evidently, the pore spaces are available forthe deposition of hydration products

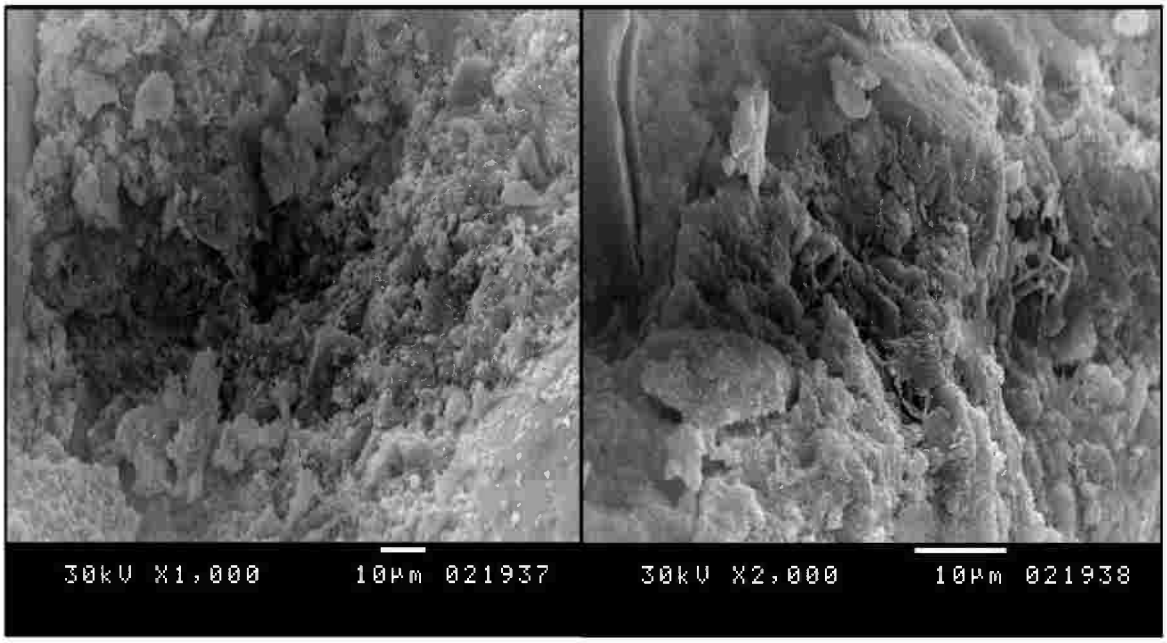

(a)(b)

Fig. 4.71 – SEM images of limestone cement mortar at a) 20ºC b) 600ºC.

4.3.5.2 SEM on bentonite mortar.

The SEM of bentonitemortarwas shown in **Fig. 4.72**, that show plenty of clay particles,C-S-H, CH and ettringite (all hydration products) and up to 600°C the clay particles were still considerably present.

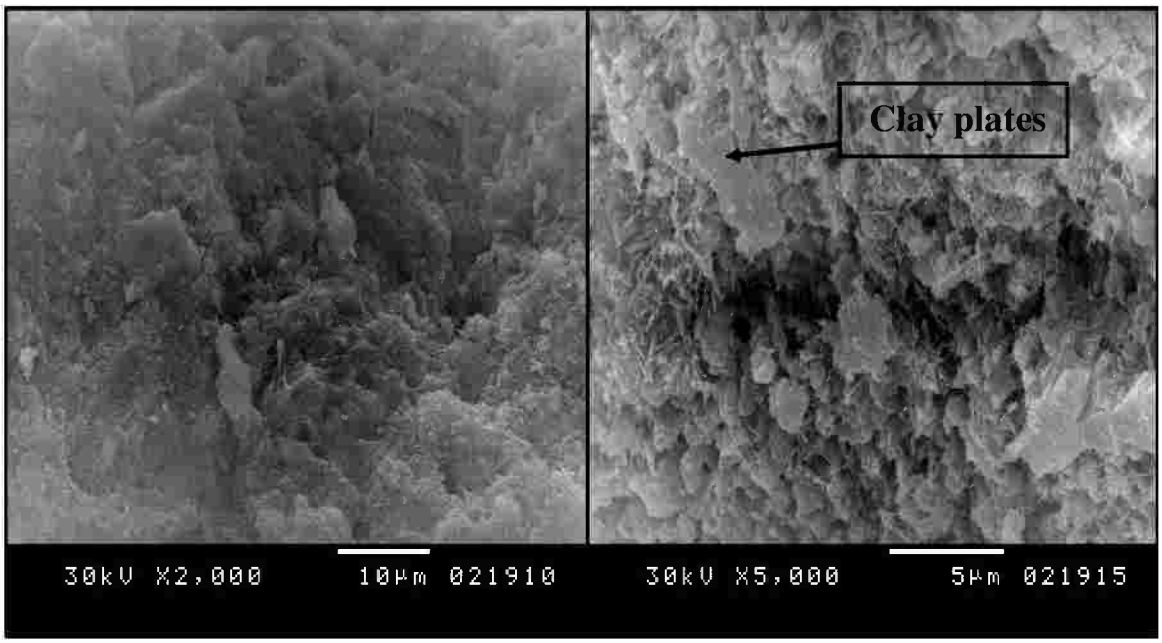

(a)

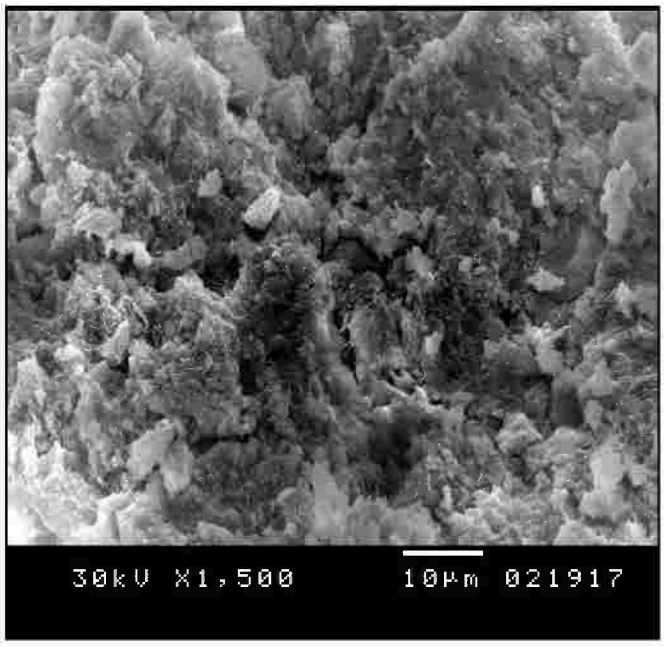

(b)

Fig. 4.72 – SEM images ofmortar with 10% bentonite as cement replacement at a) 20ºC b) 600ºC.

4.3.5.3 SEM on ceramic powder - cement mortar.

SEM of the raw material of the ceramic powder was investigated. The raw ceramic powder particles seem to be haphazard and have some conic shapes as shown in **Fig 4.73**. SEM graphs on the 10% ceramic mortar show the ceramic powder particles with about 5 μmthicknessup to 600°C without decomposition**Fig. 4.74**.Thus, this may give the 10% ceramic powder the priority on the conventional mortars. At the same time, some cracks were observed in ceramic mortars at 600°C that may increase with the increase in the percentage of ceramic powder in the mortar.

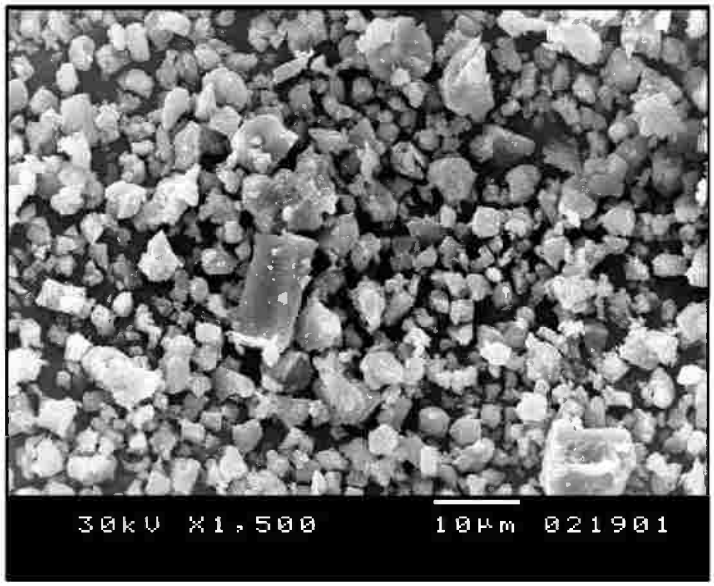

Fig. 4.73– SEM of ceramic powder raw material.

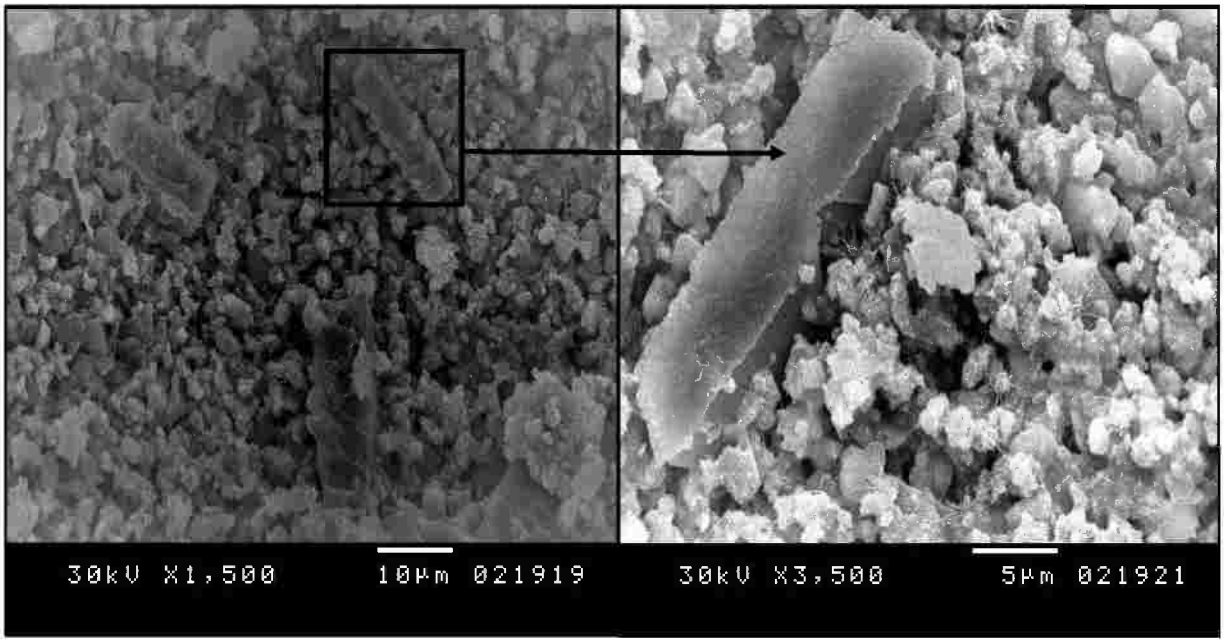

(a) 20°C

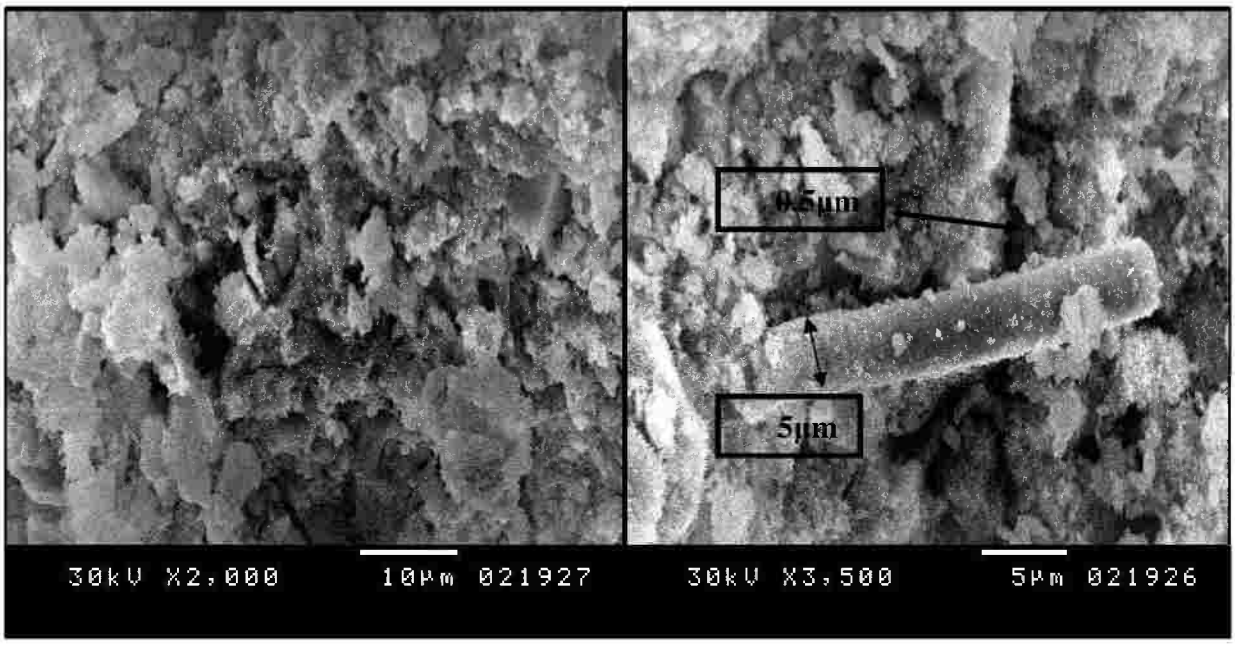

(b)

Fig. 4.74 – SEM images of mortar with 10% ceramic powder as cement replacement at a) 20ºC b) 600ºC.

4.3.5.4 SEM on melamine powder - cement mortar.

The studied raw material of melamine powder was investigated by SEM in this study. The SEM graphs show that the melamine particles consist of collectedsmall particles and plates and also particles with crystalline shapeare apparent in **Fig. 4.75**. The granules of melamine are clearly obvious, even with the mortar specimens being exposed to elevated temperature up to 600°C. As clearly obvious from **Fig. 4.76** the melamine granules take into somewhat hexagonal or oval shape and at the same time the granules are remarkable shine. As an important observation, the melamine granules seem to be cohesive and connected to one another. This perhaps explains the observed increase in compressive strength of the cement mortar when adding melamine powder.

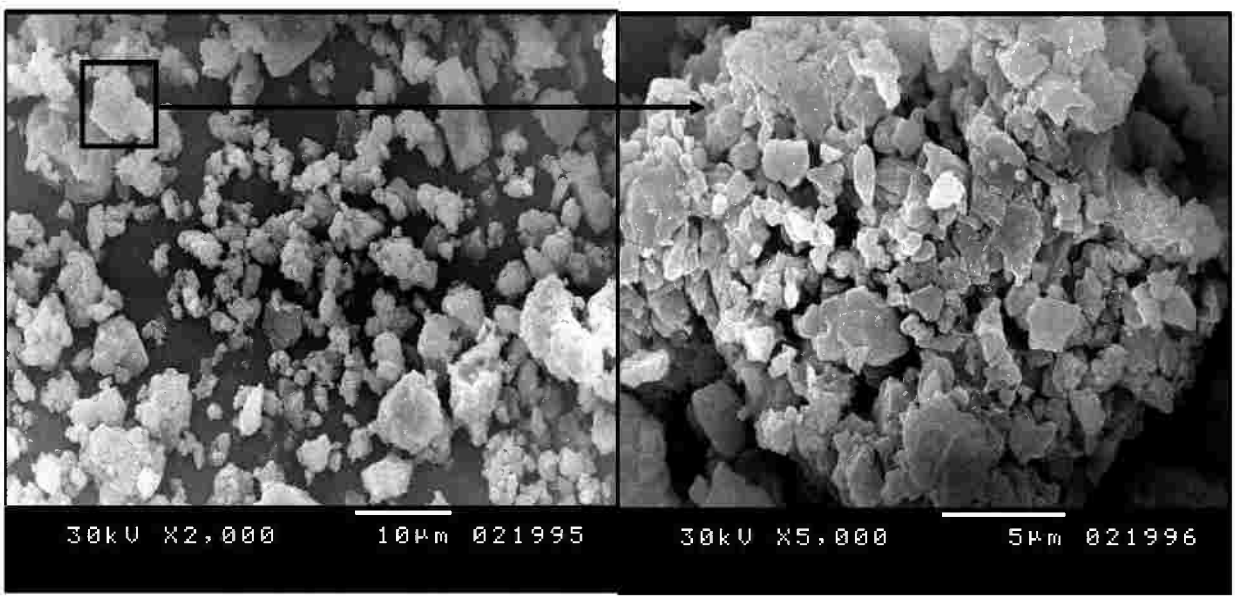

Fig. 4.75 – SEM of melamine powder raw material.

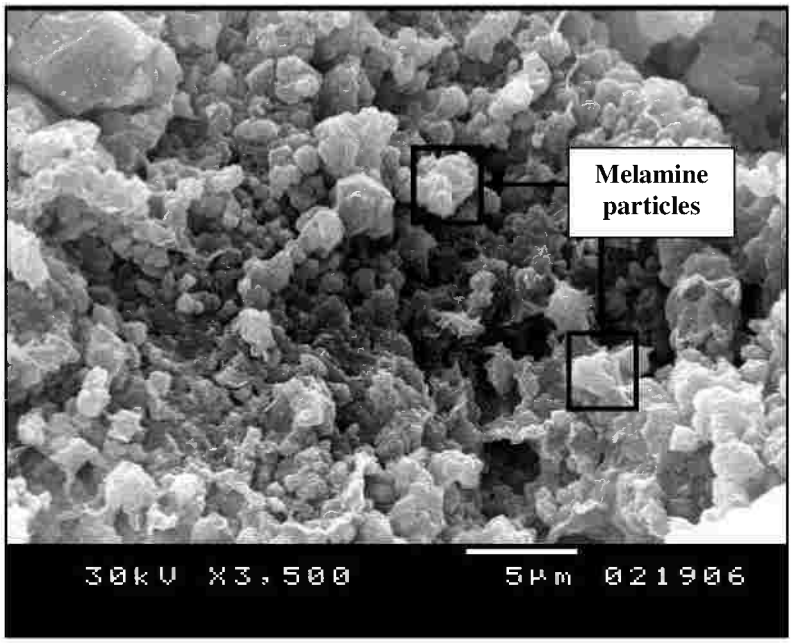

Fig. 4.76 – SEM image of the 10% melamine powderas cement replacement at a) 600ºC.

4.3.5.5 SEM on brick clay- cementmortar.

The raw materials of brick clay powder was observed by SEM which manifested a slightly large particles with 10µm as seen in **Fig. 4.77**. At 20C, SEM images show homogeneous matrix with the appearance of brick clay particles. After exposure to 600°C, an adverse degradation in the brick clay matrix with a nested and hollow shape appear with many cracks,

Fig. 4.78. SEM graphs supported the reduction that happened in 10% and 20% brick clay mortar´s compressive strength at 600°C compared to the control mortar.

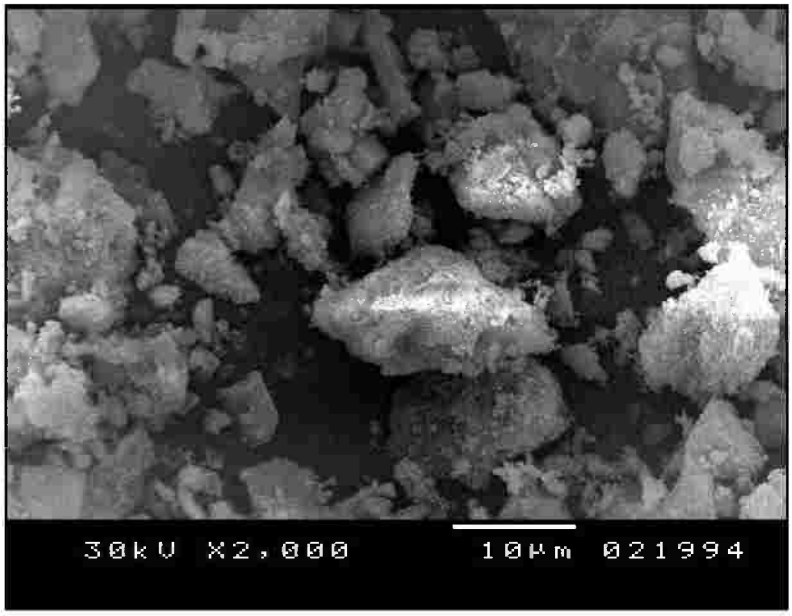

Fig. 4.77 – SEM of brick clay powder raw material.

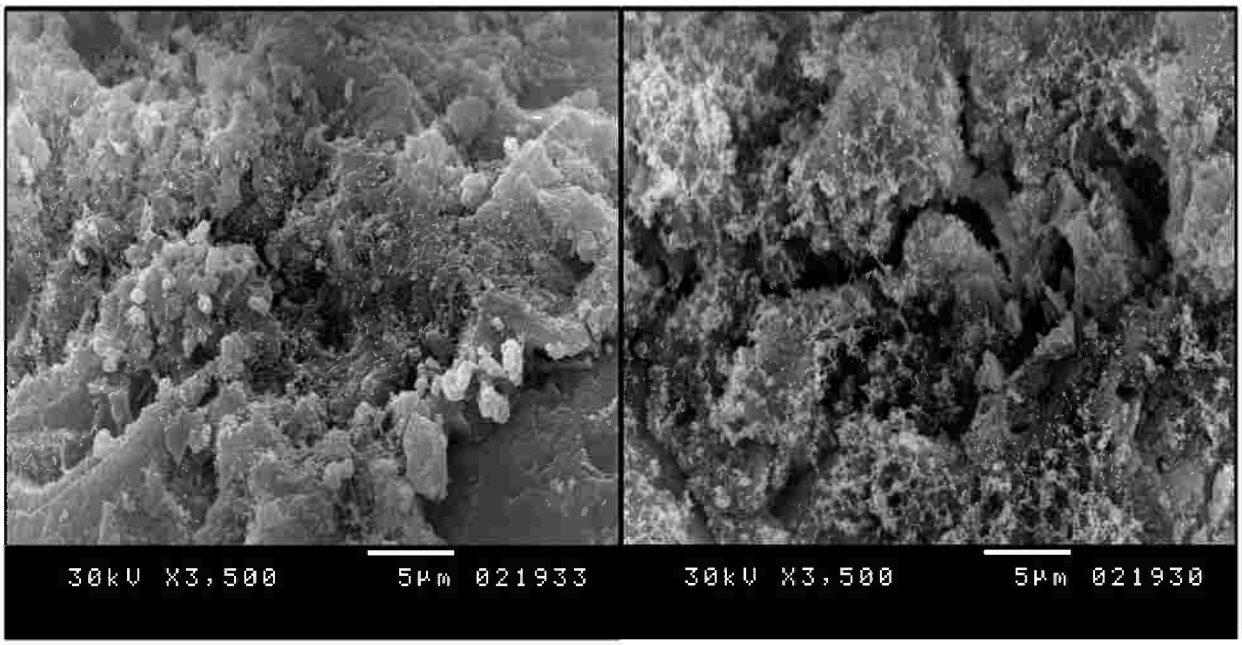

(a)(b)

Fig. 4.78 –SEM images of brick clay concrete mix at a) 20ºC b) 600ºC.

4.4 Phase 4: A Case Study.

As a practical experiment on the impact of high temperature on the reinforced concrete, a real fire test was done on a small room with 4m length, 2m width and 1.5m height. The roof of the slab was with 100 mm thickness with reinforcement 7ϕ10/m in two directions. The experiments started by puttingsix dial gauges to measure the deflection with time of the slab during the fire. The fire started inside the room and beneath the reinforced roof slab. The time-temperature relation was recorded for 2 hrs of both the exposed and unexposed surface of the reinforced roof as presented in **Table 4.21** and plottedin **Fig. 4.79**. The deflection of the slab was recorded with the time up to 2 hrs as shown in**Fig. 4.80** which shows a slight increase in the deflection in the first hour of the exposure after that, a sharp increase in the trend of the deflection.This may attribute to the increase in the temperature of the reinforcement and exhibit a slight ductile behavior.

Table 4.21: Temperature of unexposed and exposed surface of reinforced concrete roof of the experimented room.

Time (min)	Exposed surface (°C)	Unexposed surface (°C)
0	16	16
10	296	18
20	414	21
30	510	25
40	510	45
50	505	60
60	500	72
70	510	74
80	505	83
90	495	89
100	510	98
110	505	109
120	510	120

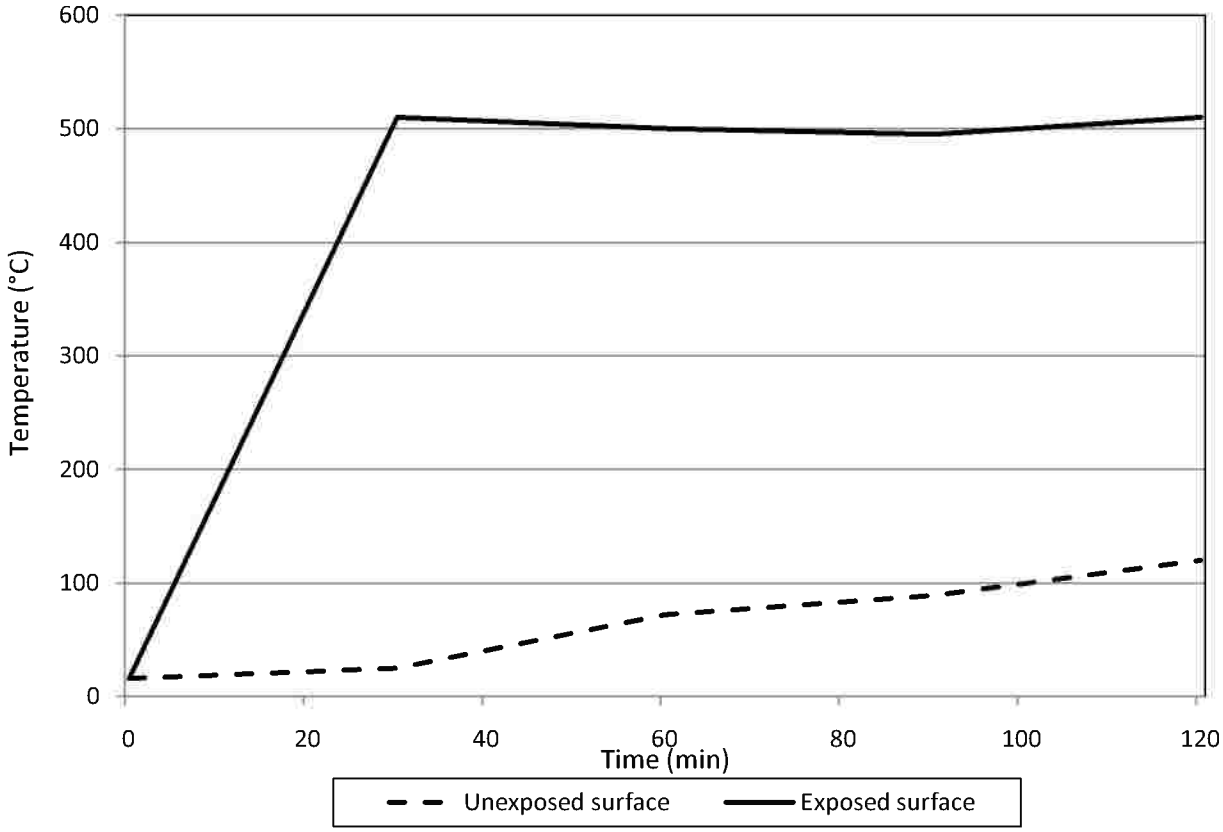

Fig. 4.79 – Time-temperature relationship of exposed and unexposed surface of the roof of the experimented room.

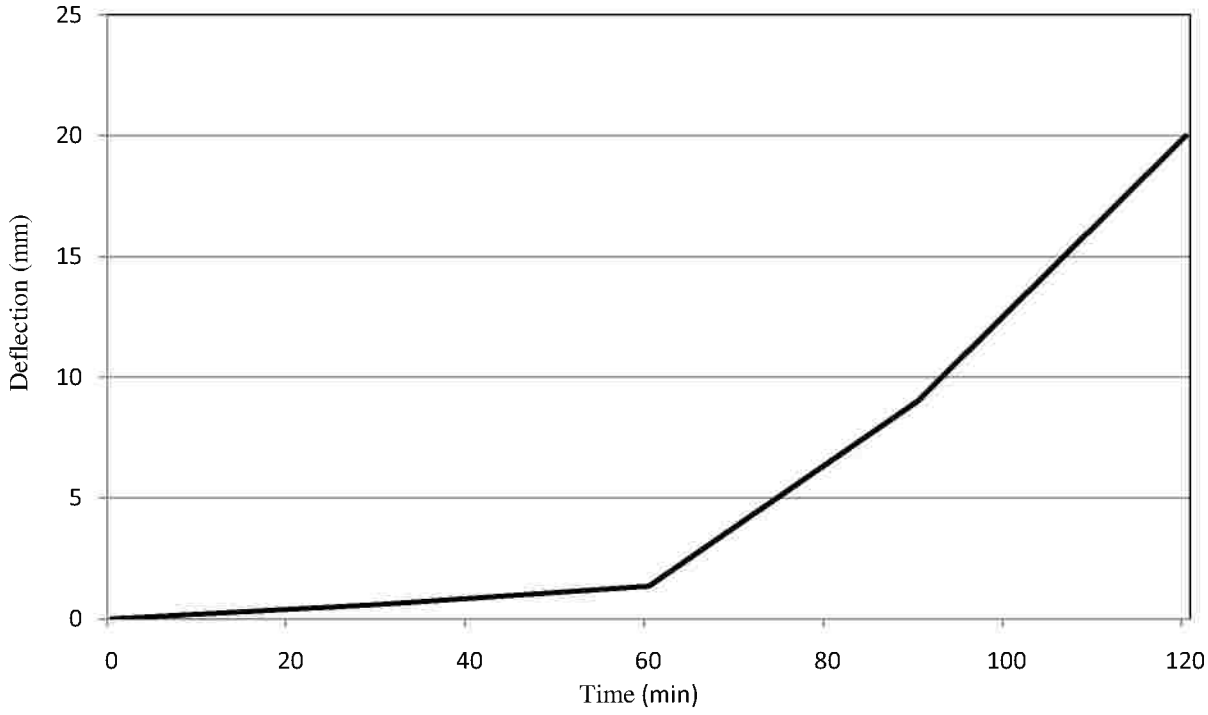

Fig. 4.80 – Time-deflection relationship of the experimented roof slab.

Qualitative observations for the slab were taken periodically on top of the slab (unexposed surface) and all sides of the room. The slab behaved well under exposure to fire, and the most interesting observations were generally made after the tests were completed. After about 10 minutes a longitudinal continuous cracks were observed in the unexposed surface of the slab as described in**Fig. 4.81**.Overall, heat transfer in reinforced slab during fire appeared after about 30 minutes, where the free water in the slab has been shown in the unexposed surface, beginning to evaporate from the cracks as shown in **Fig. 4.82**. With the increase the time of the exposure the surface cracks were increased. After 2 hrs of fire exposure the fire wasextinguished and the roof slab was cooled by water to imitate the real fire accidents. The roof slab was renounced for a week to ensure full cooling. Three cores were taken from the roof slab before and after exposure to the fire as seen in **Fig. 4.83**, the results show decreasing in the compressive strength by about 12%. These results are considerably small if they are compared to the control mix that shows a reduction in residual compressive strength by about 45% when exposed to 600°C. This is an outcome of the cores that were taken off after the fire, whenexposed to degree of temperature ranging from 120°C (unexposed surface temperature) to 510°C (exposed surface degree).

A visual inspection also was done on the reinforced roof slab that shows many surface cracks in the unexposed surface and vertical cracks along the beams that supported the slab as seen in **Fig. 4.84-(a, b).** Also a separation happened between the roof slab and the red brick clay wall as presented in **Fig. 4.84-c.** This may be due to the difference in the thermal expansion between the concrete and the red brick clay.

Fig. 4.81 – Cracking of the concrete slab of the room during the fire.

Fig. 4.82 – Water evaporation during the fire.

Fig. 4.83 – Setup of the core.

(a) (b)

(c)

Fig. 4.84 – a) Cracking in the unexposed surface of the roof slab b) Cracking in the supported beams c) The separation between roof slab and red brick clay walls.